MARTIN MARIETTA ENERGY SYSTEMS LIBRARIES
3 4456 0388821 0

142

ORNL-3973, Vol. I
UC-34 – Physics

NEUTRON PHYSICS DIVISION ANNUAL PROGRESS REPORT FOR PERIOD ENDING MAY 31, 1966

ORNL TECHNICAL INFORMATION DIVISION
Y-12 TECHNICAL LIBRARY
Document Reference Section
LOAN COPY ONLY

Do NOT transfer this document to any other person. If you want others to see it, attach their names, return the document, and the Library will arrange the loan as requested.

UCN-1624
(3 5-60)

OAK RIDGE NATIONAL LABORATORY
operated by
UNION CARBIDE CORPORATION
for the
U.S. ATOMIC ENERGY COMMISSION

Printed in USA. Price $3.00. Available from the Clearinghouse for Federal Scientific and Technical Information, National Bureau of Standards, U.S. Department of Commerce, Springfield, Virginia 22151.

LEGAL NOTICE

This report was prepared as an account of Government sponsored work. Neither the United States, nor the Commission, nor any person acting on behalf of the Commission:

A. Makes any warranty or representation, expressed or implied, with respect to the accuracy, completeness, or usefulness of the information contained in this report, or that the use of any information, apparatus, method, or process disclosed in this report may not infringe privately owned rights; or

B. Assumes any liabilities with respect to the use of, or for damages resulting from the use of any information, apparatus, method, or process disclosed in this report.

As used in the above, "person acting on behalf of the Commission" includes any employee or contractor of the Commission, or employee of such contractor, to the extent that such employee or contractor of the Commission, or employee of such contractor prepares, disseminates, or provides access to, any information pursuant to his employment or contract with the Commission, or his employment with such contractor.

ORNL-3973, Vol. I

Contract No. W-7405-eng-26

MARTIN MARIETTA ENERGY SYSTEMS LIBRARIES

3 4456 0388821 0

NEUTRON PHYSICS DIVISION ANNUAL PROGRESS REPORT

For Period Ending May 31, 1966

F. C. Maienschein, Director
A. D. Callihan, Associate Director

Group Leaders

C. E. Clifford, Reactor and Weapons Radiation Shielding
R. G. Alsmiller, Theoretical Space and High-Energy Accelerator Shielding
R. W. Peelle, Experimental Space and High-Energy Accelerator Shielding

SEPTEMBER 1966

OAK RIDGE NATIONAL LABORATORY
Oak Ridge, Tennessee
operated by
UNION CARBIDE CORPORATION
for the
U. S. ATOMIC ENERGY COMMISSION

Contents

1. NUCLEAR AND REACTOR PHYSICS 1

1.1 Deuteron Optical-Model Analysis with Spin-Orbit Potential – C. M. Perey and F. G. Perey 1

1.2 Dependence of Proton Optical-Model Parameters upon Experimental Uncertainties – J. K. Dickens 1

1.3 Elastic and Inelastic Scattering of 12.7-MeV Protons from ^{90}Zr, ^{92}Zr, and ^{94}Zr: Tabulated Differential Cross Sections – J. K. Dickens, E. Eichler, R. J. Silva, and G. Chilosi 1

1.4 Inelastic Effects in Stripping and Other Direct Reactions – S. K. Penny 2

1.5 Level Structure of ^{92}Mo – J. K. Dickens, E. Eichler, R. J. Silva, and I. R. Williams 2

1.6 Level Structure of ^{94}Zr – J. K. Dickens, E. Eichler, R. J. Silva, and G. Chilosi 2

1.7 The ^{19}F(p,α)^{16}O and ^{19}F(p,^{3}He)^{17}O Reactions at 30.5 MeV – R. K. Cole, R. Dittman, H. S. Sandhu, C. N. Waddell, and J. K. Dickens 5

1.8 Simultaneous Measurements of the Neutron Capture and Fission Cross Sections of ^{235}U and ^{233}U – G. de Saussure, L. W. Weston, R. Gwin, R. Ingle, R. W. Hockenbury, and R. R. Fullwood 5

1.9 Point-Set Representation of ^{238}U Cross Sections; Values and a FORTRAN Program for Computation – J. Wallace Webster 9

1.10 Measurement of a Portion of the Neutron Spectrum of the Bulk Shielding Reactor – R. M. Freestone, Jr., and T. V. Blosser 10

1.11 Operational Problems with the Health Physics Research Reactor – L. W. Gilley, J. W. Poston, L. B. Holland, and D. R. Ward 11

1.12 Oak Ridge Electron Linear Accelerator (ORELA) – F. C. Maienschein 12

1.13 Ratio of Capture to Fission in ^{239}Pu at keV Neutron Energies – A. Lottin, L. W. Weston, G. de Saussure, and J. H. Todd 13

2. CRITICAL EXPERIMENTS 14

2.1 Criticality of a Sphere of U(4.98)O_2F_2 Solution – E. B. Johnson 14

2.2 Critical Parameters of U(1.95) Metal Cylindrical Annuli – E. B. Johnson 15

2.3 Some Comparisons of Monte Carlo Calculations (O5R) of Low-Enriched Uranium Assemblies with Critical Experiments – J. Wallace Webster 16

2.4 Rossi-α Measurements in Subcritical Uranium Metal Cylinders – J. T. Mihalczo 17

2.5 Sensitivity of Neutron-Spectrum-Dependent Quantities in Uranium (93.2% ^{235}U) Metal Assemblies to Inelastic Scattering Models for ^{235}U – J. T. Mihalczo 18

2.6 Flight-Time Effects in Coupled Subcritical Uranium Metal Cylinders – J. T. Mihalczo 19

2.7 SORA Critical Experiments – Gustav Kistner and J. T. Mihalczo 20

2.8 Method for Estimating Critical Conditions of Large Arrays of Uranium – J. T. Thomas 22

2.9 Criticality of Lattices of Heat Transfer Reactor Experiment Fuel Elements – E. B. Johnson and R. K. Reedy 23

2.10 Experimental Determination of Safe Handling Procedures for High Flux Isotope Reactor Fuel Elements Outside the Reactor – S. J. Raffety and J. T. Thomas 24

2.11 S_n Calculations of the Aberdeen Pulse Reactor – J. T. Mihalczo 25

3. REACTOR AND WEAPONS SHIELDING 26

3.1 Measurements and Single-Velocity Calculations of Differential Angular Thermal-Neutron Albedos for Concrete – R. E. Maerker and F. J. Muckenthaler 26

3.2 Measurement of Reflected Thermal-Neutron Flux Due to Monodirectional Epicadmium Neutrons Incident on Concrete – F. J. Muckenthaler, J. L. Hull, J. J. Manning, and K. M. Henry 26

3.3 Calculations of the Differential Angular Albedo of Subcadmium Neutrons Arising from Incident Monodirectional Beams of Epicadmium Neutrons on Concrete: Comparison with Experiment – R. E. Maerker 27

3.4 Measurements of the Thermal-Neutron Flux and Fast-Neutron Dose Rate down a Rectangular Concrete Duct with One and Two Bends – F. J. Muckenthaler, J. J. Manning, J. L. Hull, and K. M. Henry 30

3.5 Calculations of Thermal-Neutron-Flux and Fast-Neutron-Dose Distributions in One-, Two-, and Three-Legged Rectangular Concrete Ducts: Comparison with Experiment – R. E. Maerker 33

3.6 Results of the Analysis by Monte Carlo of the Fast-Neutron Shielding Properties of Compound Cubical and Spherical Shields – F. H. Clark and N. A. Betz 37

3.7 Monte Carlo Calculations of the Penetration of Normally Incident Neutron Beams Through Concrete – F. H. Clark, N. A. Betz, and J. Brown 38

3.8 Measurements of Fast-Neutron Dose Rate Transmitted Through an LiH Shield with an Iron-Oil Collar Shield – F. J. Muckenthaler, J. J. Manning, J. L. Hull, and K. M. Henry 38

3.9 Monte Carlo Neutron Calculations for Determination of SNAP Collimator Design – E. A. Straker and M. B. Emmett 40

3.10 Calculations of Neutron Transport from Fission and 14-MeV Sources in Air – E. A. Straker 42

3.11 Progress in Discrete-Ordinate Transport Theory and Applications to Shielding Problems – F. R. Mynatt, W. W. Engle, Jr., and N. M. Greene 43

3.12 Monte Carlo Calculation of the Modification of the ^{235}U Fission Spectrum by a Boron Carbide Shell – R. M. Freestone, Jr. 45

3.13 Analysis of Tower Shielding Facility Neutron Scattering Data – R. M. Freestone, Jr., V. V. Verbinski, J. C. Courtney, and W. R. Burrus 46

4. RADIATION SHIELDING INFORMATION CENTER 48

4.1 Program of the Radiation Shielding Information Center – S. K. Penny, D. K. Trubey, B. F. Maskewitz, F. S. Alsmiller, and F. H. S. Clark 48

4.2 Literature Examined by the Radiation Shielding Information Center – S. K. Penny, D. K. Trubey, J. Gurney, R. G. Alsmiller, Jr., F. S. Alsmiller, B. F. Maskewitz, and B. L. McGill 49

4.3 Radiation Shielding Information Center Computer Code Collection – D. K. Trubey, B. F. Maskewitz, and S. K. Penny 50

4.4 A Monte Carlo Calculation of Fallout Gamma-Ray Dose Rates – D. K. Trubey 50

4.5 A Monte Carlo Calculation of Gamma-Ray Reflection from a Concrete Slab – D. K. Trubey and B. W. Wieland 50

5. MATHEMATICS AND COMPUTER PROGRAMS 52

5.1 SDC, a Shielding-Design Calculation Code for Fuel-Handling Facilities – E. D. Arnold and B. F. Maskewitz 52

5.2 Description of OGRE, A Monte Carlo System for Gamma-Ray Transport Studies, Including an Example (OGRE-P1) for Transmission Through Laminated Slabs – S. K. Penny, D. K. Trubey, and M. B. Emmett 52

5.3 OGRE-P4, an OGRE System Monte Carlo Code for the Calculation of Gamma-Ray Dose Rate at Arbitrary Distances from a Plane Source in Laminated Slab Geometry – D. K. Trubey 52

5.4 Computer Codes for the Calculation of Neutron and Gamma-Ray Transport Utilizing the Method of Moments – S. K. Penny 53

5.5 Variance of the Surface-Crossing Flux Estimator Used in Monte Carlo Calculations – F. H. Clark 53

5.6 Importance Functions for Monte Carlo Biasing in a Simple One-Dimensional Problem – K. J. Yost and R. R. Coveyou 53

5.7 Adjoint and Importance Functions in Monte Carlo Application – R. R. Coveyou 54

5.8 Importance Sampling Devices for Selecting Track Lengths and Directions After Scatter in O5R – F. H. Clark and N. A. Betz 55

5.9 Auxiliary Routines for O5R: O5RREAD, PICTURE, and PUNCHSIG – D. C. Irving, D. K. Trubey, and G. W. Morrison 55

5.10 A General Multigroup Cross-Section Package Using the O5R Cross-Section Library – K. J. Yost 55

5.11 Evaluated Cross-Section Library – D. C. Irving and J. Gillen 55

5.12 FORTRAN-IV Versions of the O5R Neutron Transport Code – E. C. Long 56

5.13 O6R (O5R Revised): A General-Purpose Monte Carlo Particle Transport System for IBM 360 – R. R. Coveyou 56

5.14 Random Number Generators for IBM 360 – R. R. Coveyou 57

5.15 CDC 160-A Programs for Processing Data from Neutron Time-of-Flight Cross-Section Measurements – W. E. Kinney and J. A. Biggerstaff 58

5.16 LEGENDRE, a Program to Calculate Legendre Coefficients from Angular Distributions – D. C. Irving, W. E. Kinney, and Pat Rea 59

5.17 Impossible Legendre Coefficients – D. C. Irving, R. R. Coveyou, and R. D. MacPherson 59

5.18 WATETIME – An O5R Monte Carlo Analysis Routine for the Time Behavior of Neutron Population – J. T. Mihalczo, G. W. Morrison, and D. C. Irving 59

6. RADIATION DETECTOR STUDIES (I) 60

6.1 Development of an Epithermal Neutron Spectrometer — T. V. Blosser 60

6.2 Isotropically Responding Fast-Neutron Dosimeter — T. V. Blosser 60

6.3 Progress in the Development of Instrument-Response Unfolding Methods — W. R. Burrus, B. D. Holcomb, B. Rust, C. Schneeberger, and M. Young 61

6.4 Neutron Spectrometry with Bulk Liquid Organic Scintillators — V. V. Verbinski, R. M. Freestone, Jr., R. Textor, and W. R. Burrus 62

PUBLICATIONS 65

1. Nuclear and Reactor Physics

1.1 DEUTERON OPTICAL-MODEL ANALYSIS WITH SPIN-ORBIT POTENTIAL[1]

C. M. Perey[2] F. G. Perey

An optical-model analysis of 19 deuteron elastic-scattering angular distributions in the energy range 12 to 26 MeV was performed both with and without a spin-orbit term included in the potential. The spin-orbit potential that was used is of the Thomas form, which has been found to be satisfactory for fitting the measured deuteron elastic polarization. Including the spin-orbit term always resulted in an improvement in the quality of the fits. Without the spin-orbit term, various families of potentials fitted the data equally well, but when the spin-orbit potential was added, the various families were no longer equivalent in many cases. The deuteron optical-model potential that most closely approximates the sum of the neutron and proton optical-model potentials was found to give the most consistently satisfactory results for all the angular distributions.

References

[1]Abstract of paper submitted to *The Physical Review;* also published as ORNL-TM-1529 (1966).
[2]Consultant.

1.2 DEPENDENCE OF PROTON OPTICAL-MODEL PARAMETERS UPON EXPERIMENTAL UNCERTAINTIES[1]

J. K. Dickens

The dependence of proton optical-model parameters upon experimental uncertainties was studied for four types of errors: errors in overall normalization, errors affecting the shape of the angular distribution, errors in incident energy, and errors in scattering angle. By varying the data it was found that the optical-model parameters are affected differently by the four types of errors; this suggests that a single, overall assigned error is inadequate for error analysis in optical-model studies. The minimum-χ^2 criterion was critically examined as a criterion for obtaining optimum optical-model parameters. The role of the experimental errors in the theoretical analysis was studied. Because the errors associated with the individual cross sections that form an angular distribution are not independent, it was concluded that these data do not make up a collection of several independent random samples but that collectively they resemble a single random sample. This conclusion is statistically important in the study of reaction mechanisms using results of optical-model analysis.

References

[1]Abstract of *Phys. Rev.* **143**, 758 (1966); also of ORNL-TM-1267 (September 1965).

1.3 ELASTIC AND INELASTIC SCATTERING OF 12.7-MeV PROTONS FROM ^{90}Zr, ^{92}Zr, AND ^{94}Zr: TABULATED DIFFERENTIAL CROSS SECTIONS[1]

J. K. Dickens R. J. Silva[2]
E. Eichler[2] G. Chilosi[2,3]

Numerical values of differential cross sections for elastic and inelastic scattering of 12.7-MeV protons from ^{90}Zr, ^{92}Zr, and ^{94}Zr are reported in

tabular form. Cross sections were determined at 5° intervals between laboratory angles of 20 and 165°. Inelastic-scattering data are reported for 20 excited states of ^{90}Zr (Q = −1.75, −2.18, −2.32, −2.74, −3.09, −3.31, −3.45, −3.63, −3.84, −3.97, −4.07, −4.12, −4.23, −4.33, −4.50, −4.57, −4.70, −4.82, −5.02, and −5.13 MeV); for 12 excited states of ^{92}Zr (Q = −0.93, −1.37, −1.50, −1.85, −2.07, −2.19, −2.35, −2.50, −2.76, −3.08, −3.28, and −3.49 MeV); and for 11 excited states of ^{94}Zr (Q = −0.916, −1.30, −1.47, −1.66, −2.06, −2.32, −2.36, −2.62, −3.16, −3.24, and −3.92 MeV).

References

[1]Abstract of ORNL-3934 (March 1966).
[2]Chemistry Division.
[3]Present address: INFN and Instituto di Fisica Superiore, Universita di Napoli, Italy.

1.4 INELASTIC EFFECTS IN STRIPPING AND OTHER DIRECT REACTIONS[1]

S. K. Penny

The distorted-wave theory of direct nuclear reactions such as deuteron stripping is generalized to include in the distorted waves the effects of the strong inelastic scattering which may be present when the nuclei show collective behavior. The possible changes in parity and angular momentum selection rules are discussed in detail. Formulas are given for the general case, and also for a simple model in which only one level of the target nucleus (assumed even) can be excited. Angular distributions calculated with the simple model are presented for three stripping reactions and for two cases of inelastic scattering.

References

[1]Presented to the Graduate Council of the University of Tennessee in partial fulfillment of the requirements for the degree of Doctor of Philosophy.

1.5 LEVEL STRUCTURE OF ^{92}Mo[1]

J. K. Dickens R. J. Silva[2]
E. Eichler[2] I. R. Williams[2]

Excitation energies for 34 excited states in ^{92}Mo were determined by analyzing data from inelastic scattering of 10-MeV protons and from the associated gamma-ray spectrum.

References

[1]Abstract of paper submitted to *Physics Letters*.
[2]Chemistry Division.

1.6 LEVEL STRUCTURE OF ^{94}Zr

J. K. Dickens R. J. Silva[1]
E. Eichler[1] G. Chilosi[1,2]

During the experiment to measure elastic and inelastic scattering of 12.7-MeV protons from ^{94}Zr, it became evident that the available information concerning the excited states of ^{94}Zr might not be sufficient and that the resulting theoretical analyses of these data would be hindered. Therefore the data were analyzed to obtain excitation energies for levels in ^{94}Zr which are excited by proton scattering. The analysis reported here used eight pulse-height spectra for laboratory angles of between 40 and 80°.

Figure 1.6.1 shows the spectrum obtained at 50°. Groups of protons scattered by the zirconium target can definitely be distinguished from those scattered by the target contaminants by utilizing the kinematics of the scattering as well as the expected magnitudes of the inelastic scattering. The proton groups can be distinguished from the alpha groups because the latter have much broader peaks than the former. Since the isotopic composition of the target was 97% ^{94}Zr, it is unlikely that any numbered proton group in Fig. 1.6.1 could have resulted from proton scattering by nuclei other than ^{94}Zr.

Energy calibration of the pulse-height system depended upon the relative positions of the proton peaks due to elastic scattering from ^{94}Zr and of those due to elastic and inelastic scattering from the contaminant ^{12}C. The carbon contaminant

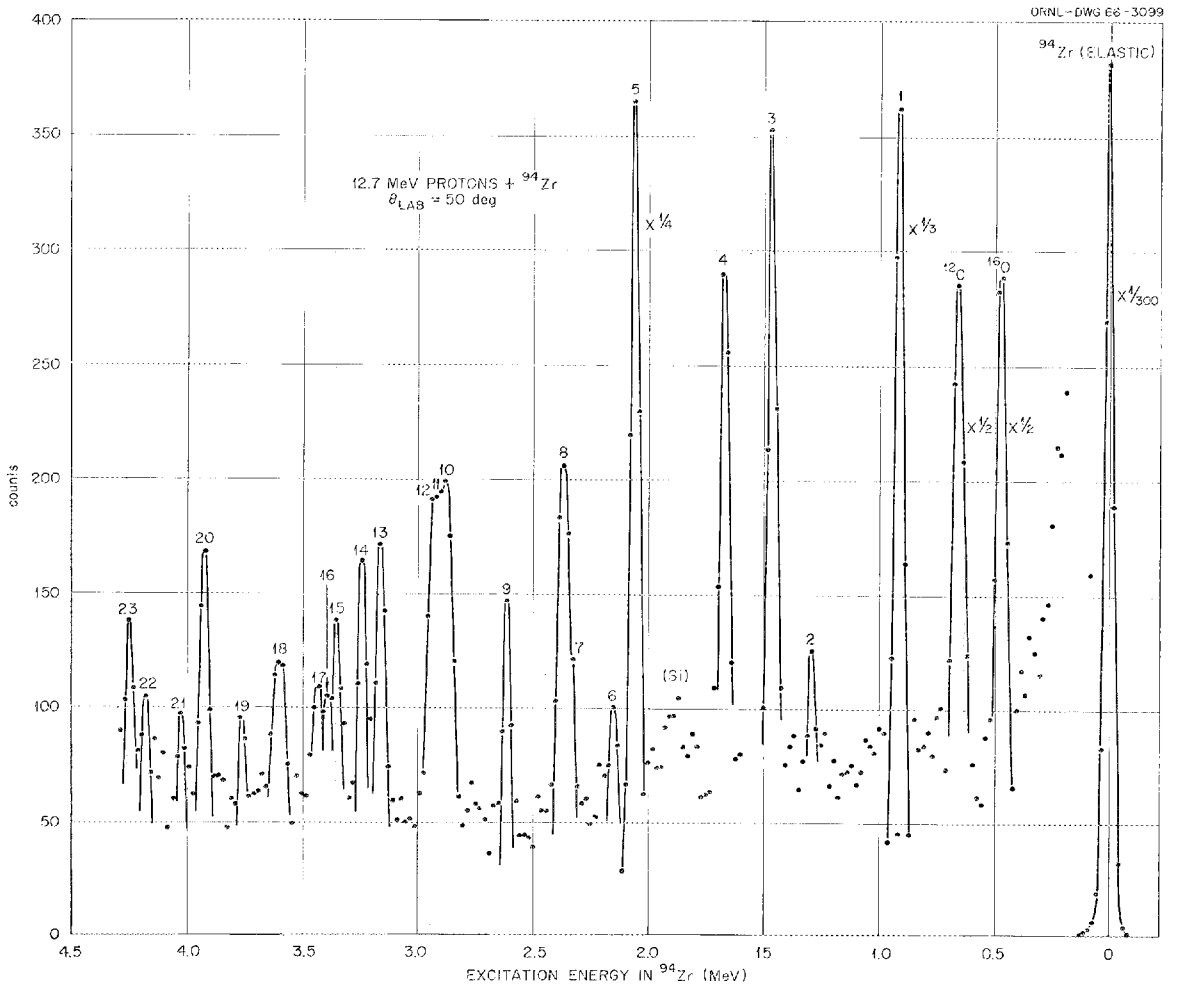

Fig. 1.6.1. Pulse-Height Spectrum of Protons Scattered from ^{94}Zr at 50°.

builds up on the surface of the target during the period of bombardment. Thus, if the carbon build-up was predominantly on one surface during the period that these particular spectra were obtained, an error would have been introduced into the calibration. The target used was ~20 keV thick to 12.7-MeV protons and ~30 keV thick to 8-MeV protons. The linearity of the pulse-height system was checked by assuming that previously reported results of excitation energies in ^{94}Zr were reasonably correct;[3,4] the system was determined to be linear for the region of interest. We suggest an error of ±30 keV for excitation energies of ~4 MeV, with the error decreasing with decreasing E_{ex}.

Table 1.6.1 presents the excitation energies and suggested spin and parity assignments, and a comparison of our results with previous work.[3,4] Several proton peaks had widths larger than our resolution (~40 keV full width at half maximum), suggesting proton scattering by more than one level in ^{94}Zr. Peak-fitting techniques were used to separate the levels; the resulting less-certain excitation energies are given in parentheses in Table 1.6.1. The broad proton peak at $E_{ex} \cong 2.9$ MeV was studied carefully in all eight spectra. We obtained a good fit to the data with three peaks (10, 11, and 12), but we cannot exclude the possibility of one or more additional levels in this group.

Table 1.6.1. ^{94}Zr Excited States and Suggested Spin and Parity Assignments, J^{π}

Peak No.[a]	12.7-MeV Protons (Present Work)		19.4-MeV Protons[b]		15-MeV Deuterons[c]	
	E_{ex} (MeV)	J^{π}	E_{ex} (MeV)	J^{π}	E_{ex} (MeV)	J^{π}
1	0.916	π^+	0.92	2^+	0.92	+
2	1.30	0^+			1.31	+
3	1.47		1.47	(4^+)	1.47	--
4	1.66	2^+	1.66	2^+	1.68	+
5	2.06	3^-	2.05	3^-	2.06	3^-
6	2.16					
7	(2.32)					
8	2.36	(2^+)	2.34	2^+	2.35	+
9	2.61	(–)	2.60	(5^-)	2.60	+
10	(2.85)		2.84			
11	(2.89)				2.89	
12	(2.94)		2.92			
13	3.16	(+)	3.14			
14	3.24		3.22		3.28	
15	3.35		3.33	(3,4)		
16	3.39					
17	3.44		3.46			
18	3.60[d]		3.57	(4,5)	3.61	–
19	3.76		3.71			
20	3.92	(–)	3.87		3.92	
21	4.02					
22	4.18					
23	4.25		4.21			

[a]Corresponding to numbering in Fig. 1.6.1.

[b]M. M. Stautberg and J. J. Kraushaar, *Bull. Am. Phys. Soc.* **10**, 527 (1965).

[c]R. K. Jolly, E. K. Lin, and B. L. Cohen, *Phys. Rev.* **128**, 2292 (1962).

[d]The proton group associated with this level has a peak width larger than expected for a single level and may include scattering by more than one excited state of ^{94}Zr.

Excitation energies for 23 levels between 0.92 and 4.25 MeV are reported, but it is unlikely that all the levels in this energy region were found. We could not separate proton groups corresponding to excitation of levels in ^{94}Zr less than 30 keV apart. In addition, levels with large spins are not appreciably excited by proton scattering; the spins of most of these 23 states will be 6 or less. Angular distributions for several of these states[5] are being analyzed so that nuclear reaction and structure information can be obtained if possible.

References

[1]Chemistry Division.

[2]Present address: INFN and Instituto di Fisica Superiore, Universita di Napoli, Italy.

[3]M. M. Stautberg and J. J. Krausharr, *Bull. Am. Phys. Soc.* **10**, 527 (1965).

[4]R. K. Jolly, E. K. Lin, and B. L. Cohen, *Phys. Rev.* **128**, 2292 (1962).

[5]J. K. Dickens *et al.*, *Elastic and Inelastic Scattering of 12.7-MeV Protons from ^{90}Zr, ^{92}Zr, and ^{94}Zr: Tabulated Differential Cross Sections*, ORNL-3934 (March 1966).

1.7 THE $^{19}F(p,\alpha)^{16}O$ AND $^{19}F(p,^3He)^{17}O$ REACTIONS AT 30.5 MeV[1]

R. K. Cole[2] H. S. Sandhu[2,4]
R. Dittman[2,3] C. N. Waddell[2]
J. K. Dickens

Absolute differential cross sections for the $^{19}F(p,\alpha)^{16}O$ reaction leading to the ground state of ^{16}O, the $^{19}F(p,^3He)^{17}O$ reaction leading to the ground state of ^{17}O, and the $^{19}F(p,^3He)^{17}O$ reaction leading to the first-excited state of ^{17}O (E_{ex} = 0.871 MeV) have been measured for angles of 7 to 155°, 16 to 111°, and 16 to 111° in the center-of-mass systems respectively. The angular distributions showed strong forward peaking for all three reactions. The experimental data were compared with theoretical angular distributions obtained by distorted-wave methods. The calculated angular distributions fit the $L = 0$ data quite well; the $L = 2$ data are not so well fitted. The ratio of the experimental spectroscopic factors for the two $(p,^3He)$ reactions agrees quite well with the computed ratio.

References

[1]Abstract of paper submitted to *Nuclear Physics;* work partially supported by the University of Southern California under AEC contract AT(04-3)-B6.

[2]University of Southern California, Los Angeles.

[3]Present address: California State College, Fullerton.

[4]Present address: San Fernando Valley State College, Northridge, Calif.

1.8 SIMULTANEOUS MEASUREMENTS OF THE NEUTRON CAPTURE AND FISSION CROSS SECTIONS OF ^{235}U AND ^{233}U

G. de Saussure R. Ingle[1]
L. W. Weston R. W. Hockenbury[2]
R. Gwin R. R. Fullwood[2]

The simultaneous measurements of the capture and fission cross sections of ^{235}U performed in October 1964 and described previously[3] have now been analyzed. Examples of the results are given in Fig. 1.8.1 and Table 1.8.1, the figure showing

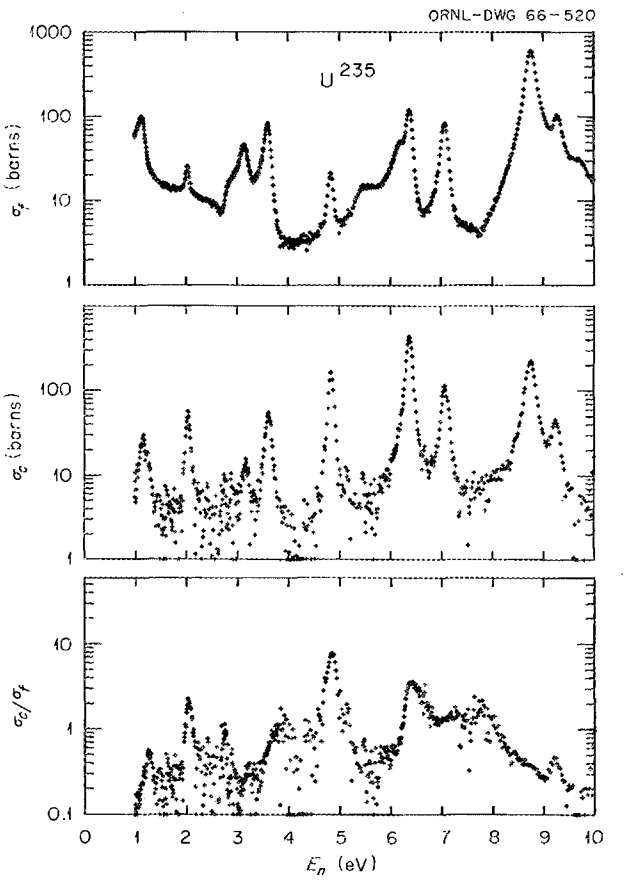

Fig. 1.8.1. Fission Cross Section, Capture Cross Section, and α for ^{235}U from 1 to 10 eV (ORNL-RPI 1964 Measurements).

the fission and capture cross sections and their ratio σ_c/σ_f in the energy range 1 to 10 eV, and the table giving the fission and capture resonance integrals over $\frac{1}{4}$ lethargy intervals. For comparison, the fission resonance integrals obtained from the data of Michaudon and Ribon[4] are included in the table.

Since October 1964 many improvements have been made in the technique and instrumentation used in measuring capture and fission cross sections at the Rensselaer Polytechnic Institute linac. A considerable reduction in background was achieved by various modifications in the beam collimation system and in the target moderator assembly. A new BF_3 ionization chamber was constructed to measure the neutron-flux spectrum with more accuracy, and an ionization chamber containing about 1 g of ^{233}U was added

Table 1.8.1. ^{235}U Capture and Fission Resonance Integrals

Energy Interval (eV)	$\int \sigma_c \, dE/E$ (barns), ORNL-RPI, 1964	$\int \sigma_f \, dE/E$ (barns)	
		ORNL-RPI, 1964	Michaudon and Ribon[a]
0.683–0.876	1.562	13.653	14.282
0.876–1.125	3.096	18.896	18.051
1.125–1.445	3.676	10.193	11.035
1.445–1.855	0.958	3.586	3.903
1.855–2.382	3.659	3.504	3.684
2.382–3.059	1.116	3.284	3.292
3.059–3.928	3.687	7.598	7.829
3.928–5.043	4.964	1.160	1.326
5.043–6.476	11.290	6.780	6.551
6.476–8.315	4.745	3.676	3.885
8.315–10.677	8.529	25.613	23.446/24.857
10.677–13.710	18.142	11.858	11.109
13.710–17.603	4.245	8.092	8.150
17.603–22.603	11.646	16.733	15.193
22.603–29.023	4.876	10.827	10.174
29.023–37.267	9.160	14.120	12.006
37.267–47.851	4.580	9.033	8.028
47.851–61.442	5.367	14.147	12.562
61.442–78.893	2.769	5.842	5.501
78.893–101	3.852	5.327	5.745
101–130	3.165	5.233	5.307
130–167	3.475	5.494	5.269
167–214	3.193	5.209	4.757
214–275	3.059	6.275	5.627
275–354	2.651	4.185	
354–454	2.206	3.385	
454–583	1.712	4.423	
583–749	1.818	3.510	
749–961	1.643	2.701	
961–1234	1.776	2.675	

[a]A. Michaudon and P. Ribon, *J. Phys. Radium* **22**, 712 (1961); also private communication.

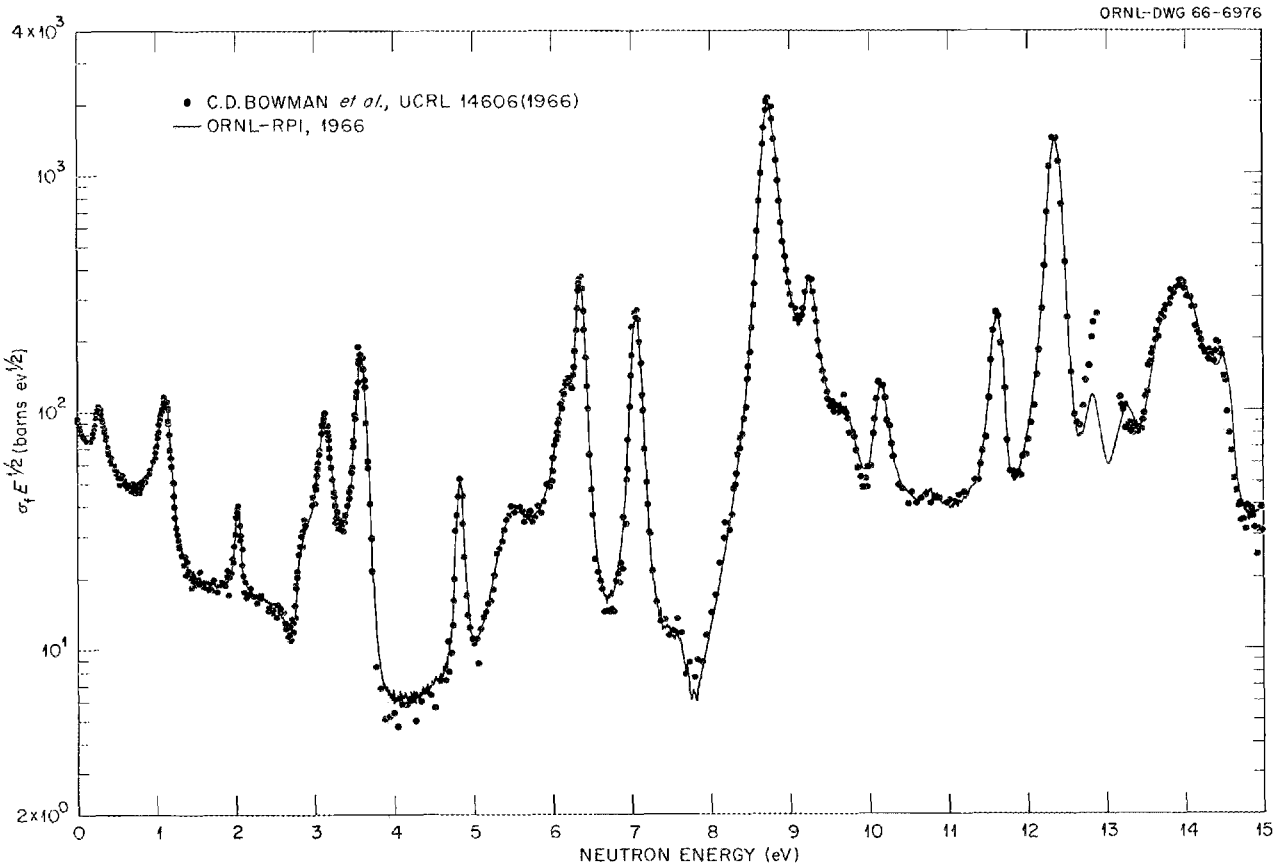

Fig. 1.8.2. Comparison of ORNL-RPI 1966 ^{235}U Fission Cross-Section Measurements from 0.4 to 15 eV with Those of Bowman *et al.*

to the equipment.[5] This new fission chamber was used to simultaneously measure the fission and capture cross sections of ^{233}U in April 1966. At the same time the ^{235}U measurements were repeated to take advantage of the improvements in the technique to decrease the uncertainties in the data.

The analysis of the new measurements is incomplete. Some preliminary results are shown in Figs. 1.8.2 and 1.8.3 and in Tables 1.8.2 and 1.8.3. In Fig. 1.8.2 the ^{235}U fission cross section from the 1966 measurements is compared in the neutron energy range from 0.4 to 15 eV with data recently obtained by Bowman *et al.*[6] Table 1.8.2 is a comparison between the two same sets of data in terms of resonance integrals over $\frac{1}{4}$ lethargy intervals. The average discrepancy between the resonance integrals obtained from the two sets of data is smaller than 3% and smaller than 0.25 barn. Since the two experiments are independent, the probable error of the fission resonance integral over a $\frac{1}{4}$ lethargy interval from either measurement must be smaller than 3% and 0.25 barn.

In Fig. 1.8.3 the ^{235}U fission cross section from the 1966 measurements is compared in the neutron energy range from 20 to 50 eV with data obtained by Brown *et al.*[7] using neutrons generated by an underground nuclear explosion. The agreement between the two sets of data is very good except below 22 eV, where the flux from the nuclear explosion was not well determined, and in the "valleys" below 35 eV, where the value of the cross section measured by Brown *et al.* is lower by as much as a factor of 2 than our value. This discrepancy is not well understood. Table 1.8.3 compares the integrated fission cross-section data from this measurement with those from three other

Table 1.8.2. ^{235}U Fission Resonance Integrals

Energy Interval (eV)	$\int \sigma_f \, dE/E$ (barns)		Difference	
	ORNL-RPI, 1966	Bowman *et al.*, UCRL-14606	barns	%
0.414–0.532	22.140	22.127	0.013	0.1
0.532–0.683	16.436	16.274	0.162	1.0
0.683–0.876	13.859	13.755	0.104	0.8
0.876–1.13	18.098	17.980	0.118	0.7
1.13–1.44	10.457	10.467	–0.010	0.1
1.44–1.86	3.758	3.704	0.054	1.5
1.86–2.38	3.689	3.666	0.023	0.6
2.38–3.06	3.407	3.261	0.146	4.5
3.06–3.93	7.971	8.002	–0.031	0.4
3.93–5.04	1.331	1.227	0.104	8.5
5.04–6.48	7.017	7.010	0.007	0.1
6.48–8.32	3.511	3.601	–0.090	2.5
8.32–10.7	25.943	26.549	–0.606	2.3
10.7–13.7	11.822	11.863[a]	–0.041	0.35
13.7–17.6	8.313	8.382	–0.069	0.8
17.6–22.6	16.861	17.319	–0.458	2.6
22.6–29.0	11.228[b]	11.346	–0.118	1.1
29.0–37.3	13.763	14.090	–0.327	2.3
37.3–47.9	8.618	8.950	–0.332	3.7
47.9–61.4	13.954	14.174	–0.220	1.6

[a]Corrected for an instrumental error in this set of data at 13.1 eV; see Fig. 8 on p. 14 of UCRL-14606.

[b]This set of data has been corrected for a small flux depression near 28 eV.

Table 1.8.3. Integrated ^{235}U Fission Cross Sections from 20 to 60 eV

Energy Interval (eV)	$\int \sigma(E) \, dE$ (barn-eV)			
	Brooks *et al.*[a]	Bowman *et al.*[b]	Brown *et al.*[c]	ORNL-RPI, 1966
20.5–33.0	418	450	415[d]	446
33.0–41.0	415	499	489	507
41.0–60.0	834	932	950	929
Total	1667	1881	1854	1882

[a]F. D. Brooks *et al.*, *Eta and Neutron Cross Sections of U-235 from 0.04 to 200 eV*, AERE-M-1670 (1966).

[b]C. D. Bowman *et al.*, *The Epithermal Fission Cross Section of U-235*, UCRL-14606 (1966); paper FF-15 in *Conference on Neutron Cross Section Technology, Washington, D.C., March 22–24, 1966.*

[c]W. K. Brown, D. W. Bergen, and J. D. Cramer, *Fission Cross Section of U-235, 20 eV–2 MeV*, LADC-7618; paper FF-11 in *Conference on Neutron Cross Section Technology, Washington, D.C., March 22–24, 1966.*

[d]Flux not well determined below 22 eV.

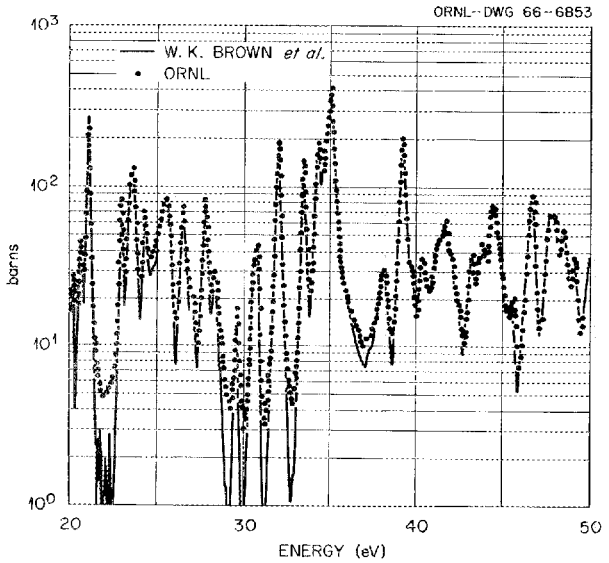

Fig. 1.8.3. Comparison of ORNL-RPI 1966 ^{235}U Fission Cross-Section Measurements from 20 to 50 eV with Those of Brown *et al.*

measurements.[6–8] Our data agree much better with those of Bowman *et al.* than with the other sets of data.

References

[1]Instrumentation and Controls Division.

[2]Rensselaer Polytechnic Institute, Troy, N.Y.

[3]L. W. Weston *et al., Neutron Phys. Div. Ann. Progr. Rept. Aug. 1, 1965,* ORNL-3858, vol. I, p. 9.

[4]A. Michaudon and P. Ribon, *J. Phys. Radium* **22,** 712 (1961); also private communication.

[5]Both the BF_3 ionization chamber and the ^{233}U fission chamber were designed and assembled by F. E. Gillespie of the Instrumentation and Controls Division.

[6]C. D. Bowman *et al., The Epithermal Fission Cross Section of U-235,* UCRL-14606 (1966); paper FF-15 in *Conference on Neutron Cross Section Technology, Washington, D.C., March 22–24, 1966.*

[7]W. K. Brown, D. W. Bergen, and J. D. Cramer, *Fission Cross Section of U-235, 20 eV–2 MeV,* LADC-7618; paper FF-11 in *Conference on Neutron Cross Section Technology, Washington, D.C., March 22–24, 1966.*

[8]F. D. Brooks *et al., Eta and Neutron Cross Sections of U-235 from 0.04 to 200 eV,* AERE-M-1670 (1966).

1.9 POINT-SET REPRESENTATION OF ^{238}U CROSS SECTIONS; VALUES AND A FORTRAN PROGRAM FOR COMPUTATION[1]

J. Wallace Webster

As part of the current effort in reactor analysis to obtain representations of cross sections as sets of values at discrete energy points rather than as sets of averaged values over broad intervals of the energy domain, a FORTRAN program has been prepared which computes total and capture cross sections of ^{238}U at specified energy points over a resonance. The resonance parameters and the temperature are used as input data. Using the resonance parameters given in BNL-325,[2] 862 point representations were computed for the cross sections of ^{238}U for neutron energies of less than 1000 eV and a temperature of 300°K. The results are presented as machine printouts and as Calcomp plots. They have also been recorded on punched cards in the format

(Energy, Cross Section) = (E15.5, E15.5) ,

and duplicate decks may be obtained by contacting the author.

References

[1]Abstract of ORNL-TM-1448 (1966).

[2]J. R. Stehn *et al., Neutron Cross Sections, Z = 88 to 98,* BNL-325, vol. III, 2d ed., suppl. 2 (February 1965).

1.10 MEASUREMENT OF A PORTION OF THE NEUTRON SPECTRUM OF THE BULK SHIELDING REACTOR[1]

R. M. Freestone, Jr. T. V. Blosser

In collaboration with the Army Nuclear Defense Laboratory (ANDL) a series of measurements were initiated for calibration of several solid-state and fission-type neutron detectors used by ANDL. For this purpose a neutron beam was extracted from the water surrounding the Bulk Shielding Reactor (BSR) through a temporary beam tube. The beam tube consisted of a 6-in.-diam air-filled aluminum pipe hung from the BSR instrument bridge and extending vertically downward to the midplane of the reactor, approximately 20 cm from its north face. The upper 7-ft-long portion of the tube was diminished to a 1-in. diameter by a water collimator. The device thus served as a convenient well-collimated beam source of thermal and epithermal neutrons. The ANDL work required that the intensity and spectrum of this source be known. These parameters were measured by using the 22 ^{10}B filters and the isotropically responding spherical BF_3 proportional counter which are the principal components of the epithermal neutron spectrometer described in Sect. 6.1, this report.

The experimental procedure was simple and straightforward. Each of the 22 filters was placed in succession over the 1-in.-diam opening of the collimator, and a set of at least three ½- or 1-min counts was made with the BF_3 counter suspended at a fixed distance of a few centimeters above the filter. Counts were also made with the counter in the unobstructed beam and with a 20-mil-thick cadmium disk as a filter. Additionally, indium and gold foils, bare and cadmium-covered, were exposed at the counter position in the beam.

Though obtaining the experimental data was essentially routine, its analysis was not. Initially, much time was lost in a futile attempt to utilize the rather elegant FERD methods of Burrus *et al.* The FERD system produces a reasonably reliable estimate of error in the unscrambled spectrum, but, unfortunately, the response functions associated with a ^{10}B filter (a $1/v$ absorber) combined with a BF_3 counter (a $1/V$ detector) possess a long, slowly decreasing tail, with which FERD could not readily cope without being modified by suitable a priori assumptions.

The analysis method finally adopted consisted basically in making a first guess at the probable shape of the spectrum, using the previously measured transmission functions of the filters to calculate the counts to be expected from such a spectrum, and iterating by successive guesses until a count-rate curve which matched the experimental count-rate curve was obtained. In the present case, iteration was concluded when all calculated counts were within 5% of experimental values.

The analyzed spectrum, not surprisingly, consists of a Maxwellian distribution of thermals with a neutron temperature of 336°K, plus a tail described by $1.967 \times 10^{-3}/E$ extending to $\sim 8 \times 10^4$ eV. Beyond this point the data appear to demand a flatter spectrum, falling roughly as $E^{-1/2}$, but they may not be reliable. The spectrum was normalized to absolute values by compelling the integral from 0.001 to 0.4 eV to agree with the experimentally determined subcadmium flux value of 1.56117×10^5 neutrons cm^{-2} sec^{-1} at 1 MW, measured with indium foils. A plot of the spectrum, which appears to be consistent in shape with published spectra for reactor neutrons in water, is shown in Fig. 1.10.1.

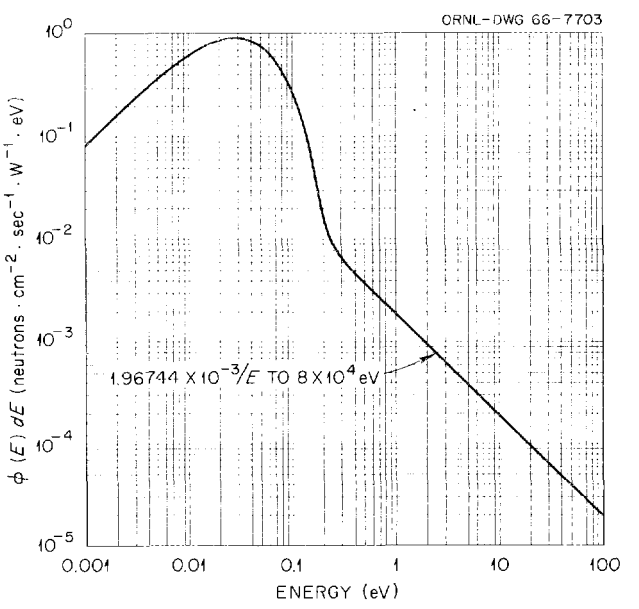

Fig. 1.10.1. Spectrum of the Bulk Shielding Reactor from Thermal to 10^5 eV.

References

[1]Work supported by the Army Nuclear Defense Laboratory, Edgewood Arsenal, Maryland.

1.11 OPERATIONAL PROBLEMS WITH THE HEALTH PHYSICS RESEARCH REACTOR

L. W. Gilley L. B. Holland
J. W. Poston[1] D. R. Ward

In the operation of the Health Physics Research Reactor (HPRR),[2] a pulse-generating reactor having an unmoderated uranium-molybdenum core (10 wt % Mo), two major difficulties have been encountered: electrical noise in the instrument channels, and scatter in the burst size (variations as large as ±40%). (Previous difficulties with the plating on the U-Mo fuel pieces have been minimized, and further improvements have been recommended.) It was necessary to identify and eliminate the sources of these problems not only to permit orderly operation of the HPRR but also because the Aberdeen Pulse Reactor,[3] being very similar in design to the HPRR, may suffer from similar difficulties.

Electrical noise in the instrument channels frequently interrupted operation due to spurious signals, which resulted in a reactor shutdown. The source of the trouble was isolated in the ionization chambers, and examination revealed that tighter quality control during their assembly will eliminate this problem. One reassembled chamber was placed back in operation, and no difficulty has been observed over a three-month period.

The problem related to our inability to achieve a target burst with better than 40% accuracy was more troublesome, not only because it is an annoyance to experimenters but also because it is inherently more dangerous than the first problem. Because of the danger, therefore, the target burst size was arbitrarily limited to 0.8×10^{17} fissions. (The largest burst during preliminary testing was 1.8×10^{17} fissions.) Several steps were taken to identify the cause for the scatter in the burst size. The first step was to examine the core mounting framework and to periodically check the dimensions of the core and the individual fuel pieces. No anomalies or changes were noted. The bolts holding the core together were checked for tightness after each series of three bursts, and they appeared to be loosening. It was feared that this might be due to the bolts stretching, but it was later attributed to a peening action on the plating on the core bolts and fuel pieces. The torque on the bolts was increased in several steps to 50 ft-lb, at which value it was shown that after 100 bursts the torque did not change and that over a period of a year the bolt dimensions did not vary. For the same operating conditions the measurements of the safety block, the individual fuel disks, and the assembled core did not change.

Tests were also made to determine to what degree of accuracy we could measure the various parameters that can affect the burst size, that is, the core temperature, the reactivity in the core prior to the burst, the reproducibility of the position of the safety block in the core, and the position of the burst rod prior to insertion. The results showed that the combined errors should permit a burst to be within 5% of the target size.

Next, attention was focused on the position of the burst rod at the time of the burst. Fastax film of the burst rod action revealed that the effectiveness of the shock absorber was inadequate, allowing the rod to bounce for as much as $\frac{3}{4}$ in. and as long as 110 msec. Since the mean time for a burst of 8×10^{16} fissions was of the order of 100 msec, it was obvious that the displacement of the rod from its fully inserted position at the time of burst could introduce some error, but not, however, enough to account for the spread in the data.

Mechanical checkout of the action of the burst rod without the core present revealed that the poorly damped impact of the burst rod caused an oscillation of the safety block and its associated supporting magnet through the action of the overtravel spring on the safety-block drive-motor system. Tests showed that the burst rod had to be critically damped to completely eliminate the safety-block oscillation.

A program was initiated to design a better shock absorber system. Since it was realized that such a program would require a fair amount of time, a longer burst rod was fabricated so that the burst rod would extend through the core when it was in the fully inserted position. Thus the reactivity change associated with any bounce would be

minimized, hopefully making it easier to isolate other sources of reactivity change. With the reactor reassembled, investigations were continued, and for each burst the following information was obtained: the insertion time of the burst rod, its position (either fully inserted or not) at the time of burst, the time lapse between initial insertion of the burst rod and the time of the burst, the initial period or initial rate of power rise during a burst, the shape of the fission-rate curve as a function of time during a burst, and the position of the safety block as a function of time for its first ½ in. of movement from its inserted position.

The last measurement also showed the movement of the safety block when the burst rod was inserted, which, together with a knowledge of the reactivity worth of the safety block as a function of position, indicated that motion of the safety block when the burst rod was inserted was the major cause of scatter in the burst size. A temporary change in the burst-rod pneumatic system made it possible for data to be accumulated in the range of 1 to 9×10^{16} fissions per burst with only a ±4% variation. This success was achieved with a fairly long burst-rod insertion time, which results in a fair number of bursts being initiated before the burst rod is completely inserted, especially at the higher burst levels; these preinitiated bursts are not included in the ±4% variation. A program has been initiated to reduce the burst-rod insertion time while still maintaining critical damping when the rod is inserted.

The original nickel plating on the fixed U-Mo fuel pieces and the chromium flash over nickel plating on the movable fuel pieces are still in service except for the bottom fuel disk and some of the core bolts. The original plating on these items was stripped, since it was not satisfactory, and the items were carefully replated with nickel and the bolts were given an additional flash coating of gold. Inspection of all pieces after a year of operation, which included 136 bursts, revealed that there was still essentially no change in the original plating (some minor flaws that were apparent a year ago had changed no further), that the overall condition of the plating on the bolt threads was fair, but that there were some cracks in the plating at the crown of the threads, indicating poor adhesion in this area. It is recommended therefore that a Whitworth thread with rounded crown and thread be used in the future for pieces that require plating.

References

[1]Health Physics Division.

[2]*Procedures Manual for the Health Physics Research Reactor*, ORNL-3519 Rev. Special.

[3]J. R. Tomlinson *et al.*, *Preliminary Safeguards Report for the Aberdeen Pulsed Reactor Facility*, BRL-1255 (September 1964).

1.12 OAK RIDGE ELECTRON LINEAR ACCELERATOR (ORELA)

F. C. Maienschein

During the past year, construction was approved for an electron linear accelerator to be used as a source of short intense pulses of neutrons. The pulsed neutrons will, for the main part, be used for making cross-section measurements by the time-of-flight technique, with emphasis given to the energy region (~1 keV to ~1 MeV) which is most important for fast-breeder reactor design.

Progress to date includes signing a contract with an accelerator manufacturer, Varian Associates of Palo Alto, California, for delivery of the accelerator components by the fall of 1967. The performance specified in the contract includes 15-A pulses of ≧140-MeV electrons with beam powers up to 50 kW for pulse widths as narrow as 2.3 nsec. This electron current should produce neutrons at a peak rate of a few times 10^{18} per second when it is incident on the water-cooled tantalum target which is now being designed by the General Engineering and Construction Division.

The accelerator and neutron target room will be placed under ~20 ft of earth shielding just south of Swan Lake and west of the Oak Ridge Isochronous Cyclotron. Ten neutron flight paths of various lengths will radiate from the neutron target room, which will be 12 ft in diameter and 10 ft high and will be evacuated to eliminate the production of radiation-induced noxious gases. The title I design of the facility was started in January 1966 by Charles T. Main of Boston, Massachusetts, the architect-engineer, and was completed in May 1966. Title II or final design was started for portions of the facility in March 1966, and it should be completed during 1966.

Since ORELA will be a versatile source of electrons, photons, and neutrons, it will be potentially useful in many ORNL programs, including studies of electron scattering, photonuclear reactions, and radiation effects. The facility design includes experimental areas which can be later adapted for such research. ORELA will be operated jointly by the Neutron Physics and Physics Divisions. ORNL participants in the design of ORELA include W. R. Burrus, G. de Saussure, R. Gwin, F. C. Maienschein,[1] V. V. Verbinski, and L. W. Weston from the Neutron Physics Division; R. C. Block, J. A. Harvey,[1] R. L. Macklin, P. D. Miller, and G. G. Slaughter from the Physics Division; A. L. Boch[2] from the Directors Division; and J. A. Murray from the General Engineering and Construction Division.

References

[1]Program codirector.

[2]Construction project director.

1.13 RATIO OF CAPTURE TO FISSION IN ^{239}Pu AT keV NEUTRON ENERGIES

A. Lottin[1] G. de Saussure
L. W. Weston J. H. Todd[2]

The ratio of the neutron capture cross section to the fission cross section (α) for ^{239}Pu has been measured for incident neutron energies from about 20 to 600 keV. The technique was very similar to that used for earlier measurements on ^{235}U.[3] The results are not yet fully analyzed.

References

[1]On assignment from Centre d'Etudes Nucléaire, Saclay.

[2]Instrumentation and Controls Division.

[3]L. W. Weston, G. de Saussure, and R. Gwin, *Nucl. Sci. Eng.* **20**, 80 (1964).

2. Critical Experiments

2.1 CRITICALITY OF A SPHERE OF $U(4.98)O_2F_2$ SOLUTION

E. B. Johnson

An extensive program of critical experiments with an aqueous solution of UO_2F_2 in which the uranium is enriched to 4.98% in ^{235}U has been under way for some time. Earlier measurements described the critical spacing of a number of cylinders of the solution contained in aluminum and polyethylene vessels[1,2] to provide guidance in storage and transport of low-enriched uranium. More recent measures have attempted to define the critical quantity of the solution, essentially unreflected, in single units of simple geometry. The results of these experiments will guide the application of analytical methods and the selection of nuclear properties, particularly neutron cross sections, necessary to satisfactorily calculate the effective neutron multiplication factor.

The first of the more recent experiments consisted of a cylinder of solution contained in thin stainless steel.[3] The experimentally observed value of k_{eff} was 1.000, which is to be compared with 1.002 calculated[3] by S_4 transport theory and with 0.99 calculated (Sect. 2.3) with the O5R Monte Carlo code.

For the second experiment of this type a spherical container 19.99 ± 0.01 in. in inside diameter was constructed of 0.02-in.-thick stainless steel. The dimensions and shape were preserved by the installation of "ribs" as shown in Fig. 2.1.1. The sphere was suspended by cables to reduce the effect of support structures. The UO_2F_2 solution contained in this sphere was critical at 19°C. The ^{235}U content of the uranium was 4.98%, and the chemical concentration at this temperature was 910.18 g of uranium per liter at a density of 2.0298 g/cm^3, corresponding to an H:^{235}U atomic ratio of 490. The reactivity contributed by the container wall, the supporting members, and the column of solution in the filling connection was determined experimentally to be 16.8 cents. On the basis of $\beta_{eff} = 0.0075$, k_{eff} of the solution was 0.999. The calculated value was 0.99 (Sect. 2.3).

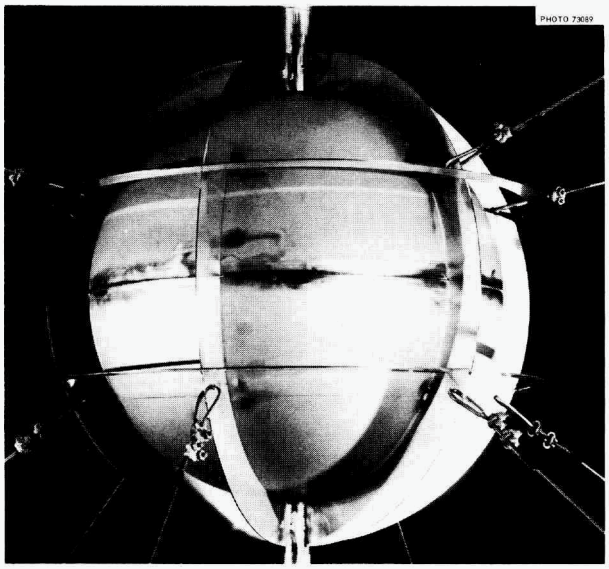

Fig. 2.1.1. Stainless Steel Sphere Used in Critical Experiments with Uranyl Fluoride Solutions.

An indication of the neutron spectrum within the sphere and on the surface of its container was obtained from irradiated U(93) foils with and without cadmium covers. The cadmium fraction had a constant value of 0.929 across a diameter; the value on the surface of the container was 0.855.

References

[1]E. B. Johnson and D. F. Cronin, *Neutron Phys. Div. Ann. Progr. Rept. Aug. 1, 1964*, ORNL-3714, p. 31; E. B. Johnson and D. F. Cronin, *Trans. Am. Nucl. Soc.* **17**, 301 (1964).

[2]E. B. Johnson, *Neutron Phys. Div. Ann. Progr. Rept. Aug. 1, 1965,* ORNL-3858, p. 15.

[3]J. Wallace Webster and E. B. Johnson, *Criticality of a Single Unit of Aqueous Uranyl Fluoride Solution Enriched to 5% in* ^{235}U, ORNL-TM-1195 (1965).

2.2 CRITICAL PARAMETERS OF U(1.95) METAL CYLINDRICAL ANNULI[1]

E. B. Johnson

Experiments have been performed to determine the critical parameters of lattices of cylindrical annuli of uranium enriched to 1.95% in ^{235}U.

In the first series of experiments the dimensions of the units were a 7.2-in. outside diameter, a 2.6-in. inside diameter, and a 40-in. length; the units had an average mass of 442 kg, of which 8.6 kg was ^{235}U. A total of 25 units was available. For the next series the outside diameter was reduced to 6.2 in., which decreased the mass of a unit to 308 kg (6.0 kg of ^{235}U); the other dimensions were unchanged.

The units were latticed in water in both square and triangular patterns to determine the critical number as a function of spacing. With the units which were 7.2 in. in outside diameter, it was found that the minimum critical number for each pattern occurred at a water-to-uranium volume ratio of 0.65 and that the critical number of units arranged in a triangular pattern was half that required for a square pattern, as shown in Fig. 2.2.1. For the 6.2-in.-OD units the minimum was found at a water-to-uranium volume ratio of 0.8, and the difference between the critical number of units arranged in square and triangular patterns was appreciably reduced.

In several critical lattices, water was excluded from the central region of each annulus by inserting coaxial Styrofoam cylinders (density = 0.024 g/cm^3) of three different diameters. In all cases exclusion of water from the central region decreased the reactivity. For example, the presence of 1.55-in.-diam Styrofoam cylinders in a lattice of 7.2-in.-OD annuli increased the critical number of units from 10 to 12.5 and shifted the volume ratio for minimum mass from 0.65 to 0.60. This minimum occurred at a surface separation of 1 in. in a triangular pattern.

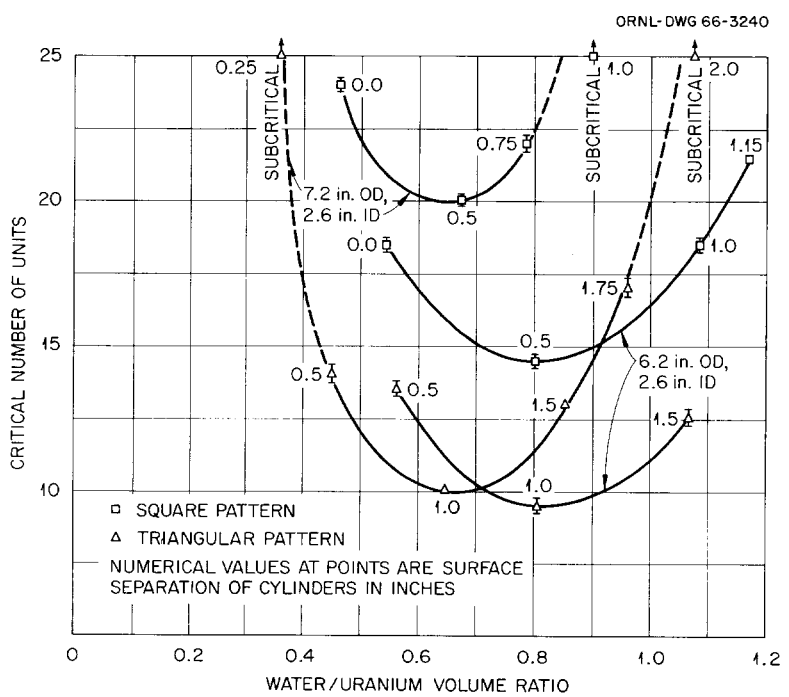

Fig. 2.2.1. Critical Lattices of U(1.95) Metal Annular Cylinders Moderated and Reflected by Water.

References

[1]Summary of paper presented at American Nuclear Society Twelfth Annual Meeting, Denver, Colo., June 20–23, 1966; to be published in *Trans. Am. Nucl. Soc.* **9**, No. 1 (1966).

2.3 SOME COMPARISONS OF MONTE CARLO CALCULATIONS (O5R) OF LOW-ENRICHED URANIUM ASSEMBLIES WITH CRITICAL EXPERIMENTS

J. Wallace Webster

A comparison with experiments has been made of the values of k_{eff} of various hydrogen-moderated assemblies of low-enriched uranium calculated by a Monte Carlo method using the O5R code. This is part of the continuing program of correlation of theory with experiment at the Critical Experiments Facility.

The cross sections of ^{238}U used in the calculations were those recently expressed (Sect. 1.9, this report) in the form of point-set representations using the latest data. The cross sections for ^{235}U below 1000 eV were taken from the recently updated UK nuclear data library;[1] those above 1000 eV were a selection from cross sections assembled and evaluated by Mihalczo[2] for the O5R library. The cross sections for the remaining elements needed in the calculations were taken directly from the O5R library without any updating. In the case of fluorine, only the total cross-section set was in the library; so the elastic cross sections were equated to the total cross section, and the inelastic and other high-energy interactions with fluorine were neglected. Scattering by fluorine was taken to be isotropic in the center-of-mass system since the angular distribution has not yet been expressed in the form necessary for the O5R code. The above-thermal interactions with all other elements were treated correctly with the best available data.

Thermal-neutron ($E \leqq 0.625$ eV) interactions were represented by the one-group option. For the computation of water-moderated experiments the cross sections, averaged over a Wigner-Wilkins spectrum for thermal neutrons, were taken from the compendium prepared by Amster.[3] For the computation of the paraffin-moderated experiments the cross sections as a function of energy below 0.625 eV were averaged over a measured spectrum obtained by Beyster[4] for a mixture in which the H:^{235}U atomic ratio was 195. The transport cross section of hydrogen, averaged over the measured spectrum, was obtained by the method of Radkowsky[5] which utilizes (1) a simple relation, due to Bethe,[6] between the measured scattering cross section and the "effective mass" of the bound hydrogen and (2) measurements by Melkonian[7] of the scattering cross section of hydrogen bound in hydrocarbons.

A variety of critical assemblies have been calculated by the O5R Monte Carlo code utilizing the values of the cross sections described above. Included were a single cylindrical and spherical volume of an aqueous solution of $U(5)O_2F_2$ (Sect. 2.1), arrays of seven and nine cylindrical units of this same solution,[8] and parallelepipeds of a mixture of $U(2)F_4$ and paraffin at two concentrations.[9]

The computed values of k_{eff} for the $U(5)O_2F_2$ solution were, on the average, lower than experimental values by about 1%; those computed for the $U(2)F_4$-paraffin assemblies were low by about $3\frac{1}{2}$%. Inadequacies in the data for the fluorine cross sections necessitating neglect of inelastic scattering and the assumption of isotropic elastic scattering are believed to be the principal causes of the discrepancies in the values of k_{eff}.

The times for the computations on the CDC 1604-A computer ranged between 118 and 204 min for 6000 neutron batches. These times are rather long, partly because no special effort was made to minimize them other than by the various reduction techniques of (1) not letting neutrons be absorbed but simply reducing their weight and (2) playing Russian roulette with neutrons of weight less than 0.2 and boosting to 0.4 the weight of those surviving. By use of the IBM 360 computer and by further attempts at variance reduction, these times may be reduced by an order of magnitude.

References

[1]R. G. Freemantle, *The Reactions of Neutrons with U^{235} – An Interim Revision of the File in the UK Nuclear Data Library,* AEEW-M502 (May 1965).

[2]J. T. Mihalczo, personal communication, 1966.

[3]H. J. Amster, *A Compendium of Thermal Neutron Cross Sections Averaged over the Spectrum of Wigner and Wilkins*, WAPD-185 (January 1958).

[4]J. R. Beyster *et al.*, "Integral Neutron Thermalization," *Quarterly Progress Report for Period Ending December 31, 1963*, GA-4881 (1964).

[5]A. Wattenberg *et al.*, pp. 95–96 in *Report for April, May, and June 1950, Physics Division of Argonne National Laboratory*, ANL-4476 (1950).

[6]H. A. Bethe, *Rev. Mod. Phys.* **9**, 122 (1937).

[7]E. Melkonian, *Phys. Rev.* **76**, 1750–59 (1949).

[8]E. B. Johnson and D. F. Cronin, *Neutron Phys. Div. Ann. Progr. Rept. Aug. 1, 1964*, ORNL-3714, p. 31; E. B. Johnson and D. F. Cronin, *Trans. Am. Nucl. Soc.* **7**, 301 (1964).

[9]J. T. Mihalczo, *Trans. Am. Nucl. Soc.* **3**, 74 (1960); J. T. Mihalczo and V. I. Neeley, *Nucl. Sci. Eng.* **13**, 6 (1962).

2.4 ROSSI-α MEASUREMENTS IN SUBCRITICAL URANIUM METAL CYLINDERS[1]

J. T. Mihalczo

Prompt-neutron decay constants were measured by the Rossi-α technique[2] in subcritical 7-, 11-, and 15-in.-diam cylinders of enriched uranium metal (93.15% ^{235}U) of heights varying in $\frac{1}{8}$-in. decrements from slightly subcritical to half critical. Using the measured values of β/l for delayed critical cylinders[3] of the same diameter and calculated changes in β/l due to the decrease in height, multiplication factors were obtained.

Two detectors were used in these measurements, and the time distribution of pulses from detector B relative to a pulse from detector A was observed. A PDP-4 digital computer processed binary information from a timing device which measured intervals down to 5 nsec. The probability of a fission-chain correlated event in detector B at a time Δt after an event in detector A is exp $(-\alpha\Delta t)$, since the probability that a prompt neutron exists in the assembly is also exponential (α is the prompt-neutron decay constant). The pulses from detector B were delayed with respect to those from detector A so that events occurring in detector B prior to those occurring in detector A could also be measured. These events in detector B have the distribution exp $(+\alpha\Delta t)$.

The generators of the fission chains in subcritical assemblies are external source neutrons, whereas in delayed-critical assemblies they are delayed neutrons emitted in the fundamental mode. Although there was concern with the establishment of a fundamental mode in the subcritical measurements, Monte Carlo calculations showed that the spatial distribution converges to within a few percent in about three generations, which in this case is less than 20 nsec.

A set of Rossi-α data for an 11-in.-diam 2.125-in.-high subcritical cylinder is shown in Fig. 2.4.1 and is representative of all the results from about 25 cylinders studied. A least-squares fit of the data to the function $A(\exp \pm \alpha\Delta t) + B$ by an IBM 7090 gave the same value of α for both exponentials. The expected symmetrical distribution was observed. The reactivity of this cylinder as obtained from the expression $\alpha l/\beta = \rho - 1$ was

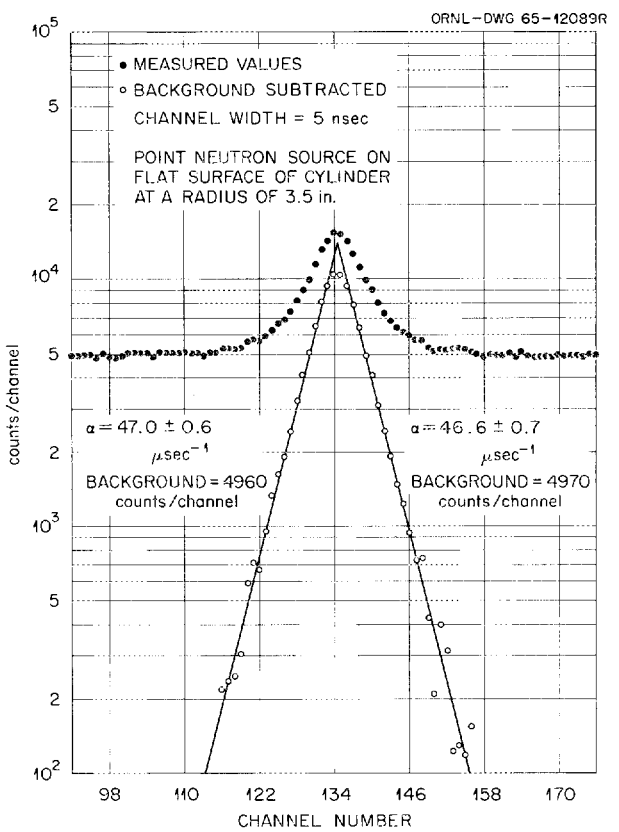

Fig. 2.4.1. Time Distribution of Fission Events in Rossi-α Measurements in 11-in.-diam, 2.125-in.-thick Uranium Metal Cylinder.

–33 dollars. The measured delayed-critical value, β/l, in a cylinder of the same diameter was reduced 26.6% by Monte Carlo calculations for the change in neutron lifetime with height. The multiplication factor, based on $\beta = 0.0068$, was 0.785, which compares very well with 0.777 ± 0.005 computed directly by a Monte Carlo method.[4]

References

[1]Summary of paper presented at the American Nuclear Society Twelfth Annual Meeting, Denver, Colo., June 20–23, 1966; to be published in *Trans. Am. Nucl. Soc.* **9**, No. 1 (1966).

[2]J. D. Orndoff, *Nucl. Sci. Eng.* **2**, 450 (1957).

[3]J. T. Mihalczo, *Nucl. Sci. Eng.* **20**, 60 (1964).

[4]D. C. Irving *et al.*, *O5R, A General Purpose Monte Carlo Neutron Transport Code*, ORNL-3622 (1965).

2.5 SENSITIVITY OF NEUTRON-SPECTRUM-DEPENDENT QUANTITIES IN URANIUM (93.2% ^{235}U) METAL ASSEMBLIES TO INELASTIC SCATTERING MODELS FOR ^{235}U

J. T. Mihalczo

The existing discrepancy between the measured and the calculated neutron lifetime in fast critical assemblies has motivated a study of the sensitivity of this and other quantities dependent on the neutron energy spectrum to the inelastic scattering properties of ^{235}U. The energy distributions of neutrons after one, two, and three successive inelastic collisions with the ^{235}U nucleus were determined by using the evaporation model at all energies and by using a combination of the evaporation model and the level excitation model. In one variation of the latter, the calculated cross sections of Yiftah, Okrent, and Moldauer[1] were used in the excitation level model up to 2.3 MeV; in another variation the cross sections of Parker[2] were used in level excitation up to 2.0 MeV. The evaporation model was used for higher energies in both cases. The source neutrons for these scattering studies were assumed to have a Maxwellian spectrum with a mean temperature corresponding to that resulting from fissions produced by neutrons having an energy of 1 MeV. The results of these three calculations are summarized in Table 2.5.1.

The effects of these variations on a number of characteristics of the Godiva I critical assembly were calculated by a Monte Carlo code and are summarized in Table 2.5.2. The effect of a 30% decrease in the nuclear temperature used in the evaporation model was also investigated. The results are expressed as differences, in percent, between the values obtained from using the evaporation model at all energies at the higher temperature and the values obtained by each of the other variations.

Table 2.5.1. Average Energy of Neutrons Inelastically Scattered from ^{235}U

Method	Energy (MeV)			Energy of Source Neutrons (MeV)
	After First Collision	After Second[a] Collision	After Third[a] Collision	
Evaporation model at all energies	0.461	0.184	0.089	1.975
Level excitation model with cross sections of ref. 1 below 2.3 MeV; evaporation model above	0.689	0.486	0.357	1.968
Level excitation model with cross sections of ref. 2 below 2.0 MeV; evaporation model above	1.418	1.068	0.810	1.964

[a]The values here refer to the distribution after two or three successive inelastic collisions.

Table 2.5.2. Sensitivity of Neutron-Spectrum-Dependent Quantities in Godiva I to Inelastic Scattering Models for ^{235}U

Quantity	Percentage Change from Value Calculated by the Evaporation Model[a]		
	Reference 1 Cross Sections[b]	Reference 2 Cross Sections[b]	Evaporation Theory with Temperature Reduced 30%
Time to loss by absorption and leakage	−5.7	−10.2	+6.7
Time to loss minus escape flight time	−7.4	−12.3	+8.2
Generation time	−9.0	−13.6	+10.6
Number of collisions before loss	−1.9	−4.2	+1.8
Average energy of neutrons in core	+7.9	+12.2	−14.0
Average energy of the leakage flux distribution	+1.4	0.3	~0
Multiplication factor	−0.13	−1.8	+0.7
Central spectral indices			
$\sigma_f(^{235}U)/\sigma_f(^{238}U)$	−4.3	−2.7	
$\sigma_f(^{237}Np)/\sigma_f(^{238}U)$	+3.0	+8.3	
Probability of leakage of fission neutrons	+2.8	+2.4	−0.9

[a]The nuclear temperature of ^{235}U in the evaporation model was 0.36 MeV.
[b]The calculational methods are described in the first column of Table 2.5.1.

References

[1]S. Yiftah, D. Okrent, and P. A. Moldauer, *Fast Reactor Cross Sections*, Pergamon Press, London, 1960.

[2]K. Parker, *Neutron Cross Sections of ^{235}U and ^{238}U in the Energy Range 1 keV to 15 MeV, Part I*, AWRE 0-82/63 (December 1963).

2.6 FLIGHT-TIME EFFECTS IN COUPLED SUBCRITICAL URANIUM METAL CYLINDERS

J. T. Mihalczo

The time dependence of fission events in a subcritical assembly consisting of two coaxial 11-in.-diam uranium (93.2 wt % ^{235}U; ρ = 18.7 g/cm^3) metal cylinders 2.625 in. thick separated by 14.55 in. has been measured by the Rossi-α technique.[1] Neutrons with 1-MeV energy can travel across the air gap between the flat faces in 52 nsec. The inverse of this transit time is comparable to the prompt-neutron decay constant, 25.7 μsec^{-1}, measured in a single isolated cylinder.

Variation of the location of the two detectors used in the Rossi-α measurements has resulted in the isolation of one of the components in the decay. With the two detectors sampling leakage neutrons from the same cylinder, two exponential decays, shown in Fig. 2.6.1, were observed, and with the detectors sampling leakage neutrons from different cylinders, only the slower of the two components was measured. A least-squares fit of the first set of data to the sum of a constant background and two exponential terms gave prompt-neutron decay constants of −15.5 ± 0.06 μsec^{-1} and −34.3 ± 2.9 μsec^{-1}. Fitting the second set of results to the sum of a constant background

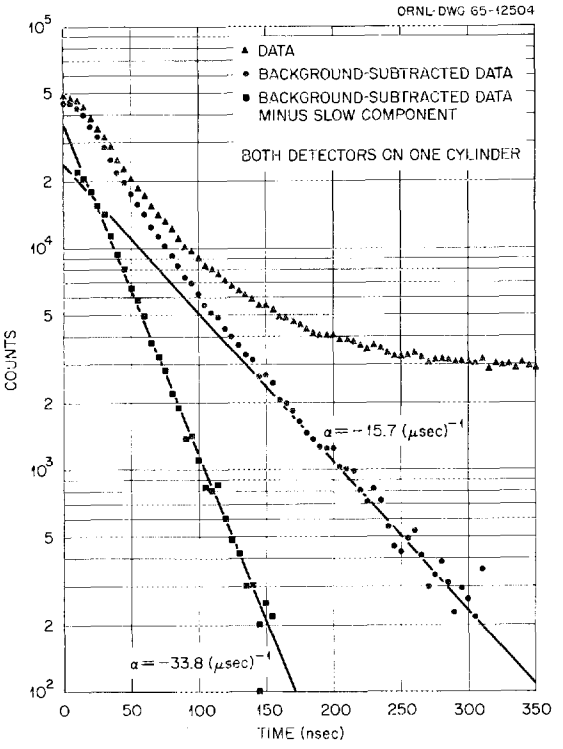

Fig. 2.6.1. Prompt-Neutron Decay in Two Coaxial 11-in.-diam 2.625-in.-thick Cylinders Spaced with 14.55 in. Between the Flat Surfaces.

and a single exponential gave a decay constant of $-15.7 \pm 0.09\ \mu\text{sec}^{-1}$. Analysis of the first set of data, assuming the slower decay constant to be $-15.7\ \mu\text{sec}^{-1}$, gave $-34.0 \pm 0.7\ \mu\text{sec}^{-1}$ for the faster decay.

The neutron kinetics in this coupled assembly are also described by two coupled equations representing the neutron population in each core, taking into account a flight time between cores. This is equivalent to the treatment of Kistner[2] for a reflected fast assembly except that it includes the effect of the flight time. The experimental results are fitted to the Rossi-α correlations computed by using the solutions of these two equations by nonlinear least-squares analysis techniques.

References

[1]J. Orndoff, *Nucl. Sci. Eng.* **2**, 450 (1957).
[2]G. Kistner, *Nukleonik* **7**, 106 (1964).

2.7 SORA CRITICAL EXPERIMENTS[1]

Gustav Kistner[2] J. T. Mihalczo

A program of critical experiments was performed at the ORNL Critical Experiments Facility in cooperation with Euratom, supporting the design of the Sorgente Rapida[3] (SORA). SORA is a fast, NaK-cooled, repetitively pulsed nuclear reactor which will be used as a source for neutron research.

The experiments were performed with a mockup which differs from SORA principally in the use of iron to represent NaK and of uranium instead of clad uranium-molybdenum alloy as fuel. Enriched uranium rods (93.2 wt % ^{235}U), 1.379 cm in diameter and 24 cm in length, closely fitted holes located on a triangular pattern (1.630-cm pitch) in an iron block. Of the 95 holes available, only about 85 contained uranium: the others contained iron. The core volume fractions were 0.649 U, 0.344 Fe, and 0.007 void. A 28-cm-thick iron reflector, containing six control rods and two 14.1-cm-diam scatterers made of polyethylene, iron, or beryllium (used to change the spectrum of the neutrons leaking out the horizontal beam holes), enclosed five sides of the hexagonal core. A movable reflector of various sizes and materials could be located adjacent to the sixth side. The arrangement is shown in Fig. 2.7.1.

The critical mass, the reactivity of the various parts, and the parameters relevant to the pulsed operation of the reactor are presented in Table 2.7.1.

The expected pulse width of SORA was calculated by using one-group space-independent neutron kinetics according to the method of Bondarenko and Stavisskii.[4] Assuming that the reactivity of the movable reflector as a function of time is parabolic in the prompt-critical region, the half-width θ is

$$\theta = \frac{1.67}{\sqrt[4]{\alpha_x(\alpha_1 v)^2\ \epsilon}}\ ,$$

where α_x and α_1 are defined in Table 2.7.1, v is the speed of the movable reflector, and ϵ is the reactivity above prompt critical which satisfies the condition[2] that the pulse characteristics and the mean power remain constant in time; ϵ is a function of α_1, α_x, v, and the pulse repetition

ORNL-DWG 66-3241

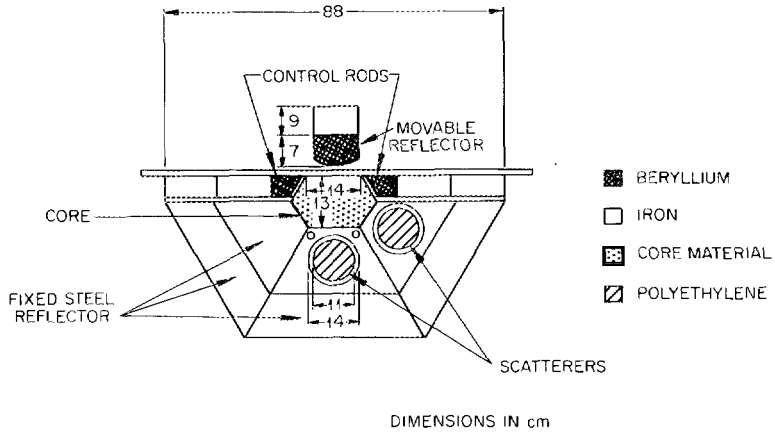

Fig. 2.7.1. Horizontal Cross Section of SORA Critical Experiment Mockup.

Table 2.7.1. Results of SORA Mockup Critical Experiments

Movable reflector[a]						
Material	Beryllium			Iron[b]		
Width (cm)	11	16	21	11	16	21
Reactivity (dollars)	6.2	9.1	11.2	3.7	5.2	6.5
α_x (cents/cm^2)[c]	8.6	9.5	9.9	5.3	4.2	4.0
Fast component,[d] α_1, of prompt-neutron decay constant (μsec^{-1})	0.32	0.34	0.30	0.55	0.48	0.49
Mass of uranium loading (kg)	57.2	54.0	51.2	57.7	56.4	55.2
Experimental multiplication factor[e]	1.0010	1.0005	1.0007	1.0013	1.0007	1.0004
Predicted neutron pulse half-width,[f] θ (μsec)	61	58	50	52	60	60

[a]The height and thickness of the movable reflector were fixed at 24 and 7 cm respectively.

[b]For these experiments the polyethylene scatterers and the beryllium control rods were replaced by iron.

[c]α_x is a measure of the shape of the reactivity-displacement curve for the movable reflector and equals $[\rho(0) - \rho(x)]/x^2$, where $\rho(x)$ is the reactivity as a function of the linear displacement x from the position of maximum reactivity.

[d]The slow component has not been measured precisely.

[e]Based on $\beta_{eff} = 0.00645$.

[f]These values assume a pulse repetition rate of 100 sec^{-1} and a reflector speed of 2.83×10^4 cm/sec.

rate. Values of θ, derived from α_x and α_1 measured in these experiments and other design parameters, appear in Table 2.7.1. The results substantiate the nuclear design of SORA and show that a movable reflector of either beryllium or iron will produce satisfactory neutron pulses.

References

[1]Summary of paper presented at American Nuclear Society Twelfth Annual Meeting, Denver, Colo., June 20–23, 1966; to be published in *Trans. Am. Nucl. Soc.* **9** (1966).

[2]On assignment to ORNL from Euratom, Ispra, Italy.

[3]V. Raievski, p. 553 in *Proceedings of a Symposium on Pulsed Neutron Research, Karlsruhe, May 10, 1965,* vol. II, International Atomic Energy Agency, Vienna, 1965.

[4]I. I. Bondarenko and Yu. Ya. Stavisskii, *Reactor Sci. Technol.* **14**, 55–58 (1961).

2.8 METHOD FOR ESTIMATING CRITICAL CONDITIONS OF LARGE ARRAYS OF URANIUM

J. T. Thomas

In view of the large safety factors presently used in the specification of storage and transport of fissile materials, it seems reasonable that knowledge to within 5% of the number of units required to be critical at a given spacing would be a satisfactory basis for nuclear safety evaluations. Experimental data from critical arrays of enriched uranium metal cylinders of various sizes and shapes are correlated by a neutron nonleakage parameter $(1 + NB_N^2)^{-1}$, which leads to

$$NB_N^2 = \text{constant} . \tag{1}$$

Here N is the total number of units in a cuboidal array, and B_N^2 is defined as

$$B_N^2 = \sum_{i=1}^{3} \frac{\pi^2}{[n_i(d_i + \delta) + 2\lambda]^2} ,$$

where

n_i = number of units along ith edge,

d_i = dimension of unit in direction of i,

δ = unit surface separation,

λ = a suitable extrapolation distance, determined empirically.

Multiplication factors for several arrays whose critical spacings were determined by Eq. (1) were computed by a Monte Carlo code (the GEM-3 code)[1] that had been used successfully to calculate multiplication factors for five critical experiments[2] performed with various units. The results

Table 2.8.1. Unreflected Critical Arrays of Enriched Uranium Metal Cylinders and Computed Multiplication Factors

Unit[a]	Mass (kg)	Diameter (cm)	Height-to-Diameter Ratio	n_1	n_2	n_3	Surface Separation (cm)	Calculated k_{eff}
A[6]	10.434	11.481	0.47	4	4	4	3.952	0.9937
A[4]	10.489	9.116	0.95	3	3	3	2.436	0.9919
B	15.683	11.490	0.70	3	3	3	4.204	0.9836
C	20.877	11.484	0.94	3	3	3	6.363	0.9961
D	26.113	11.486	1.17	3	3	3	8.494	0.9955

[a]The entries in this column identify the types of units, which are described in detail in ref. 1; each unit consists of U(93.2) metal at a density of 18.76 g/cm^3.

Table 2.8.2. Multiplication Factors from Monte Carlo Calculations of Arrays of Uranium Metal Cylinders

Unit[a]	64 Units		216 Units		512 Units		1000 Units	
	δ^b (cm)	k_{eff}	δ (cm)	k_{eff}	δ (cm)	k_{eff}	δ (cm)	k_{eff}
A^6	3.952	0.9937	7.060	0.9875	9.619	0.9978	11.852	0.9916
A^4	4.625	1.0006	8.118	0.9766	10.973	1.0074	13.451	0.9758
B	6.816	0.9983	11.032	1.0084	14.504	1.0004	17.531	1.0202
C	9.601	1.0046	14.818	0.9937	19.107	1.0023	22.841	0.9914
D	12.363	1.0022	18.567	0.9982	23.653	0.9853	28.074	0.9800

[a]The entries in this column identify the types of units, which are described in detail in ref. 1.
[b]Values of the surface separation of the units in the critical arrays were determined with Eq. (1).

of the experiments and the corresponding calculated multiplication factors are given in Table 2.8.1. Table 2.8.2 summarizes typical results for the arrays, all of which had large values of N. The similarity of the multiplication factors for the arrays to those calculated for the experiments may be regarded as a credible evaluation of the applicability of Eq. (1) to large arrays of units.

References

[1]Furnished by the United Kingdom Atomic Energy Authority, Health and Safety Branch.

[2]J. T. Thomas, *Critical Three-Dimensional Arrays of Neutron-Interacting Units, Part II. U(93.2) Metal*, ORNL-TM-868 (July 1964); H. C. Paxton *et al.*, *Critical Dimensions of Systems Containing U^{235}, Pu^{239}, and U^{233}*, TID-7028, p. 132 (June 1964).

2.9 CRITICALITY OF LATTICES OF HEAT TRANSFER REACTOR EXPERIMENT FUEL ELEMENTS

E. B. Johnson R. K. Reedy

A series of experiments has been completed to determine the critical parameters of lattices of Heat Transfer Reactor Experiment (HTRE) fuel elements, primarily in geometries and environments of interest for transport, storage, and chemical dissolution. The variety of critical lattices was limited by the small number of elements available.

These elements are of three types, as shown in Table 2.9.1. They consist of thin concentric annular fuel plates clad with Nichrome; each plate is slightly more than 1 in. long and adjacent clusters are spaced 0.125 in. The core material is a UO_2-Nichrome cermet containing uranium enriched to 93.2% in ^{235}U.

Arrays of these elements were made critical with water and with dilute aqueous $U(92.6)O_2(NO_3)_2$ solution of two concentrations (to simulate dissolver environments) as moderator and reflector; one solution concentration was 3.97 g of ^{235}U per liter and the other was 8.02 g of ^{235}U per liter. In some of the slab lattices in water, sheets of cadmium were placed between rows to serve as a neutron absorber as they might in a shipping container.

Typical of the results obtained in the three liquids which served as moderator and reflector were those with a lattice of nine of the elements, containing 1036 g of ^{235}U each, arranged in a square pattern; in water the critical surface separation of the elements was 1.15 in., in the solution containing about 4 g of ^{235}U per liter it was 1.70 in., and in the solution containing about 8 g of ^{235}U per liter it was 2.85 in.

A linear array of 26 elements (15 elements containing 1036 g of ^{235}U, 8 containing 1198 g, and

Table 2.9.1. Dimensions of the HTRE Fuel Elements

Mass of ^{235}U (g)	Overall Length (in.)	Maximum Fuel Plate Diameter (in.)	Length of Fuel Plate (in.)	Number of Annular Fuel Plates per Section[a]	Number of Elements Available
1198.0	30.750	2.690	1.615	12	8
1036.4	29.125	3.432	1.530	14	15
781.8	29.125	2.460	1.530	10	8

[a]The longitudinal separation of clusters of concentric annular plates was 0.125 in.; the radial separation of adjacent plates within a cluster was not uniform, even within an element of a particular type, but ranged between about 0.115 and 0.200 in. The thickness of the plates ranged from 0.013 to 0.027 in.

3 containing 782 g) was subcritical in water, and a line of six of the 1036.4-g elements (as many as could be installed in the smaller tank used for the solution experiments) was also subcritical at the lower solution concentration; however, five of the latter elements in line in the more concentrated solution were subcritical by only 8 cents.

Three rows of elements in slab geometry were made critical in water with a surface spacing of 3.25 in. between the rows and with the elements within a row in contact; this lattice consisted of two rows each of seven of the 1036-g elements with a row of eight of the 1198-g elements between. The critical separation of the rows when sheets of 30-mil-thick cadmium were centered between them was 1.5 in.

2.10 EXPERIMENTAL DETERMINATION OF SAFE HANDLING PROCEDURES FOR HIGH FLUX ISOTOPE REACTOR FUEL ELEMENTS OUTSIDE THE REACTOR[1]

S. J. Raffety J. T. Thomas

A series of experiments has been performed with the fuel element fabricated for the third High Flux Isotope Reactor Critical Experiment (HFIRCE-3) to establish safe conditions for the routine handling, shipping, and storage of HFIR fuel outside the reactor. The negative reactivity, or the shutdown margin, of the HFIRCE-3 fuel element when submerged in an effectively infinite water reflector was found to be 1.15 ±0.09 dollars. The shutdown margin with a storage post in the target region was 8.57 ± 0.32 dollars, and the shutdown margin with a 0.026-in.-thick cadmium sheet wrapped around the element leaving a ⅛-in. water gap was about 17 dollars. The effect of displacing water from the target region was studied by placing Styrofoam cylinders in the submerged element. It was found, for example, that the submerged HFIRCE-3 element would be critical if 15% of the water was displaced from the target region and that the maximum increase in reactivity, about 4 dollars, would be produced by displacing approximately 69% of the water from the target region. Displacing water inside the storage post reduced the shutdown margin of this system to a minimum of 3 dollars when all the water had been displaced from the post. The negative reactivity value of various stainless steel strips, with and without boron, which could be inserted between the fuel plates of the element was determined and is reported in tabular and graphical form. The effect of steel or combinations of steel and lead or steel and concrete as reflectors displacing water adjacent to the submerged element was also studied. Reflectors of steel or lead less than 3.5 in. thick reduced the reactivity of the system, but greater thicknesses increased the reactivity, with lead producing the greater increase. The HFIRCE-2 fuel element was used with the HFIRCE-3 element to study the interaction of two submerged elements in close proximity. The interaction was found to be very small if the elements were separated by 6 in. or more, but was quite important if the separation was less than 4 in. For example, with the axes of the two

elements in the same plane, with a surface-to-surface separation of 1 in., and with storage posts in both target regions, the two-element system was critical with a water height which produced only a 2.49-in. top reflector.

References

[1]Abstract of ORNL-TM-1488 (in publication).

2.11 S_n CALCULATIONS OF THE ABERDEEN PULSE REACTOR

J. T. Mihalczo

Some of the characteristics of the Aberdeen Pulse Reactor[1] (APR) have been estimated by S_n transport theory calculations.[2] These characteristics include the critical geometry, the peak-to-average power density ratio, and various reactivity effects. The APR is similar to the Health Physics Research Reactor,[3] modified to include a 2.16-in.-diam axial irradiation cavity. The diameter of the APR is greater, 8.90 vs 8.00 in.; the height is less, 8.08 vs 9.05 in.; and the safety block is longer, extending the full length of the core.

The calculations employed the six-group cross sections of Hansen and Roach[4] for ^{235}U, ^{238}U, iron, nickel, and molybdenum and employed those of Connolly[5] for chromium. The method was verified by the satisfactory calculation of some critical cylinders[6] of U-Mo alloy of the same composition. In the cylindrically symmetric geometry used to mock up the APR in these calculations, the structural material near the core was taken into account. The results of the calculations are given in Table 2.11.1.

Table 2.11.1. Calculated Properties of the Aberdeen Pulse Reactor[a]

Multiplication constant with all rods inserted	1.015
Overall dimensions, in.	
Diameter	8.90
Height	8.08
Worth of irradiation cavity insert (Δk)	0.00568
Peak-to-average power density ratio	1.95
Δk per cm change in height	0.014
Δk per percent change in density of U-Mo	0.0048

[a]The reactor core is a uranium-molybdenum alloy containing 10% Mo, with the uranium enriched in ^{235}U to 93.2 wt %.

References

[1]J. R. Tomlinson *et al.*, *Preliminary Safeguards Report for the Aberdeen Pulsed Reactor Facility*, BRL-1255 (September 1964).

[2]C. E. Lee, *The Discrete S_n Approximation to Transport Theory*, LA-2595 (June 1961).

[3]M. I. Lundin, *Health Physics Research Reactor Hazards Summary*, ORNL-3248 (August 1962).

[4]G. E. Hansen and W. H. Roach, *Six and Sixteen Group Cross Sections for Fast and Intermediate Critical Assemblies*, LAMS-2543 (1961).

[5]L. Connolly, *Los Alamos Group Averaged Cross Sections*, LA-2941, p. 45 (September 1963).

[6]W. E. Kinney and J. T. Mihalczo, *ORNL Fast Burst Reactor: Critical Experiments and Calculations*, ORNL-CF-61-8-71 (August 1961).

3. Reactor and Weapons Shielding

3.1 MEASUREMENTS AND SINGLE-VELOCITY CALCULATIONS OF DIFFERENTIAL ANGULAR THERMAL-NEUTRON ALBEDOS FOR CONCRETE[1]

R. E. Maerker F. J. Muckenthaler

Single-velocity Monte Carlo calculations and measurements have been performed to determine the differential angular thermal-neutron albedos for a reinforced concrete from monodirectional beams of incident thermal neutrons. Preliminary calculations using a statistical estimation technique indicate that up to 50 scatterings should be followed for each neutron in order to produce good estimates of the differential albedos, and up to 100 scatterings to produce good estimates of the capture gamma-ray differential dose albedos. Deviation between experiment and calculation can be reduced to an average of 5.1% for 72 points of comparison if an anisotropic scattering law for water deduced from earlier Argonne National Laboratory measurements is assumed.

References

[1]Abstract of paper submitted to *Nuclear Science and Engineering*.

3.2 MEASUREMENT OF REFLECTED THERMAL-NEUTRON FLUX DUE TO MONODIRECTIONAL EPICADMIUM NEUTRONS INCIDENT ON CONCRETE[1]

F. J. Muckenthaler J. J. Manning
J. L. Hull K. M. Henry

An experimental program was performed at the Tower Shielding Facility concurrently with a Monte Carlo calculation to measure, as a function of the angles of incidence and emergence, contributions made by incident subcadmium neutrons and epicadmium neutrons to the thermal-neutron flux that is scattered from a concrete slab. The reflected flux due to incident thermal neutrons, reported previously,[2] was obtained through a subtraction process involving 16 different measurements at each of 72 combinations of the angle of incidence and the polar and azimuthal angles of reflection. The contribution from incident epicadmium neutrons was determined in the same subtraction process using only eight of the measurements. These were cadmium-covered and bare-detector readings for both foreground and background measurements for the cases of cadmium over the reactor collimator and cadmium over the reactor collimator and concrete slab. (The background measurements were made with the slab rotated so that the horizontal center line of the front face of the slab was coincident with the line-of-sight of the detector.)

A tightly collimated beam of neutrons was obtained for this experiment by placing a 92-in.-thick water shield adjacent to the 15-in.-diam beam port of the Tower Shielding Reactor II beam shield. This additional shielding contained a stepped collimator, with the neutron beam emerging through a hole $2\frac{3}{4}$ in. in diameter and 36 in. long. The beam collimator contained a cadmium sleeve that extended 12 in. outward from the shield toward the slab to further reduce the spread in the thermal-neutron beam at the concrete slab. A concrete slab, 6 ft square and 9 in. thick and located 8 ft from the end of the collimator, was attached to a turntable that rotated the slab about both its vertical and horizontal axis. The pivot point was located in the middle of the surface of the slab upon which the neutrons were incident.

Thermal-neutron fluxes and fast-neutron dose rates (with the cadmium sleeve removed) were

Table 3.2.1. Thermal-Neutron Fluxes Reflected from Concrete for Incident Epicadmium Neutrons

ϕ (deg)	θ (deg)	Thermal-Neutron Flux (neutrons cm^{-2} sec^{-1} W^{-1})
15	19.0	1.08×10^{-4}
	33.5	9.20×10^{-5}
	44.0	7.44×10^{-5}
	52.0	6.32×10^{-5}
	60.0	4.64×10^{-5}
	67.0	3.30×10^{-5}
	74.0	2.10×10^{-5}
	80.4	1.15×10^{-5}
	86.8	4.06×10^{-6}
45	80.4	1.31×10^{-5}
	86.8	2.71×10^{-6}
135	19.0	1.06×10^{-4}
	33.5	8.99×10^{-5}
	44.0	7.31×10^{-5}
	52.0	5.98×10^{-5}
	60.0	4.47×10^{-5}
	67.0	3.26×10^{-5}
	74.0	2.05×10^{-5}
	80.4	1.16×10^{-5}
	86.8	3.52×10^{-6}

measured in a plane perpendicular to the axis of the beam collimator at the surface of the concrete slab. These results were integrated to obtain the total dose rate and thermal-neutron flux incident upon the slab. The fast-neutron spectrum from this reactor was determined earlier.[3]

The scattered thermal-neutron flux was measured by a BF_3 detector located in a water shield at a fixed distance of 31 ft from the center of the slab surface. The water shield contained a collimator that permitted the detector to see the whole slab when the slab was perpendicular to the detector shield. The detector shield moved through an arc in the horizontal plane that passed through the reactor beam center line while the slab was rotated about both its horizontal and vertical axis. This permitted the determination of scattered thermal-neutron fluxes for combinations of four angles of beam incidence (θ_0) and nine polar (θ) and six azimuthal (ϕ) angles of emergence.

Typical results are given in Table 3.2.1 for an incident angle of 60°.

References

[1]Work funded by Defense Atomic Support Agency under order EO-804-66.

[2]R. E. Maerker and F. J. Muckenthaler, *Neutron Phys. Div. Ann. Progr. Rept. Aug. 1, 1965*, ORNL-3858, vol. I, p. 29.

[3]M. S. Bokhari *et al.*, *Neutron Phys. Div. Ann. Progr. Rept. Aug. 1, 1963*, ORNL-3499, vol. I, p. 105.

3.3 CALCULATIONS OF THE DIFFERENTIAL ANGULAR ALBEDO OF SUBCADMIUM NEUTRONS ARISING FROM INCIDENT MONODIRECTIONAL BEAMS OF EPICADMIUM NEUTRONS ON CONCRETE: COMPARISON WITH EXPERIMENT[1]

R. E. Maerker

Calculations of doubly differential angular and energy current albedos, $d\alpha_{th}/d\Omega$, as functions of the incident energy group (ΔE_0) and the cosines of the incident and reflected polar angles (μ_0 and μ respectively) were reported previously[2] for monodirectional beams of epicadmium neutrons incident on concrete with energies up to 200 keV. (The angles are defined with respect to an inwardly drawn slab normal.) The results have since been extrapolated to 10 MeV, as shown in Table 3.3.1, and the calculated albedos have been compared with albedos obtained from a series of experiments performed at the Tower Shielding Facility and described in Sect. 3.2.

In the experiments, monodirectional neutrons were reflected from a 9-in.-thick concrete slab, and the contribution to the reflected subcadmium flux due to incident epicadmium neutrons was measured for various values of μ_0 and μ. In determining the experimental albedos, the absolute spectrum of neutrons incident on the slab was constructed as follows. Above 1 MeV the spectrum was assumed to be the same as that reported earlier for almost the same geometry,[3] and in the region from 200 keV to 1 MeV it was obtained by extrapolating the measurements above 1 MeV down to 200 keV. The spectrum in the region above 200 keV was then normalized to yield the measured fast-neutron dose rate incident upon the surface

Table 3.3.1. Curve-Fitted Values of Subcadmium Neutron Albedos Produced by Slowing Down of Incident Epicadmium Neutrons

ΔE_0	$d\alpha_{th}/d\Omega$ [(subcadmium neutrons) sr^{-1} (source neutron)$^{-1}$]	α_{th} (neutrons/source neutron)
2.64–9.57 MeV	$\lvert\mu\rvert(1 + 1.73\ \lvert\mu\rvert)(0.0024 + 0.0040\ \mu_0)$	$0.016 + 0.027\ \mu_0$
0.725–2.64 MeV	$\lvert\mu\rvert(1 + 1.73\ \lvert\mu\rvert)(0.0028 + 0.0044\ \mu_0)$ [a]	$0.019 + 0.030\ \mu_0$ [a]
200–725 keV	$\lvert\mu\rvert(1 + 1.73\ \lvert\mu\rvert)(0.0036 + 0.0049\ \mu_0)$	$0.024 + 0.033\ \mu_0$
55.1–200 keV	$\lvert\mu\rvert(1 + 1.73\ \lvert\mu\rvert)(0.0043 + 0.0058\ \mu_0)$	$0.029 + 0.039\ \mu_0$
15.2–55.1 keV	$\lvert\mu\rvert(1 + 1.73\ \lvert\mu\rvert)(0.0052 + 0.0059\ \mu_0)$	$0.035 + 0.040\ \mu_0$
4.2–15.2 keV	$\lvert\mu\rvert(1 + 1.73\ \lvert\mu\rvert)(0.0062 + 0.0071\ \mu_0)$	$0.042 + 0.048\ \mu_0$
1.15–4.2 keV	$\lvert\mu\rvert(1 + 1.73\ \lvert\mu\rvert)(0.0077 + 0.0073\ \mu_0)$	$0.052 + 0.049\ \mu_0$
0.32–1.15 keV	$\lvert\mu\rvert(1 + 1.73\ \lvert\mu\rvert)(0.0090 + 0.0099\ \mu_0)$	$0.061 + 0.067\ \mu_0$
0.087–0.32 keV	$\lvert\mu\rvert(1 + 1.73\ \lvert\mu\rvert)(0.011 + 0.012\ \mu_0)$	$0.074 + 0.081\ \mu_0$
24–87 eV	$\lvert\mu\rvert[(0.0185 + 0.0150\ \mu_0) + \lvert\mu\rvert(0.0177 + 0.0235\ \mu_0)]$	$0.095 + 0.096\ \mu_0$
6.6–24 eV	$\lvert\mu\rvert[(0.0332 + 0.0085\ \mu_0) + \lvert\mu\rvert(0.0220 + 0.0268\ \mu_0)]$	$0.150 + 0.084\ \mu_0$
1.8–6.6 eV	$\lvert\mu\rvert[\ 0.0595 + \lvert\mu\rvert(0.0290 + 0.0305\ \mu_0)]$	$0.248 + 0.064\ \mu_0$
0.5–1.8 eV	$\lvert\mu\rvert[(0.124 - 0.035\ \mu_0) + \lvert\mu\rvert(0.020 + 0.053\ \mu_0)]$	$0.431 + 0.001\ \mu_0$

[a]Extrapolated values.

Table 3.3.2. Comparison of Measured Spectrometer Responses with Calculated Responses[a]

Filter No.	Response (counts/30 sec/kW) Measured	Response (counts/30 sec/kW) Calculated	Filter No.	Response (counts/30 sec/kW) Measured	Response (counts/30 sec/kW) Calculated
0	1.96×10^5	2.19×10^5	12	2.65×10^2	2.72×10^2
1	3.16×10^3	3.05×10^3	13	2.29×10^2	2.20×10^2
2	2.32×10^3	2.40×10^3	14	1.98×10^2	1.76×10^2
3	1.45×10^3	1.60×10^3	15	1.60×10^2	1.47×10^2
4	1.17×10^3	1.27×10^3	16	1.26×10^2	1.13×10^2
5	9.75×10^2	1.15×10^3	17	1.20×10^2	9.5×10^1
6	8.7×10^2	9.8×10^2	18	9.5×10^1	7.0×10^1
7	7.4×10^2	7.9×10^2	19	7.5×10^1	4.9×10^1
8	5.65×10^2	6.0×10^2	20	4.2×10^1	2.9×10^1
9	4.85×10^2	5.0×10^2	21	3.5×10^1	1.9×10^1
10	4.2×10^2	3.9×10^2	22	2.4×10^1	7.6×10^0
11	3.35×10^2	3.36×10^2			

[a]The response of filter 23 has been subtracted from each of the measured and calculated values.

of the slab. From 10 to 200 keV the spectrum was assumed to be roughly $1/\sqrt{E}$, so that it joined smoothly with the normalized spectrum at 1 MeV.

In the region from 0.5 eV to 10 keV the spectrum was determined from measurements with a recently developed boron filter spectrometer.[4] Table 3.3.2 shows the agreement between the boron filter measurements at the point of intersection of the beam center line and the slab surface and the response as calculated by R. M. Freestone, Jr., assuming a subcadmium Maxwellian spectrum at a temperature of 336°K, a $1/E$ spectrum in the range 0.18 eV to 10 keV, and a $1/\sqrt{E}$ spectrum in the range 10 keV to 1 MeV. The counting efficiency of the spectrometer in this geometry was assumed to be 0.242 for 0.0253-eV neutrons, and the fluxes were normalized to the measured subcadmium flux and cadmium ratio.

The absolute incident neutron current spectrum integrated over the surface of the slab was thus deduced to be the one pictured in Fig. 3.3.1. The ratio of the surface-integrated value to the centerline value was 352 for neutrons above 200 keV, 216 for subcadmium neutrons, and 283 for neutrons in the epithermal range (i.e., between 0.5 eV and ~200 keV).

Taking the values of Table 3.3.1 (or, where possible, the actual Monte Carlo calculated values) for a given μ_0 and μ and weighting the contribution from each energy group by the fraction of the total number of epicadmium neutrons in that group incident upon the slab (numbers found by integrating the ordinates of Fig. 3.3.1 between appropriate limits) yielded values of the subcadmium differential angular albedos for the experimental epicadmium spectrum. Experimental values of this same quantity were obtained by multiplying the measured fluxes at a given μ_0, μ, and ϕ (conventional azimuth) by the quantity $(30.48R)^2\ e^{R/70}/\int\int J(E_0,A)\cdot d\bar{A}\ dE_0$, where R is the distance (in feet) from the detector to the geometric center of the slab surface (R has a constant value of 31 ft for all measured points), and the double integral represents the total number of epicadmium neutrons incident over the surface of the slab. Of the 34 common points of calculation and measurement, a disagreement of 23% and one of 36% represented the largest variance; the remaining 32 comparisons have a root-mean-square disagreement of 4.5%. In these comparisons, since no significant azimuthal variation of the subcadmium neutron differential albedo was measured, the average of the subcadmium differential albedos over all azimuths at which they were measured for a given μ_0 and μ was used to compare with the differential albedo from the azimuthally independent calculation. Typical results are shown in Table 3.3.3, in which a comparison of the measured and calculated subcadmium differential angular albedos is made for the case of $\mu_0 = 0.50$.

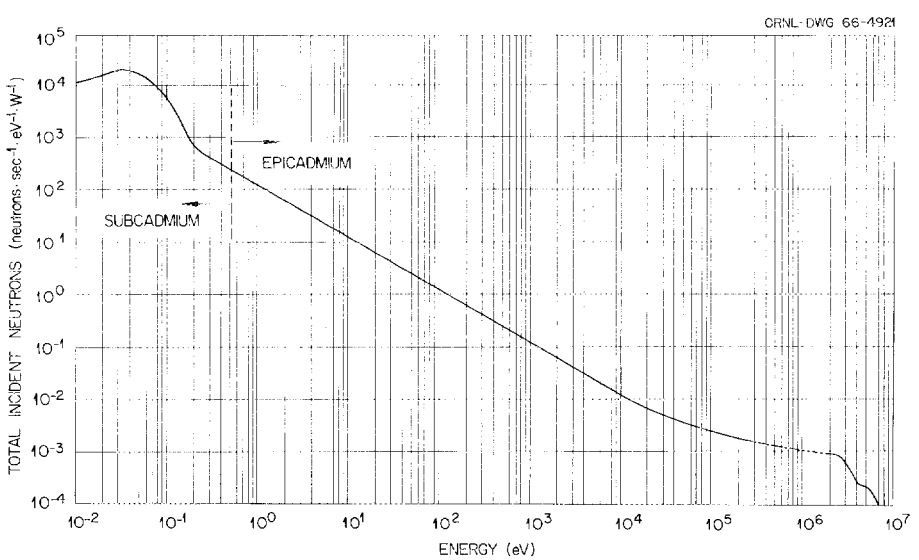

Fig. 3.3.1. Absolute Incident Spectrum of Neutrons on Concrete Slab Integrated over the Slab Surface. Slab was located at a distance of 8 ft from the outer edge of the reactor collimator.

Table 3.3.3. Comparison of Calculated and Measured Subcadmium Differential Angular Albedos Arising from the Epicadmium Spectrum of Fig. 3.3.1 Incident at 60° with Slab Normal

$\lvert\mu\rvert$	Albedos [subcadmium neutrons sr^{-1} (source neutron)$^{-1}$]		
	Measured; $\phi = 15°$	Measured; $\phi = 135°$	Calculated
0.944	2.43×10^{-2}	2.38×10^{-2}	2.47×10^{-2}
0.833	2.07×10^{-2}	2.02×10^{-2}	2.08×10^{-2}
0.722	1.67×10^{-2}	1.64×10^{-2}	1.71×10^{-2}
0.611	1.42×10^{-2}	1.34×10^{-2}	1.37×10^{-2}
0.5	1.04×10^{-2}	1.00×10^{-2}	1.05×10^{-2}
0.389	7.41×10^{-3}	7.32×10^{-3}	7.52×10^{-3}
0.278	4.72×10^{-3}	4.61×10^{-3}	4.91×10^{-3}
0.167	2.58×10^{-3}	2.60×10^{-3}	2.60×10^{-3}
0.0556	9.13×10^{-4}	7.91×10^{-4}	7.25×10^{-4}

References

[1]Summary of paper presented at the Twelfth Annual Meeting of the American Nuclear Society, June 20–23, Denver, Colo; abstract to be published in *Trans. Am. Nucl. Soc.* **9** (1966). Work funded by Defense Atomic Support Agency under order EO-804-66.

[2]R. E. Maerker, *Neutron Phys. Div. Ann. Progr. Rept. Aug. 1, 1965*, ORNL-3858, vol. 1, pp. 24–27.

[3]T. V. Blosser and R. M. Freestone, Jr., *Neutron Phys. Div. Ann. Progr. Rept. Aug. 1, 1965*, ORNL-3858, vol. I, p. 59.

[4]M. S. Bokhari *et al.*, *Neutron Phys. Div. Ann. Progr. Rept. Aug. 1, 1963*, ORNL-3499, vol. I, Fig. 3.3.5, p. 107.

3.4 MEASUREMENTS OF THE THERMAL-NEUTRON FLUX AND FAST-NEUTRON DOSE RATE DOWN A RECTANGULAR CONCRETE DUCT WITH ONE AND TWO BENDS[1]

F. J. Muckenthaler J. L. Hull
J. J. Manning K. M. Henry

Measurements of the thermal-neutron flux and fast-neutron dose rate transmitted through a straight duct with a 3-ft-square cross section were reported in the previous annual.[2,3] The work has since been extended to include measurements in the same duct containing one and two bends. The length of the duct between each bend was 15 ft, giving an L/W ratio of 5. The experimental procedure was the same as that described for the

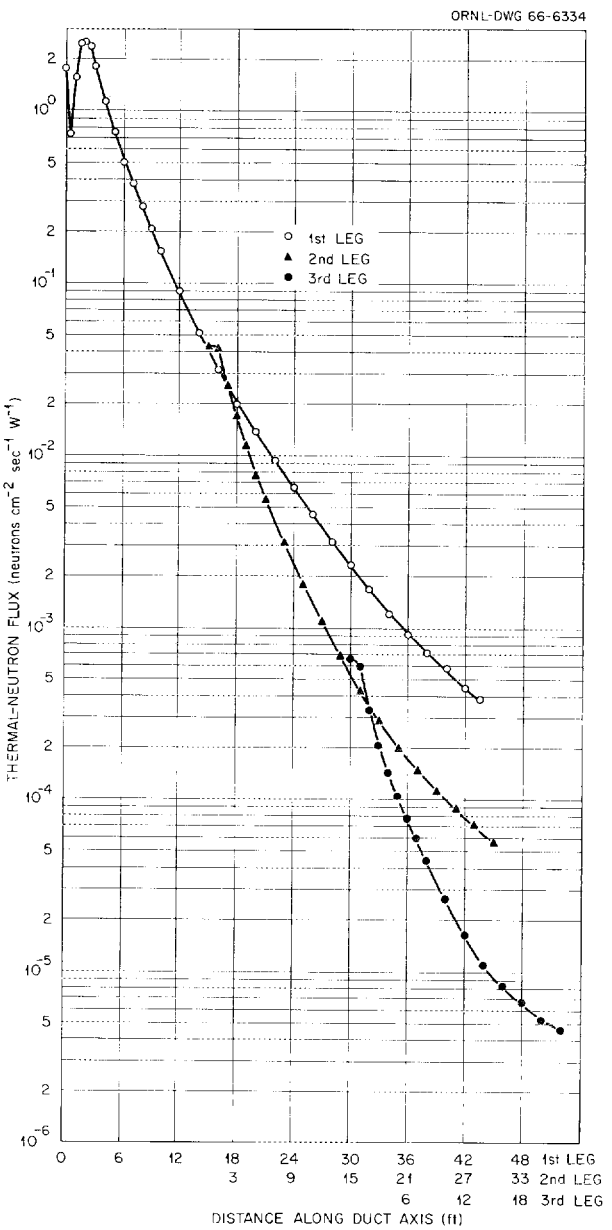

Fig. 3.4.1. Thermal-Neutron Fluxes Along Axes of One-, Two-, and Three-Legged Rectangular Concrete Ducts Due to Incident Thermal Neutrons.

straight-duct measurements, with the zero position in the second and third legs always measured at the point where the axis of the leg in which the measurements were being made intersected the axis of the preceding leg.

The results of the thermal flux measurements along the axes of three ducts having one, two, and three legs, respectively, are shown in Figs. 3.4.1 and 3.4.2. The contributions from thermal neutrons incident on the source wall are given in Fig. 3.4.1, and those from epicadmium neutrons are given in Fig. 3.4.2. The fast-neutron dose rate measurements, made with a Hurst-type dosimeter, are plotted in Fig. 3.4.3, which shows the reduction in the dose rate obtained by the introduction of a 90° bend in the duct. The measurements shown for the second leg of the duct were limited by insufficient neutron intensity.

A separate set of measurements was made with an isotropically sensitive fast-neutron dosimeter[4] designed to give a response proportional to the Snyder-Neufeld multicollision dose curve over an energy range from the epicadmium region to approximately 15 MeV. This dosimeter consists of

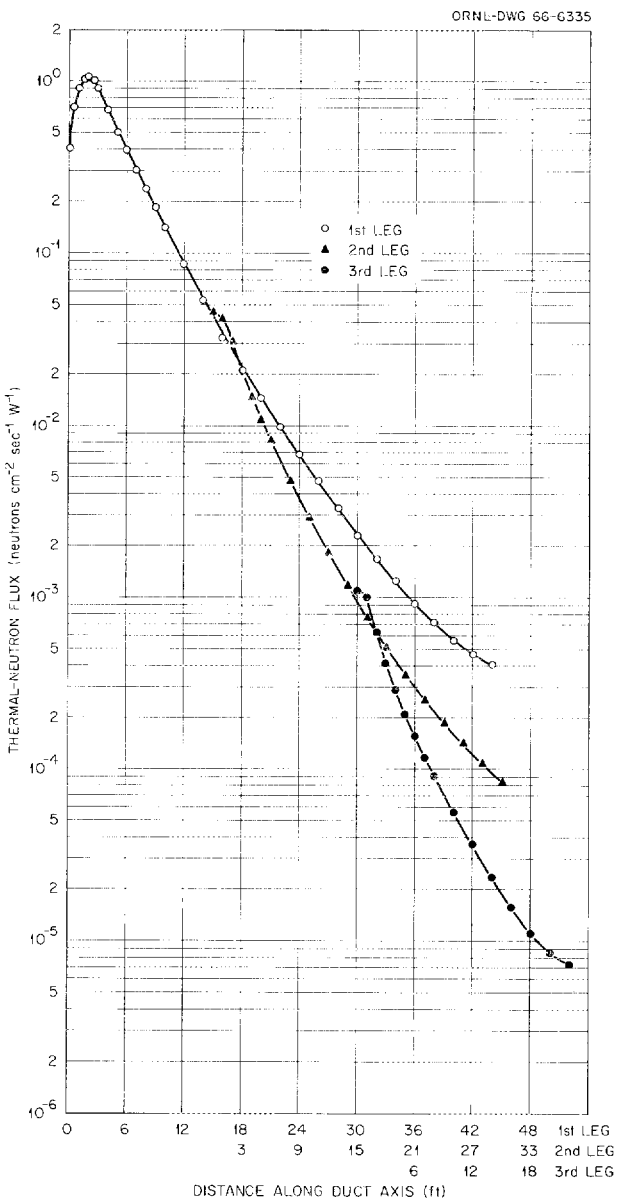

Fig. 3.4.2. Thermal-Neutron Fluxes Along Axes of One-, Two-, and Three-Legged Rectangular Concrete Ducts Due to Incident Epicadmium Neutrons.

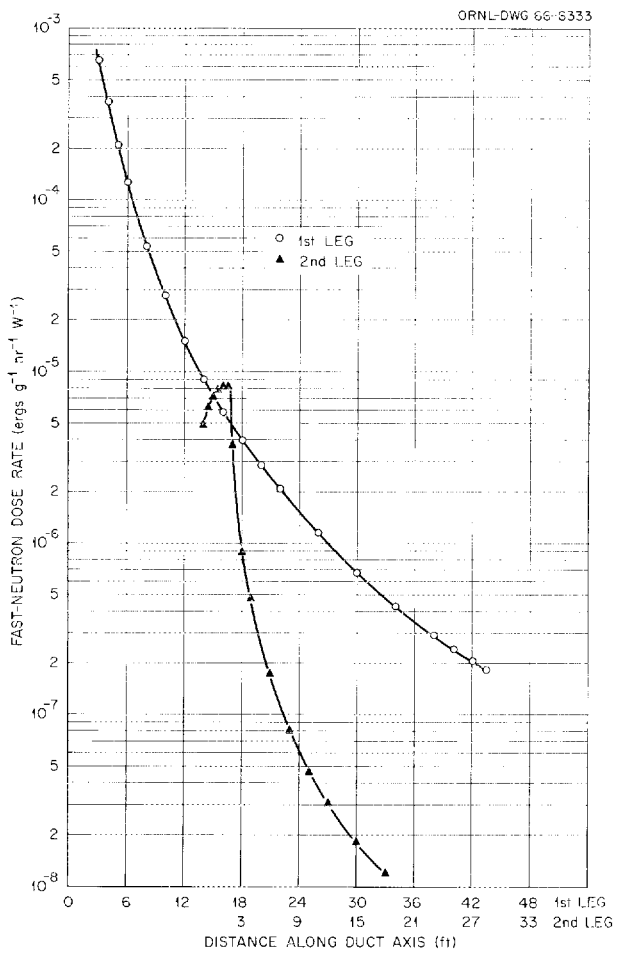

Fig. 3.4.3. Fast-Neutron Dose Rates in One- and Two-Legged Rectangular Concrete Ducts (Hurst Dosimeter Measurements).

Table 3.4.1. Multicollision Fast-Neutron Dose Rates Along the Axis of a Three-Legged Rectangular Concrete Duct

Detector Location (ft)	Dose Rate (ergs g^{-1} h^{-1} W^{-1})		
	8-in. Ball	10-in. Ball	12-in. Ball
First Leg			
0		8.30×10^{-3}	3.00×10^{-3}
1	3.25×10^{-3}	3.08×10^{-3}	1.73×10^{-3}
2	3.86×10^{-3}	2.41×10^{-3}	1.66×10^{-3}
3	2.51×10^{-3}	1.51×10^{-3}	1.01×10^{-3}
4	1.48×10^{-3}	8.88×10^{-4}	5.82×10^{-4}
5	9.15×10^{-4}	5.43×10^{-4}	3.59×10^{-4}
6	6.02×10^{-4}	3.55×10^{-4}	2.31×10^{-4}
7	4.06×10^{-4}	2.36×10^{-4}	1.56×10^{-4}
8	2.84×10^{-4}	1.63×10^{-4}	1.06×10^{-4}
9	2.04×10^{-4}	1.17×10^{-4}	7.70×10^{-5}
10	1.47×10^{-4}	8.53×10^{-5}	5.67×10^{-5}
11	1.10×10^{-4}	6.32×10^{-5}	4.19×10^{-5}
12	8.25×10^{-5}	4.74×10^{-5}	3.22×10^{-5}
13	6.32×10^{-5}	3.62×10^{-5}	2.48×10^{-5}
14	5.03×10^{-5}	2.86×10^{-5}	1.97×10^{-5}
15	4.16×10^{-5}	2.42×10^{-5}	1.65×10^{-5}
Second Leg			
0	4.64×10^{-5}	2.89×10^{-5}	1.93×10^{-5}
0.5	4.71×10^{-5}	2.99×10^{-5}	2.03×10^{-5}
1	4.55×10^{-5}	2.89×10^{-5}	1.93×10^{-5}
1.5	3.51×10^{-5}	1.90×10^{-5}	1.08×10^{-5}
2	1.48×10^{-5}	7.55×10^{-6}	4.15×10^{-6}
3	8.44×10^{-6}	4.12×10^{-6}	2.28×10^{-6}
Second Leg			
4	5.17×10^{-6}	2.49×10^{-6}	1.37×10^{-6}
5	3.32×10^{-6}	1.60×10^{-6}	8.47×10^{-7}
6	2.25×10^{-6}	1.10×10^{-6}	5.70×10^{-7}
7	1.59×10^{-6}	7.69×10^{-7}	3.98×10^{-7}
8	1.15×10^{-6}	5.49×10^{-7}	2.84×10^{-7}
9	8.68×10^{-7}	4.21×10^{-7}	2.16×10^{-7}
10	6.47×10^{-7}	3.10×10^{-7}	1.65×10^{-7}
11	5.00×10^{-7}	2.42×10^{-7}	1.26×10^{-7}
12	3.97×10^{-7}	1.91×10^{-7}	1.02×10^{-7}
13	3.27×10^{-7}	1.54×10^{-7}	8.07×10^{-8}
14	2.66×10^{-7}	1.28×10^{-7}	6.60×10^{-8}
15	2.29×10^{-7}	1.09×10^{-7}	5.74×10^{-8}
Third Leg			
0	2.17×10^{-7}	1.12×10^{-7}	5.75×10^{-8}
1	1.89×10^{-7}	8.45×10^{-8}	4.36×10^{-8}
1.5	1.12×10^{-7}	4.45×10^{-8}	1.99×10^{-8}
2	5.85×10^{-8}	2.44×10^{-8}	1.23×10^{-8}
4	2.21×10^{-8}	9.62×10^{-9}	3.70×10^{-9}
6	9.15×10^{-9}	3.86×10^{-9}	2.15×10^{-9}
8	6.46×10^{-9}	2.31×10^{-9}	8.15×10^{-10}
10	2.70×10^{-9}	1.08×10^{-9}	6.00×10^{-10}
12	1.47×10^{-9}	8.87×10^{-10}	4.44×10^{-10}
13.5	1.57×10^{-9}	6.04×10^{-10}	1.05×10^{-10}

a spherical BF_3 counter placed inside a polyethylene ball covered with cadmium. Preliminary studies indicated that the diameter of the polyethylene ball should be between 8 and 12 in. Since the development of the dosimeter was incomplete when the measurements were made, it was decided to make the duct measurements with three balls, 8, 10, and 12 in. in diameter, and then to interpolate between thicknesses as required to obtain the best approximation to the Snyder-Neufeld multicollision dose curve. The results are shown in Table 3.4.1.

The response of the balls to a known dose rate was determined with a calibrated Po-Be source. The center of detection for each ball (detector position) was considered to be a point on the surface of the ball nearest the zero position in the leg in which the measurements were being made. Thus measurements at the zero position along the axis of the second leg do not correspond to measurements at the 15-ft position in the first leg.

References

[1]Work funded by Defense Atomic Support Agency under order EO-804-66.

[2]F. J. Muckenthaler *et al.*, *Neutron Phys. Div. Ann. Progr. Rept. Aug. 1, 1965*, ORNL-3858, vol. I, p. 20.

[3]*Ibid.*, p. 21.

[4]T. V. Blosser, *Neutron Phys. Div. Ann. Progr. Rept. Aug. 1, 1965*, ORNL-3858, vol. I, p. 61.

3.5 CALCULATIONS OF THERMAL-NEUTRON-FLUX AND FAST-NEUTRON-DOSE DISTRIBUTIONS IN ONE-, TWO-, AND THREE-LEGGED RECTANGULAR CONCRETE DUCTS: COMPARISON WITH EXPERIMENT[1]

R. E. Maerker

Calculations of the thermal-neutron fluxes and fast-neutron dose rates in one-, two-, and three-legged concrete ducts having 90° bends have been performed with a modified version[2] of the flexible-geometry Monte Carlo duct code originated by Cain,[3] and the results have been compared with the data obtained in experiments performed at the Tower Shielding Facility (TSF) and described in Sect. 3.4. The modifications consisted primarily in the incorporation into the code of the doubly differential thermal-neutron flux and fast-neutron dose albedo data previously developed under this program.[4]

In the code the walls are assumed to be reflecting and absorbing surfaces which reflect the incident neutrons with reduced weight into various energy groups and directions, the probabilities for which are predetermined from the doubly differential albedo data. For each wall interaction, statistical estimates, based on the differential angular albedo data, are made of the fast-neutron dose rate or flux contribution to each of several detectors located within the duct. The neutrons are followed in a random-walk procedure down the duct until they either escape out the front or rear end of the duct or are killed by Russian roulette when their weight falls below a predetermined value.

For fast-neutron dose calculations the neutrons are killed after they suffer more than a predetermined number of scatterings in the lowest energy group (200 to 750 keV), and no biasing of the scattering probabilities is used; also, no histories are allowed for neutrons which penetrate a corner wall, although a statistical estimate based on wall penetration may be used if desired.

For single-velocity thermal-neutron calculations, biasing of the random-walk scattering probabilities may be used in order to force more neutrons deeper into the duct; the bias procedure employed in the code is not a strong one and simply amounts to sampling from an isotropic angular distribution for the postscattering direction. As with the fast neutrons, however, no history of a neutron which penetrates a corner wall during the course of its random walk is allowed, although a statistical estimate based on wall penetration may be made.

In calculations of the slowing down of epicadmium neutrons to thermal energies, the manner in which the code traces an individual history is similar to its treatment of incident thermal neutrons with two exceptions. First, the energy of the neutron is, of course, kept track of in the random walk; second, when the energy falls below 0.5 eV, the random walk samples from the thermal-neutron distribution. An option in the code also permits a calculation of the slowing-down spectrum described by absolute fluxes in each of 13 energy groups between 0.5 eV and 8 MeV at several detector locations. Secondary capture gamma-ray dose rates may also be calculated, the differential dose albedo data being taken from previously reported values.[5]

The calculations were carried out for three 3- by 3-ft-square duct configurations for which measurements were made at the TSF (see Sect. 3.4). They include (1) a straight duct 45 ft long, (2) a two-legged duct with a right-angle bend located 15 ft down the first leg, the second leg being 30 ft in length, and (3) a three-legged duct with two right-angle bends, one located 15 ft down the first leg and the second 15 ft down the second leg, the third leg being 20 ft in length. In all three cases the source of neutrons was incident at an angle of 45° with respect to a side wall normal, confined to an area approximately one-eighth that of the mouth, and centered approximately at the geometric center of the mouth. The 45° geometry was used to serve as a rigorous test of the calculation, because the fluxes for detector locations greater than several feet from the duct mouth would be due entirely to wall-scattered radiation. The source spatial distribution was determined for the experimental results of the beam mapping.

Fast-Neutron Dose Rates

Fast-neutron dose rates were calculated for only the straight duct and the two-legged duct, since the experimental results were limited to these cases.[6] The calculations were normalized to the total number of neutrons incident on the duct wall in each of the six energy groups used by the code in the range 200 keV to 8 MeV, a number found by integrating the fast-neutron dosimeter response over the plane of the wall, and, using the fast-

neutron spectrum previously reported,[7] converting the dose rate to an incident absolute number spectrum. Figure 3.5.1 shows a comparison of the calculated and measured results. In general, the agreement averages better than 10% through five orders of fast-neutron dose attenuation.

Thermal-Neutron Distributions from a Thermal Source

The calculations were normalized to the total number of subcadmium neutrons incident on the duct wall, a number found by integrating the thermal-neutron flux over the plane of the source wall as measured by a BF_3 detector. The total number of incident subcadmium neutrons was found to be 1.65×10^4 neutrons sec^{-1} W^{-1}.

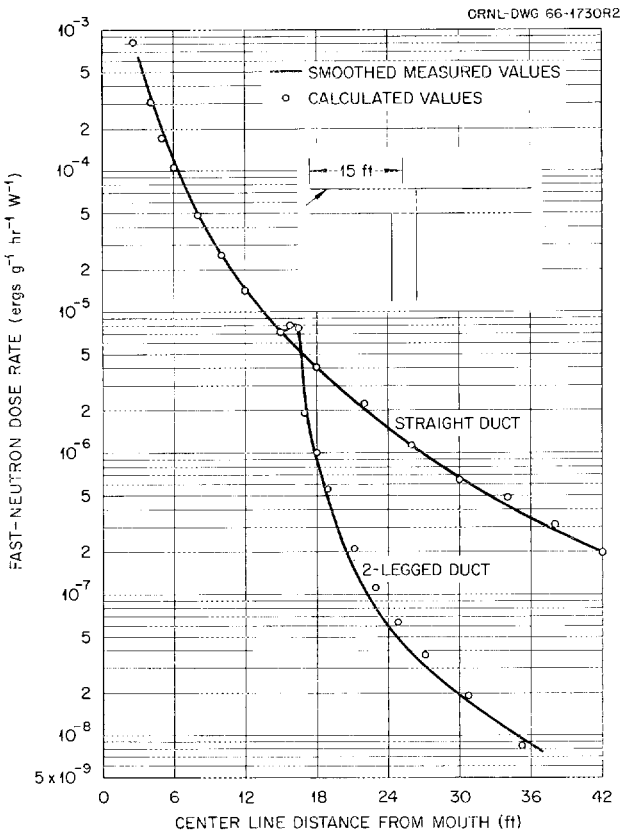

Fig. 3.5.1. Comparison of Calculation and Measurement of the Single-Collision Dose Rate Along the Center Lines of a Straight and a Two-Legged Square Duct.

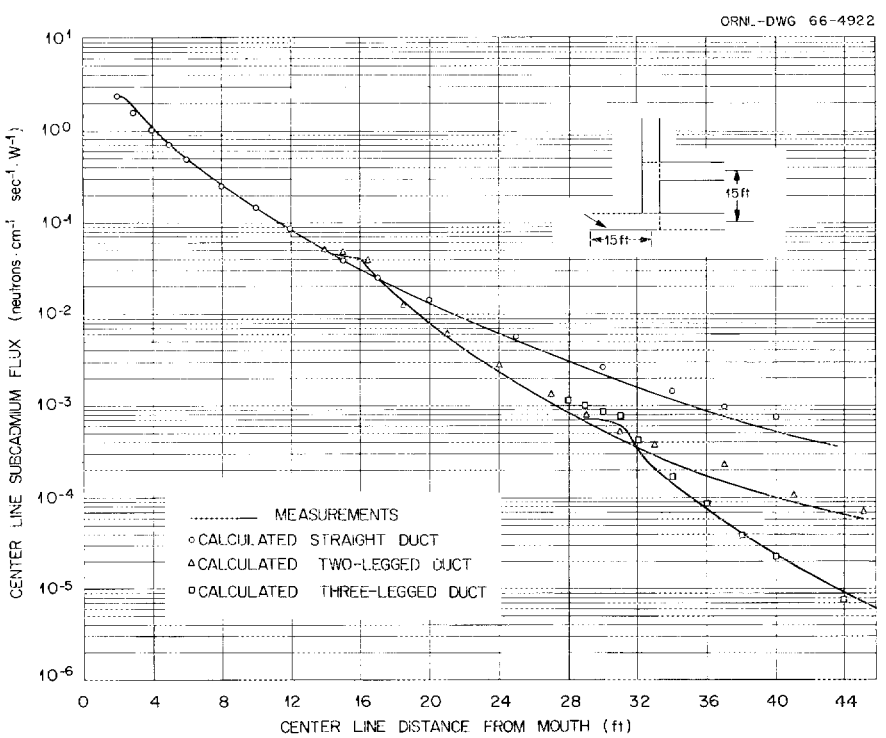

Fig. 3.5.2. Comparison of Calculation and Measurement of the Subcadmium Flux Along the Center Lines of a Straight, a Two-Legged, and a Three-Legged Square Duct (Thermal Source).

Figure 3.5.2 shows a comparison of the calculated and measured results. The agreement averages about 20% in the second and third legs and 5% for most of the straight duct. For the three-legged duct, it was necessary to follow approximately 18 wall backscatterings to obtain 90% of the flux contribution in the middle of the second leg; 25 wall backscatterings were required for the third leg. With isotropic biasing, statistical errors in the second leg averaged approximately 10% for 20,000 source histories in a running time on the CDC 1604 of 2 h; in the third leg the errors averaged approximately 15% for 50,000 source histories in a running time of close to 3 h. Although the code calculates the dose arising from wall-capture secondary gamma rays as well, these results will not be presented until some comparisons with TSF measurements have been made.

Thermal-Neutron Distributions from an Epicadmium Source

In order to test the accuracy of the code for the slowing-down problem, calculations were made of the thermal-neutron flux along the center line of the three duct configurations, and the results were compared with measurements made at the TSF.

The absolute epicadmium spectrum incident upon the source wall was determined in a manner similar to that described in Sect. 3.3. Since the reactor collimator arrangement used for the duct measurements differed from that used for the albedo measurements and since the center of the source wall was at a different distance from the reactor collimator than the center of the slab surface had been, a separate set of measurements with the boron filter spectrometer was made by T. V. Blosser at the geometric center of the mouth of the duct. The calculations of R. M. Freestone, Jr., were then used to predict the spectrometer response, assuming a Maxwellian subcadmium shape at a neutron temperature of 336°K, a $1/E$ tail in the region 0.185 eV $\leq E_0 \leq$ 10 keV, and a $1/\sqrt{E}$ transition shape in the region 10 keV $\leq E_0 \leq$ 1 MeV, with an efficiency of 0.217 at 0.0253 eV, the whole normalized to the measured subcadmium flux and cadmium ratio. A comparison of the measured and calculated responses is shown in Table 3.5.1.

The absolute incident neutron current spectrum integrated over the surface of the source wall was thus deduced to be the one shown in Fig. 3.5.3. The ratio of the surface integral of the current to the flux at the point of measurement was 472 for all neutrons above 200 keV, and was 545 for all neutrons below 200 keV.

Using the spectrum above 0.5 eV shown in Fig. 3.5.3 in the duct code produces the center-line subcadmium fluxes illustrated in Fig. 3.5.4, where comparisons are made with the measured values. Agreement, in general, averages about the same as that for incident subcadmium neutrons, and the statistical errors, number of wall backscatterings, and running times for the same number of source histories are comparable.

Table 3.5.1. Comparison of Measured and Calculated Spectrometer Responses at Geometric Center of Duct Mouth[a]

Filter No.	Response [counts (30 sec)$^{-1}$ kW^{-1}]	
	Measured	Calculated
0	8.18×10^5	8.18×10^5
1	1.21×10^4	1.09×10^4
2	8.34×10^3	8.20×10^3
3	5.21×10^3	5.55×10^3
4	4.35×10^3	4.45×10^3
5	3.83×10^3	4.05×10^3
6	3.29×10^3	3.38×10^3
7	2.68×10^3	2.75×10^3
8	2.00×10^3	2.07×10^3
9	1.78×10^3	1.78×10^3
10	1.38×10^3	1.36×10^3
11	1.23×10^3	1.18×10^3
12	9.85×10^2	9.50×10^2
13	8.22×10^2	7.78×10^2
14	6.70×10^2	6.12×10^2
15	5.26×10^2	5.10×10^2
16	4.90×10^2	3.95×10^2
17	4.00×10^2	3.22×10^2
18	2.86×10^2	2.45×10^2
19	2.49×10^2	1.69×10^2
20	1.79×10^2	1.02×10^2
21	1.00×10^2	6.7×10^1
22	5.1×10^1	2.6×10^1

[a]The response of filter 23 has been subtracted from each of the measured and calculated values.

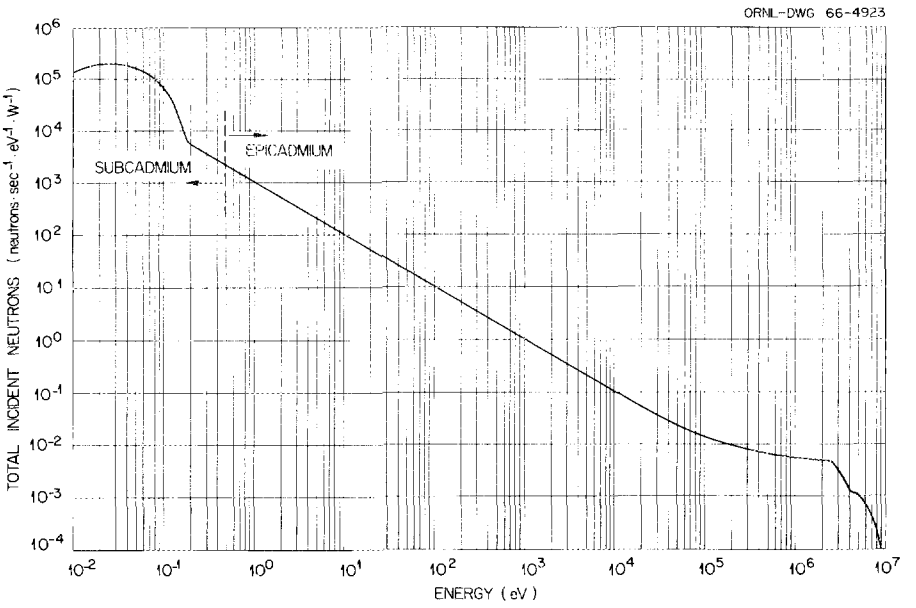

Fig. 3.5.3. Absolute Incident Spectrum of Neutrons on Source Wall Integrated over the Surface Located at an Average Distance of Approximately 7 ft from the Outer Edge of the Reactor Shield Collimator.

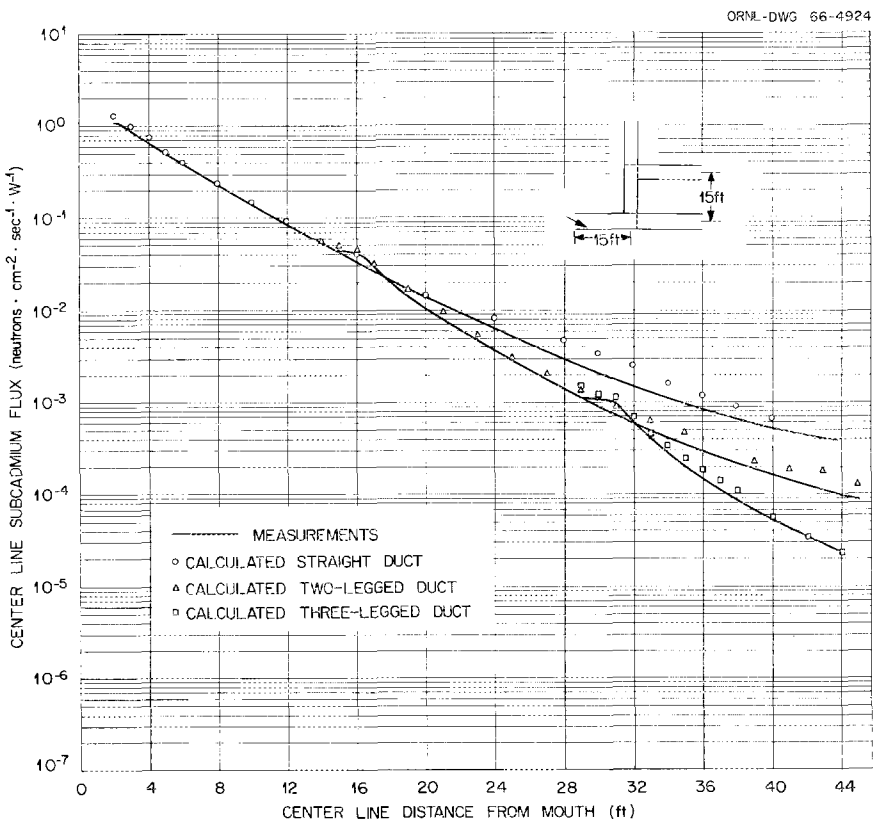

Fig. 3.5.4. Comparison of Calculation and Measurement of the Subcadmium Flux Along the Center Lines of a Straight, a Two-Legged, and a Three-Legged Square Duct (Epicadmium Source).

Table 3.5.2. Comparison of Calculated Multicollision Dose Rate with Ball Measurements

Leg	Center-Line Distance of Center of Detection from Mouth (ft)	Dose Rate (ergs g^{-1} h^{-1} W^{-1})		
		Measured 10-in. Ball	Calculated	Measured 12-in. Ball
2	19	2.5×10^{-6} (2.1×10^{-6})[a]	1.9×10^{-6}	1.35×10^{-6} (1.1×10^{-6})
2	23	5.5×10^{-6} (4.9×10^{-7})	4.5×10^{-7}	2.85×10^{-7} (2.45×10^{-7})
2	29	1.28×10^{-7} (1.2×10^{-7})	1.05×10^{-7}	6.6×10^{-7} (6.1×10^{-8})
3	33	1.45×10^{-8} (1.2×10^{-8})	9.2×10^{-9}	6.4×10^{-9} (4.8×10^{-9})
3	40	1.08×10^{-9} (9.0×10^{-10})	6.5×10^{-10}	6.0×10^{-10} (5.1×10^{-10})

[a]The dose rates in parentheses are those obtained when the center of detection was assumed to be the center of the ball rather than the leading edge.

The epicadmium spectra at several locations along the duct center line were also calculated for the three-legged duct. Using the flux-to-multicollision-dose factors of Snyder and Neufeld,[8] epicadmium multicollision dose rates may be calculated at these locations. Table 3.5.2 shows the results of this calculation and a comparison with the 10- and 12-in.-diam ball measurements described in Sect. 3.4.

References

[1]Work funded by the Defense Atomic Support Agency under order EO-804-66.

[2]R. E. Maerker and V. R. Cain, *AMC, A Monte Carlo Code Utilizing the Albedo Approach for Calculating Neutron and Capture Gamma-Ray Distributions in Rectangular Concrete Ducts*, ORNL-3964 (to be published).

[3]V. R. Cain, *Calculations of Thermal-Neutron Flux Distributions in Concrete-Walled Ducts Using an Albedo Model with Monte Carlo Techniques*, ORNL-3507 (1964).

[4]R. E. Maerker and F. J. Muckenthaler, *Differential Fast-Neutron Albedo for Concrete*, ORNL-3822, vols. I–VI (July 1965).

[5]R. E. Maerker, *Neutron Phys. Div. Ann. Progr. Rept. Aug. 1, 1965*, ORNL-3858, vol. I, pp. 24–27.

[6]Preliminary calculations for the straight duct were reported in the previous annual: R. E. Maerker, *Neutron Phys. Div. Ann. Progr. Rept. Aug. 1, 1965*, ORNL-3858, vol. I, pp. 23–24.

[7]M. S. Bokhari, V. V. Verbinski, and H. A. Todd, *Neutron Phys. Div. Ann. Progr. Rept. Aug. 1, 1963*, ORNL-3499, vol. I, Fig. 3.3.5, p. 107.

[8]Cited by H. Goldstein, *Fundamental Aspects of Reactor Shielding*, chap. 2, Addison-Wesley, New York, 1959.

3.6 RESULTS OF THE ANALYSIS BY MONTE CARLO OF THE FAST-NEUTRON SHIELDING PROPERTIES OF COMPOUND CUBICAL AND SPHERICAL SHIELDS[1]

F. H. Clark N. A. Betz[2]

An extensive program of calculations was performed to check certain fast-neutron dose-rate measurements made at Project BREN in 1962. The response characteristic of the modified long counter was computed. Nitrogen and oxygen cross sections were reviewed and used in calculations of the transport in air of neutrons from a Godiva source to a distance of 66 g/cm^2. Transport results obtained by Monte Carlo were compared with those obtained by the moments method. A spectrum at an 80-g/cm^2 penetration was determined. The perturbating effect of a structure on the neutron field in its neighborhood was estimated. The effect of variations of the spectrum with penetration distances on doses computed with different weight functions was also examined; the Snyder-Neufeld multicollision physical dose was found to vary with distance in a way markedly different from

others examined. Work was also done on importance sampling techniques, especially the exponential transform, and the sampling problem was formulated in a simplified, approximate expression to facilitate statistical interpretations. Finally, a number of shield penetration calculations were performed to compare with the measurements and to determine the effects of shield shape, shield cavity size, and source angular distributions incident on the shields. The agreement between the calculations and the measurements was within the uncertainty in the detector response characteristic.

References

[1]Abstract of ORNL-TM-1433 (in publication); work supported under AEC-BRL interagency agreement 40-40-64.

[2]Mathematics Division.

3.7 MONTE CARLO CALCULATIONS OF THE PENETRATION OF NORMALLY INCIDENT NEUTRON BEAMS THROUGH CONCRETE[1]

F. H. Clark N. A. Betz[2] J. Brown[3]

O5R, a Monte Carlo neutron-transport code, has been adapted to calculate fast-neutron doses within and outside concrete slab shields. Such calculations were performed for a variety of shield thicknesses (0 to 180 cm) and for various monoenergetic sources from 0.7 to 14 MeV. The concrete chosen is ordinary concrete with approximately 6% water content. Results are plotted as tissue kerma vs penetration distance for each source energy. The source is in each case a broad normally incident beam.

References

[1]Abstract of ORNL-3926 (in publication); work partially supported under Army Nuclear Defense Laboratory Project No. 137-65.

[2]Mathematics Division.

[3]Central Data Processing Facility, Oak Ridge Gaseous Diffusion Plant.

3.8 MEASUREMENTS OF FAST-NEUTRON DOSE RATE TRANSMITTED THROUGH AN LiH SHIELD WITH AN IRON-OIL COLLAR SHIELD

F. J. Muckenthaler J. L. Hull
J. J. Manning K. M. Henry

Since experiments for measuring the radiation transmitted through an LiH shadow shield designed for use with the Space Nuclear Auxiliary Power plants will be conducted in air at the Tower Shielding Facility, auxiliary shielding in the form of a collar will be required in order to minimize the contribution of air-scattered neutrons to the measured dose. An experiment was performed at the TSF to verify the Monte Carlo calculations which were done to determine the effect of the collar shield. For this experiment the shadow shield was placed in an oil-filled tank into which movable iron slabs were also placed as a mockup of the collar shield. The neutron dose transmitted through this assembly was then determined for various source geometries. Prior to the collar shield experiment the homogeneity of the shadow shield was determined by utilizing a tightly collimated neutron beam and detector.

Since the LiH was cast in its container, measurements were made to check on possible cracks in the LiH as well as voids between it and the walls of the cone-shaped container. The LiH shield was centered in a cylindrical oil-filled iron vessel 4 ft in diameter through which the larger end of the LiH shield protruded. A collimated beam of neutrons approximately $1\frac{1}{4}$ in. in diameter was impinged on the smaller end of the LiH shield. The neutron intensity transmitted through the shield was measured with a modified long counter placed inside a collimating water shield. The axes of the detector and the neutron beam were always coincident. The LiH shield was mapped by moving the assembly perpendicular to the neutron beam and rotating it 360° about its axis. The mappings did not reveal any cracks in the LiH but did show a separation between the container walls and the LiH. After the LiH container was filled with mineral oil, no neutron streaming was observed.

The LiH (oil-compensated) shield was then placed in another iron vessel through which both ends of the LiH protruded (Fig. 3.8.1). A 6-in.-diam collimator was used for the neutron beam to obtain adequate neutron intensity. The neutrons

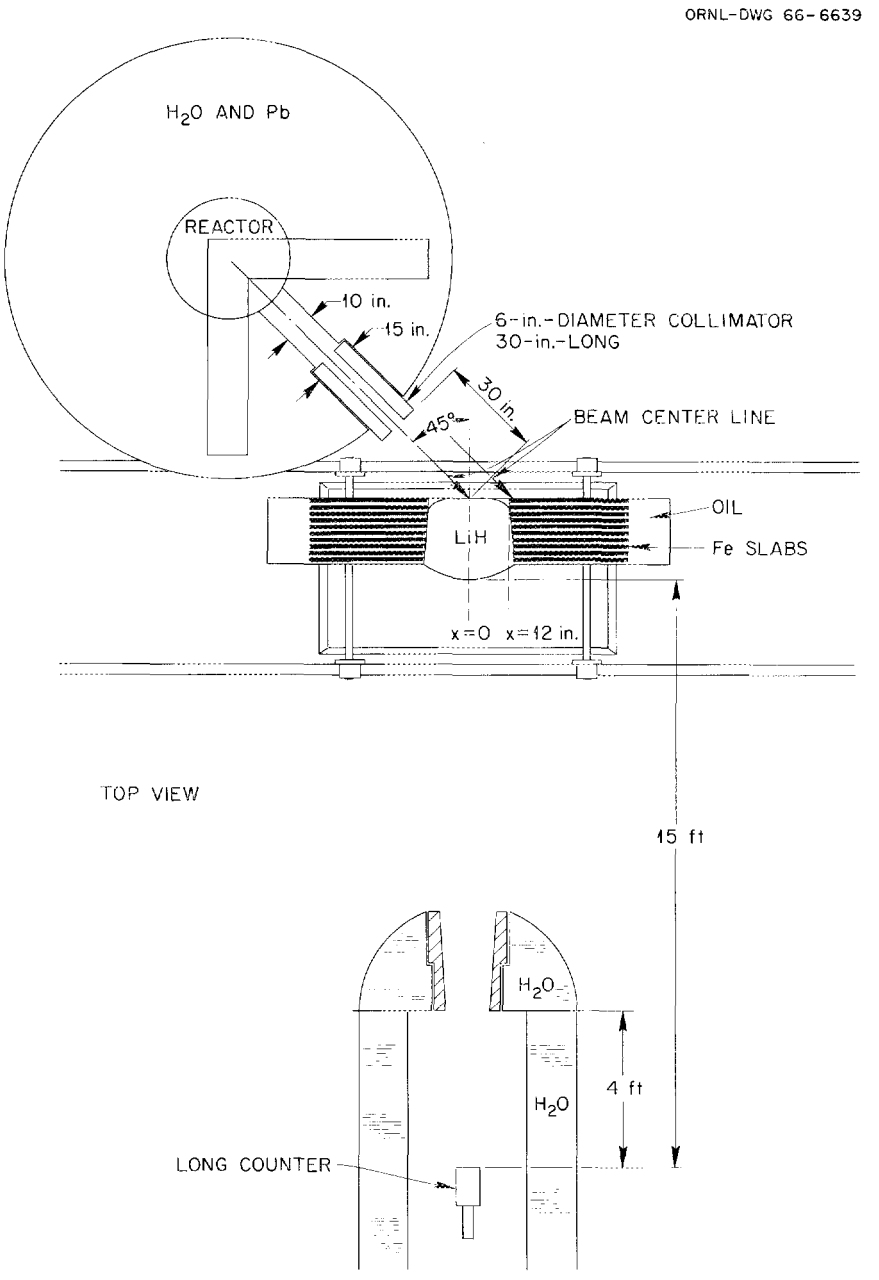

Fig. 3.8.1. Experimental Arrangement for LiH and Collar Shield Neutron Transmission Measurements.

were incident on the smaller end of the LiH shield, which was mounted so that its axis was in the same horizontal plane as the neutron beam. The iron vessel, which was approximately 4 ft high, 10 ft wide, and 20 in. thick, contained all oil or a combination of oil and 10-in.-thick slabs of iron. Three configurations of oil and iron were used, varying from 1-in.-thick alternating layers to 10 in. of iron followed by 10 in. of oil.

The detectors were placed in the collimating shield at a distance of 15 ft from the LiH shield. The neutron dose rate profile was mapped both at the point of incidence on the collar shield and at the 15-ft detector position with the LiH and collar

Table 3.8.1. Measurements of the Fast-Neutron Dose Rate Transmitted Through an LiH Shield Placed in a Collar Shield Consisting of 10 in. of Iron and 10 in. of Oil

θ (deg)	X (in.)	Long Counter (counts min^{-1} W^{-1})	Dosimeter (ergs g^{-1} h^{-1} W^{-1})
		No Shield Behind LiH and Collar	
0	0	7.19×10^{-3}	9.04×10^{-8}
	6	9.80×10^{-3}	1.28×10^{-7}
	12	1.12×10^{-2}	1.69×10^{-7}
	18	6.62×10^{-3}	8.88×10^{-8}
25	0	3.48×10^{-3}	4.60×10^{-8}
	6	6.31×10^{-3}	9.09×10^{-8}
	12	6.94×10^{-3}	9.67×10^{-8}
	18	3.29×10^{-3}	4.05×10^{-8}
45	0	1.90×10^{-3}	2.43×10^{-8}
	6	2.86×10^{-3}	
	12	2.76×10^{-3}	
	18	1.51×10^{-3}	
		12-in. of Polyethylene Behind LiH Shield Only	
0	0	1.52×10^{-3}	
	6	2.37×10^{-3}	
	12	3.88×10^{-3}	
	18	4.38×10^{-3}	
25	0	1.27×10^{-3}	1.44×10^{-8}
	6	3.68×10^{-3}	4.39×10^{-8}
	12	4.67×10^{-3}	6.53×10^{-8}
	18	2.68×10^{-3}	3.96×10^{-8}
45	0	1.06×10^{-3}	1.11×10^{-8}
	6	1.93×10^{-3}	
	12	2.21×10^{-3}	
	18	1.26×10^{-3}	
		19 in. of H_2O Behind LiH Shield and Collar	
0	0	3.88×10^{-4}	
	6	3.49×10^{-4}	
	12	3.25×10^{-4}	
	18	1.07×10^{-4}	
25	0	5.70×10^{-5}	
	6	8.70×10^{-5}	
	12	9.20×10^{-5}	
	18	1.11×10^{-4}	
45	0	9.40×10^{-5}	
	6	6.30×10^{-5}	
	12	4.90×10^{-5}	
	18	4.60×10^{-5}	

shield removed. Measurements were made for angles (θ) of neutron incidence of 0, 25, and 45°. For each angle the collar shield was moved so that the beam was centered at distances (X) of 0, 6, 12, and 18 in. from the axis of the LiH shield and in its horizontal midplane. For each position of the collar shield the detector shield was also moved so that the axis was always parallel to and coincident with the LiH shield axis.

In order to determine separately the contributions to the measurement from the neutrons which penetrated the outer surface of the LiH shield, those which penetrated the collar shield, and those which scattered around the shields, additional measurements were required. These were taken with 12 in. of polyethylene covering the LiH shield only and with 19 in. of water covering both shields. By taking the differences between these measurements and the unshielded measurements, the contributions from each of the above components could be determined.

Typical results are given in Table 3.8.1 for a collar shield consisting of 10 in. of iron followed by 10 in. of oil.

3.9 MONTE CARLO NEUTRON CALCULATIONS FOR DETERMINATION OF SNAP COLLIMATOR DESIGN

E. A. Straker M. B. Emmett[1]

To aid in the design of a specific collimator for the SNAP core-mapping experiments,[2] a series of Monte Carlo calculations using the O5R code were made to determine the effect of the collimator geometry on the ratio of foreground-to-background neutrons. (As used here, "foreground" refers to those neutrons that arrive directly at the detector, and "background" refers to those neutrons that are transmitted or scattered by the walls of a collimator shield. The background neutrons must be minimized, since they have different energy and angular distributions from the foreground neutrons.)

In addition to essentially 4π shielding for the detector and a reasonable detector-source distance, the following specific criteria had to be met for the SNAP core-mapping collimator: The spatial response of the collimator at the source plane had to be such that at least 80% of the detector counts would come from a circular area less than 2.5 in.

in diameter. The direct intensity transmitted by the collimator had to be relatively uniform over the detector surface area, and the calculated ratio of background-to-foreground neutrons at the detector had to be less than 5%.

Basic principles of collimator design[3,4] indicate that for point sources and detectors the entrance and exit ends should be tapered. The same principles apply to collimators designed for distributed sources and detectors, but the calculation has to be performed by Monte Carlo rather than by analytical methods. In the O5R calculations, statistical estimation was used to determine the scattered intensity resulting from events in various regions of the collimator; thus it was possible to separate the scattered intensity due to events in the collimator liner. Source angle biasing and Russian roulette were used to improve the statistics of the calculation.

To illustrate the importance of tapering the ends of the collimator, comparative calculations were made for a straight cylindrical collimator and for a double-tapered design in which the tapered length at each end was one-half the length of the remaining cylindrical region. (The diameter was adjusted so that the direct flux was the same for the two cases.) The collimator was assumed to consist of a water tank with a $\frac{1}{8}$-in.-thick liner to define the air column. The isotropic fission source was essentially infinite in extent, and the detector was a disk of the same diameter as the opening in the straight cylindrical collimator. The total background flux was reduced from 11.7% to 6% by tapering the ends of the collimator. The scattered intensity was reduced by a factor of 5, but the transmitted flux was reduced by a factor of less than 2. For both geometries approximately 85% of the scattered component of the background neutrons came from scattering events in the liner. When the iron liner was replaced by an aluminum one, the percentage of background neutrons scattered by the liner was somewhat smaller; but there was no significant change in the total background.

As a result of the calculations the design obtained for the SNAP collimator was a modification of the double tapered geometry. To reduce the transmitted flux, an additional tapered region was added at the entrance of the collimator; thus to maintain the same aperture, the source-detector distance was increased. Also, shielding was added around the detector. Figure 3.9.1 illustrates

ORNL-DWG 66-6550

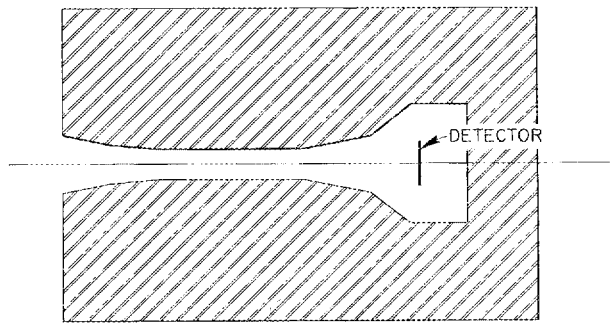

Fig. 3.9.1. Schematic of SNAP Core-Mapping Collimator Showing the Shape of the Air Column.

a collimator design which meets the experimental requirements and for which the background neutron contribution was calculated to be less than 3% of the foreground neutron contribution. For this particular design 45% of the scattered contribution comes from scattering events in the liner, and approximately 40% is due to neutrons scattered in the shielding around the detector cavity; the other 15% is due to scattering in the bulk shield. Approximately two-thirds of the total background neutrons were uncollided neutrons from the source (transmitted component).

The calculations indicated that the transmitted part of the background flux may be reduced by removing all corners at the entrance to the collimator which lie between any part of the source and detector. The scattered contribution may be reduced by decreasing the amount of liner which is viewed directly by the source and detector. However, for a particular experiment, the degree of collimation desired limits the length of the tapered regions which may be utilized and thus sets a lower limit on the ratio of background-to-foreground neutrons.

References

[1]Mathematics Division.

[2]C. E. Clifford, F. J. Muckenthaler, and J. Lewin, *Neutron Phys. Div. Ann. Progr. Rept. Aug. 1, 1965*, ORNL-3858, vol. I, p. 36.

[3]J. B. Marion and J. L. Fowler, pp. 770 ff. in *Fast Neutron Physics, Part I*, Interscience, New York, 1960.

[4]A. Simon and C. E. Clifford, *Nucl. Sci. Eng.* 1, 156 (1956).

3.10 CALCULATIONS OF NEUTRON TRANSPORT FROM FISSION AND 14-MeV SOURCES IN AIR[1]

E. A. Straker

The transport of neutrons from point isotropic fission and 14-MeV sources in an infinite air medium has been calculated by the Monte Carlo O5R code[2] and by the discrete-ordinate code ANISN. (A brief description of ANISN is given in Sect. 3.11.) Both first-collision tissue dose and differential energy spectra are determined as a function of distance from the source.

The present results for dose from a point fission source are compared in Fig. 3.10.1 with doses calculated by Trubey,[3] using the moments code RENUPAK,[4] by Wells,[5] using a Monte Carlo code, by Eisenhauer,[6] using an NBS moments code, by Ritchie,[7] using a Monte Carlo code, and by Johnson,[8] using the Monte Carlo code K-74. Variations in the dose conversion factors used in the various calculations may account for small differences but not for calculations differing by a factor of nearly 2 as noted at a range of 1000 m. A comparison of differential energy spectra at several penetrations indicated that there probably were significant differences in the total cross sections used in the various codes; this has been verified by a comparison of the cross sections used in RENUPAK, O5R, ANISN, and the NBS code.

Monte Carlo and S_8P_3 calculations have also been performed for a point monoenergetic source of 14-MeV neutrons. Dose as a function of distance from the source is shown in Fig. 3.10.2 with several other calculated results. Moments calculations by Trubey[3] and Eisenhauer[6] differ by a factor of nearly 4 at 1000 m. Monte Carlo calculations by Wells[5,9] using "new" and "old" cross sections also differ by a factor of 4. Additional Monte Carlo results by Marcum,[10] Ritchie,[7] and Johnson[8] are also shown. Differential energy spectra also illustrate large variations between the calculations, with general agreement existing between RENUPAK and ANISN results.

The increased spread in results for 14-MeV neutrons over similar results for fission neutrons was believed to have resulted from variations in

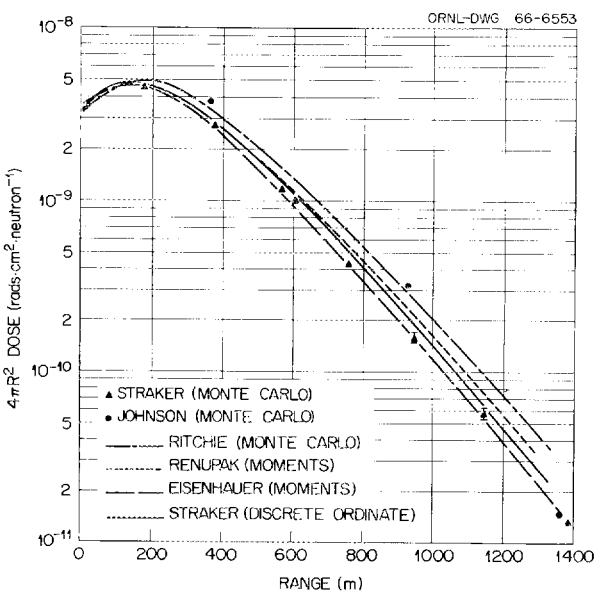

Fig. 3.10.1. $4\pi R^2$ Dose vs Range for Point Isotropic Fission Source in an Infinite Air Medium of Density 1.29×10^{-3} g/cm^3.

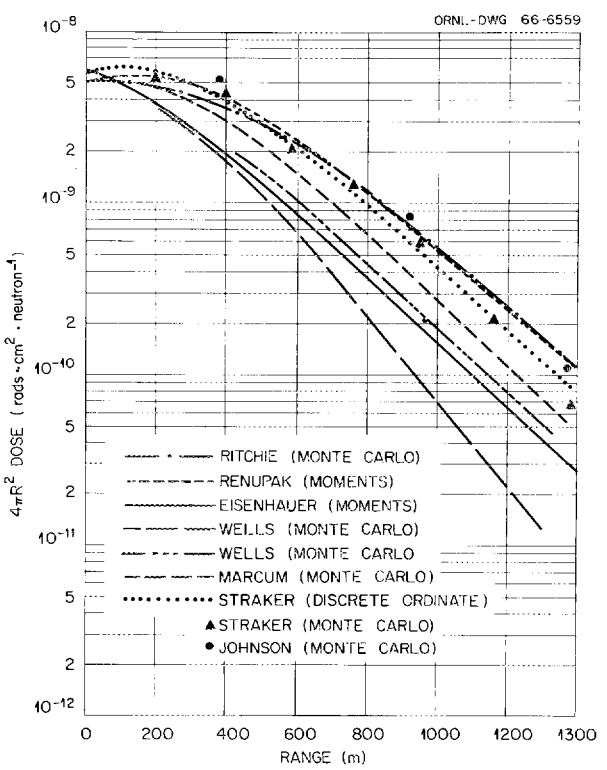

Fig. 3.10.2. $4\pi R^2$ Dose vs Range for a 14-MeV Source in an Infinite Air Medium of Density 1.29×10^{-3} g/cm^3.

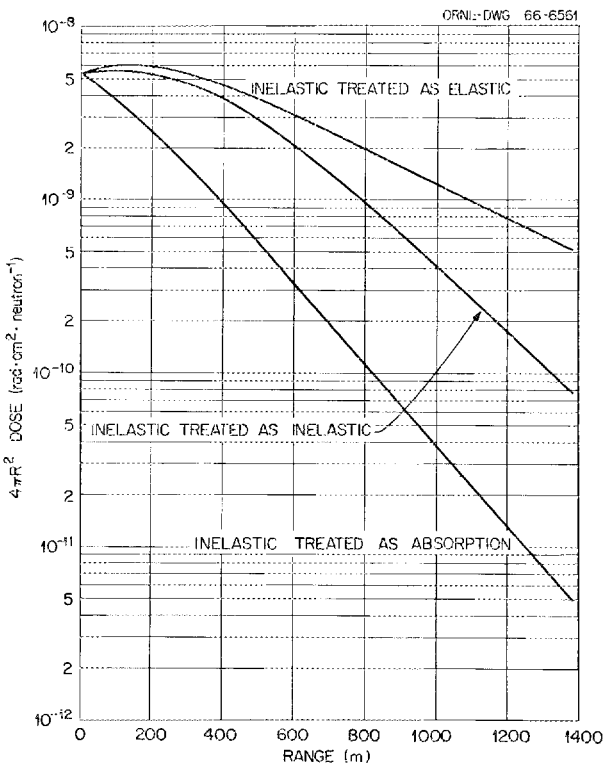

Fig. 3.10.3. Effect of Inelastic Scattering on First-Collision Dose from a 14-MeV Source in Air. Density = 1.29×10^{-3} g/cm^3.

the inelastic scattering cross sections. As a preliminary investigation of the effect on the dose from altering the inelastic scattering cross section, Monte Carlo calculations were performed for the cases in which inelastic scattering was treated correctly, using the cross sections presently on the O5R library tape; only elastic scattering was allowed, that is, an inelastic event was treated as absorption; and inelastic scattering was considered to be elastic. Variations in the first-collision dose calculated with these three assumptions are shown in Fig. 3.10.3. It is noted that there are very large differences in the dose calculated with the two extreme treatments of inelastic scattering.

All the calculated doses in Fig. 3.10.2 lie between the two extreme curves of Fig. 3.10.3. The differences in the various results probably reflect variations in inelastic cross sections as well as in the treatment of energy lost in an inelastic event.

It is concluded that differences in the calculated doses for the two sources cannot be traced to the calculational techniques but are most likely due to variations in cross sections stemming from lack of updating and detail of representation. The importance of inelastic scattering for high-energy sources illustrates the necessity of obtaining accurate inelastic cross-section data.

References

[1]The author is indebted to M. B. Emmett for her assistance in performing the O5R calculations and to N. M. Greene of the Data Processing Facility for performing the S_N calculations.

[2]D. C. Irving *et al.*, *O5R, A General-Purpose Monte Carlo Neutron Transport Code*, ORNL-3622 (1965).

[3]D. K. Trubey, private communication, 1965.

[4]J. Certaine, E. DeDufour, and G. Rabinowitz, *RENUPAK, An IBM-704 Program for Neutron Moments Calculations*, NDA-2130-3 (1959).

[5]M. B. Wells, *NRDL-CDM Shielding Symposium Proceedings*, NP-10038 (1960).

[6]C. Eisenhauer, National Bureau of Standards, private communication, 1965.

[7]R. H. Ritchie, private communication, 1965.

[8]C. F. Johnson, *Radiological Armor Program Methods and Data Compilation – vol. 2, Radiation Environments*, FZK-200-2 (1965).

[9]M. B. Wells, Radiation Research, private communication, 1966.

[10]J. I. Marcum, *Monte Carlo Calculations of the Transport of 14-MeV Neutrons in the Atmosphere*, RM-3531-PR (1963).

3.11 PROGRESS IN DISCRETE-ORDINATE TRANSPORT THEORY AND APPLICATIONS TO SHIELDING PROBLEMS

F. R. Mynatt[1] W.W. Engle, Jr.[1]
N. M. Greene[1]

In support of the SNAP Shielding Program, two codes, ANISN and DOT, have been developed. These codes solve the linear, energy-dependent, Boltzmann transport equation in one and two dimensions, respectively, using the finite-difference technique known as discrete ordinates or Carlson's

S_N method. The angular distribution of the scattering cross section is approximated by a Legendre series expansion which allows the in-scatter integral to be computed by quadrature.

Shielding calculations are being performed with these codes as checkout problems and to develop efficient routine procedures. Both codes are operational, but since only preliminary checks have been made with DOT, the following results are restricted to ANISN calculations. Figure 3.11.1 shows the fast-neutron dose rate from a point fission source in a water sphere of 150-cm radius.

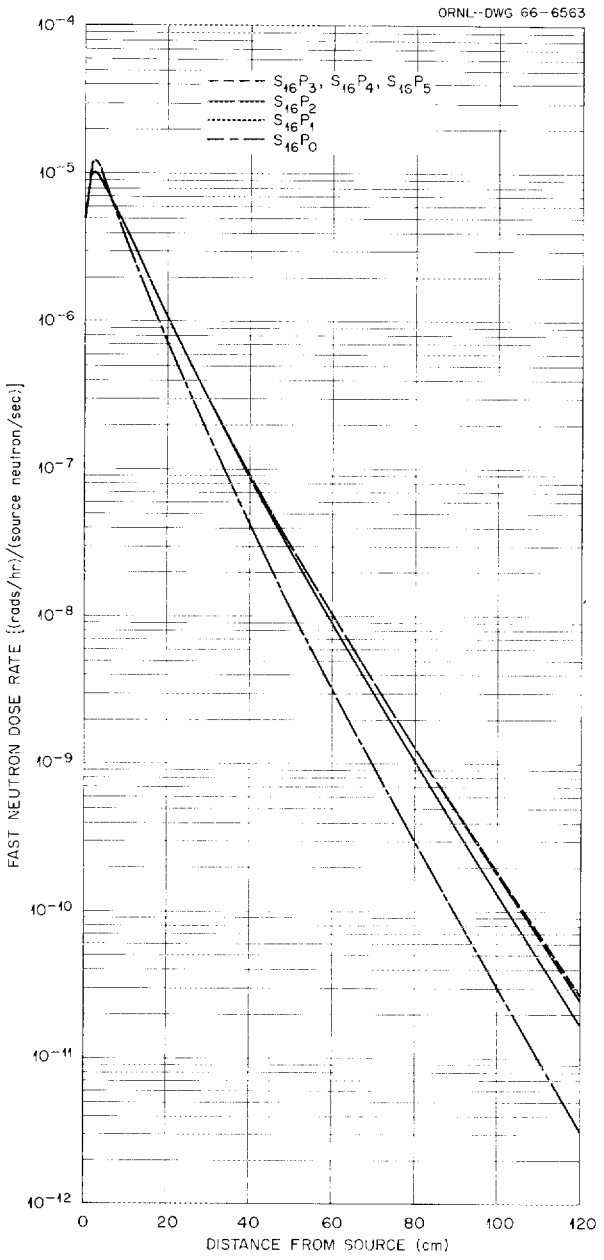

Fig. 3.11.1. ANISN Calculation of Fast-Neutron Dose Rate from a Point Fission Source in a Water Sphere of 150-cm Radius.

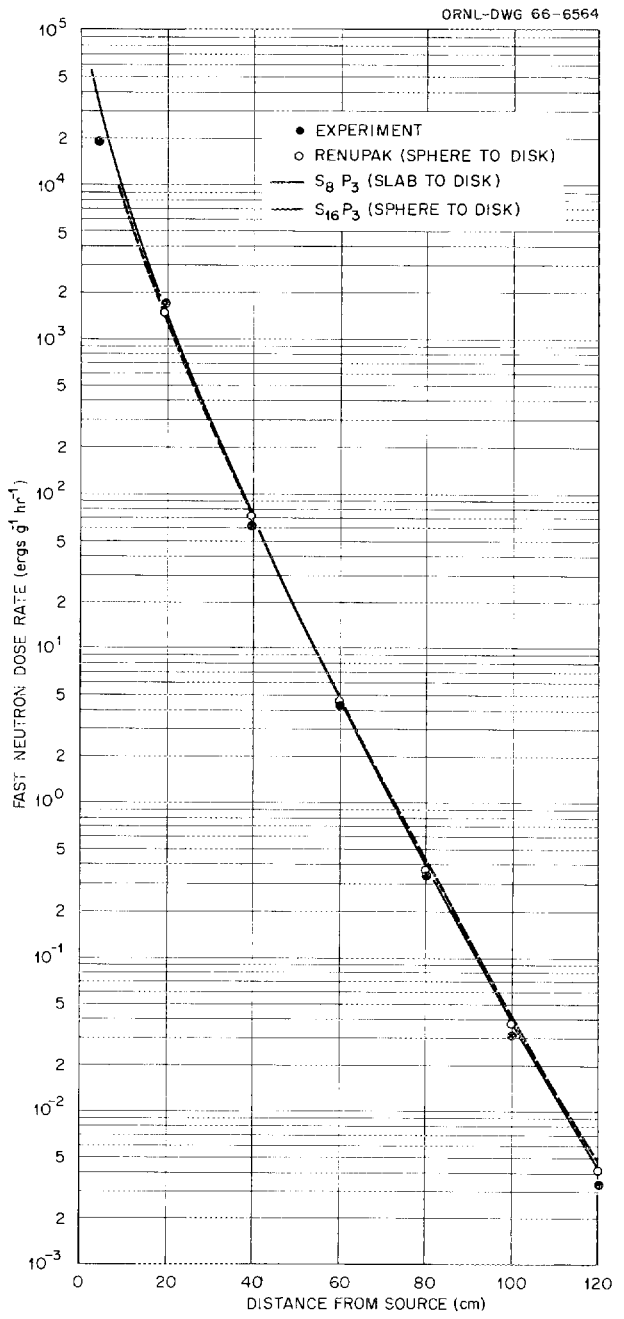

Fig. 3.11.2. Comparison of Results from Two ANISN Calculations with Fast-Neutron Dose Rate Measured at Lid Tank Shielding Facility and with Previously Calculated RENUPAK Results.

With the number of energy groups (27) and the spatial interval size (2 cm) fixed, the order of S_N and P_l was varied with the following results:

1. For S_{16} calculations the fast-neutron dose and the individual group fluxes converged at P_3; P_l was increased up to P_5 in these calculations.
2. For P_3 calculations the dose and group fluxes converged at S_{16} as S_N was varied from S_4 to S_{32}.

Figure 3.11.2 shows the fast-neutron dose rate in water with the 28-in.-diam Lid Tank Facility (LTF) disk source at a power of 1.62×10^{11} fissions/sec. The $S_{16}P_3$ curve from Fig. 3.11.1 is shown transformed to disk geometry and normalized to the LTF power. Also shown is a disk transformation of an ANISN S_8P_3 slab calculation with infinite plane source. These are compared with previously reported experimental data and a RENUPAK moments method calculation.[2] The sphere and slab calculations present widely differing difficulties in the finite difference techniques in ANISN. In the sphere the geometric angular redistribution is given an extreme test, while in the slab the flight path attenuation and rapid change in flux angular distribution severely test the capabilities of the code.

Similar calculations of a point fission source in a sphere of lithium hydride have been performed. Variation of S_N and P_l gives the same results as for the water sphere. Comparisons with experiment have not yet been made, and lithium cross-section differences have confused comparisons with other calculations.

References

[1]Central Data Processing Facility, Oak Ridge Gaseous Diffusion Plant.

[2]D. K. Trubey and M. B. Emmett, *A Comparison of First and Last Flight Expectation Values Used in an O5R Monte Carlo Calculation of Neutron Distributions in Water*, ORNL-RSIC-3 (1965).

3.12 MONTE CARLO CALCULATION OF THE MODIFICATION OF THE ^{235}U FISSION SPECTRUM BY A BORON CARBIDE SHELL[1]

R. M. Freestone, Jr.

In making measurements of epithermal and fast-neutron spectra it has become nearly traditional, whatever the detection device, to enclose the detector by a shell of B_4C, in order to shield out the usually high thermal-neutron flux which would otherwise saturate the detector response. It has apparently been assumed that the effect of this shell upon the spectrum of those neutrons which penetrate it is qualitatively and quantitatively negligible. Recently, however, some curiosity concerning the validity of this assumption has been evidenced.[2]

In order to satisfy this curiosity, a Monte Carlo calculation utilizing the O5R Neutron Transport Code[3] has been initiated. The versatility of the O5R code makes it possible to perform such a calculation without any compromises with geometry, energy structure, or permissible interactions being required; and a high degree of statistical confidence should be obtained.

The initial calculation considers a nearly spherical shell of B_4C having a ^{10}B density of 1.75 g/cm^3. This shell is typical of those being used by Kinch and McNeilly, of the Army Nuclear Defense Laboratory, to enclose a series of solid-state detectors. The code is sufficiently flexible that other densities may be substituted in later computations. A mock detector consisting of a thin aluminum disk is positioned at the center of the shell, so that buildup effects due to reflection by the detector will be taken into account.

The source for the calculation consists of an essentially isotropic selection from the Cranberg[4] description of the ^{235}U fission spectrum. Efficiency is improved by forcing all initial neutron paths to be directed toward the surface of the shell.

Cross sections to be used in the computation are the recent compilation of D. C. Irving, of this Division, and represent the most up-to-date information available.

Although the calculation is still in progress, nearly all the routines involved have been at least partially tested and debugged. It is expected that at least preliminary results will have been obtained by the time this Annual is published.

References

[1]Work supported by the Army Nuclear Defense Laboratory, Edgewood Arsenal, Maryland.

[2]J. W. Kinch and J. H. McNeilly, ANDL, private communication.

[3]D. C. Irving *et al.*, *O5R, A General-Purpose Monte Carlo Neutron Transport Code*, ORNL-3622 (1965).

[4]L. Cranberg *et al.*, *Phys. Rev.* **103**, 662 (1956).

3.13 ANALYSIS OF TOWER SHIELDING FACILITY NEUTRON SCATTERING DATA

R. M. Freestone, Jr. V. V. Verbinski
J. C. Courtney[1] W. R. Burrus

Three years ago an extensive experimental investigation of the scattering of neutrons from cylinders of various materials as a function of scattering angle was carried out at the Tower Shielding Facility (TSF). These experiments included both measurements of neutron dose, using a conventional (Hurst) dosimeter, and measurements of pulse-height spectra using a 2-in.-diam, 2-in.-high cylindrical liquid organic scintillator, NE-213.[2] The data were expected to be of particular interest to the Space Nuclear Auxiliary Power program, but to also be of value to various other shielding programs then current at the TSF.

The dosimetric data were briefly reported in a previous annual report.[3] The spectrometric data, however, were not analyzed beyond the pulse-height spectrum stage. At the time the experiments were carried out no reliable and convenient device for further analysis, that is, to neutron spectra as functions of energy and scattering angle, was felt to exist. Recent years, however, have seen the rather full development of the FERD group of analysis codes developed by Burrus,[4] and work is now under way to apply these codes to the slightly dusty TSF data.

The TSF measurements were made with 1-, 2-, 4-, and 6-in.-diam cylinders of carbon, polyethylene, iron, beryllium, concrete, and aluminum, at scattering angles of 45, 90, and 135° from the source-sample axis. In all, some 60 individual runs were made. Figure 3.13.1 shows the experimental configuration common to all runs.

Early attempts to apply the FERD codes to the unfolding of the TSF data were somewhat less than successful. Judged by comparison of unfolded TSF experimental spectra with accepted standard spectra such as the neutron spectrum of a calibrated Po-Be source, curve shapes were badly distorted and absolute magnitudes appeared to be in error. Intensive study of all components of both the spectrometer system and the unfolding codes during the last six months has, however, been successful in identifying and eliminating nearly every one of the difficulties. In general, the sources of the difficulties were traced to inadequate phototube base performance, nonlinearities in various regions of the electronics, etc. A few stemmed from simple lack of knowledge of the analysis codes; that is, in the beginning we were not able to recognize the areas within which maximum care was needed in processing data.

With essentially all of the "bugs" out of the systems, we are now going ahead with large-scale processing of the TSF data. Simple auxiliary codes have been written so that the data containing errors stemming from tube-base and analyzer nonlinearities can be effectively corrected to resemble data obtained with our present "good" system. Using such treatment, we should be able to obtain quite useful data from the old measurements.

References

[1]Former Graduate Fellow, Oak Ridge Associated Universities.

[2]NE-213, a product of Nuclear Enterprises, Ltd., Winnipeg, Canada, contains xylene, naphthalene, activators, and a spectrum shifter.

[3]F. J. Muckenthaler *et al.*, *Neutron Phys. Div. Ann. Progr. Rept. Aug. 1, 1963*, ORNL-3499, vol. 1, p. 155.

[4]A complete documentation of the FERD system has been nearly completed by W. R. Burrus and B. Holcomb.

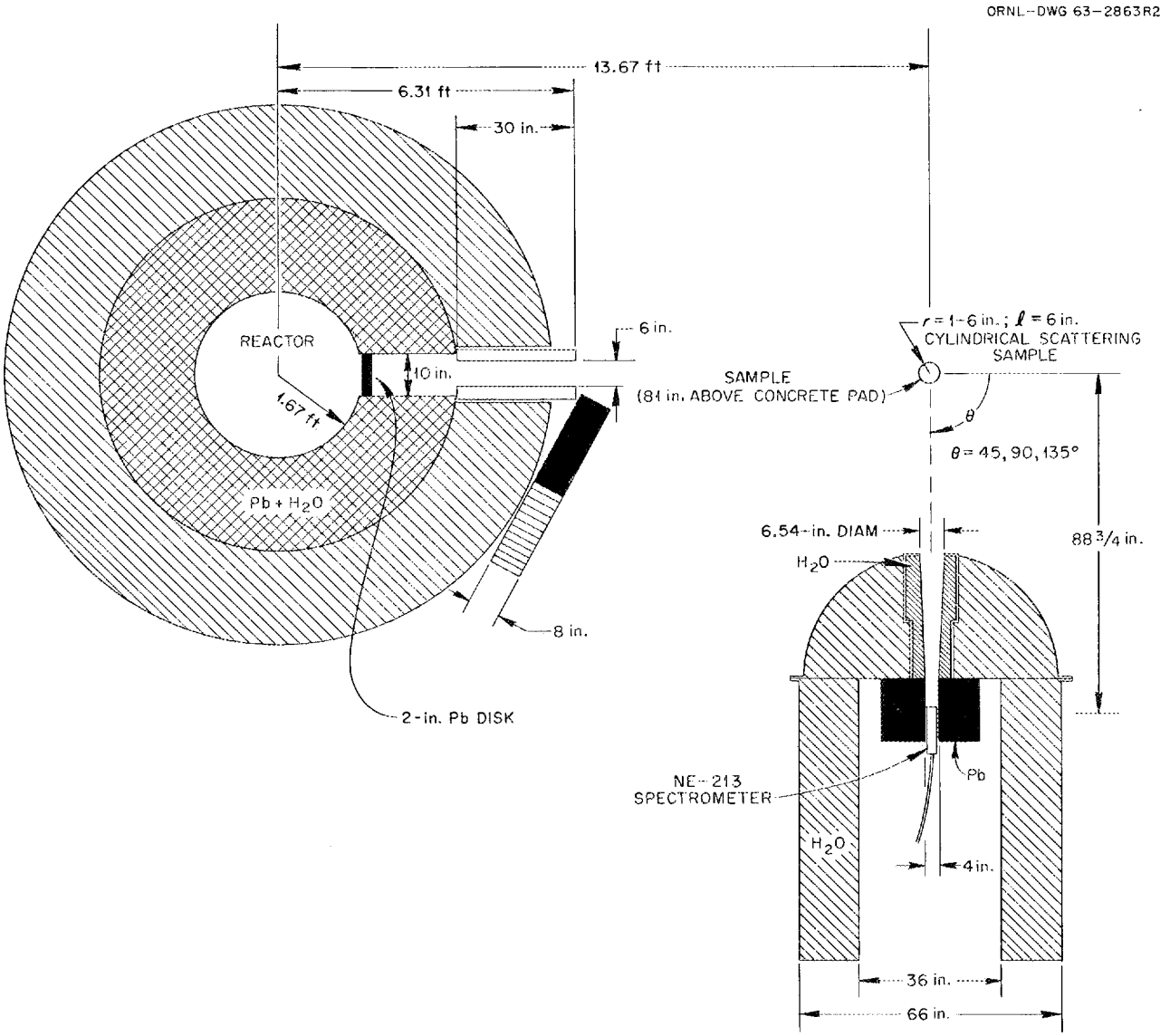

Fig. 3.13.1. Experimental Arrangement for Measuring Scattered Neutron Spectra from Cylindrical Samples in TSR-II Beam.

4. Radiation Shielding Information Center

4.1 PROGRAM OF THE RADIATION SHIELDING INFORMATION CENTER

S. K. Penny B. F. Maskewitz
D. K. Trubey F. S. Alsmiller
F. H. S. Clark

The Radiation Shielding Information Center continues to serve the technical community engaged in radiation shielding research and development. As reported previously,[1] the shielding information provided by RSIC now covers radiations from reactors, radioisotopes, weapons,[2] and accelerators and radiations which will be encountered by space vehicles.[3] The status of the literature surveys made by the Center in these various areas is described in Sect. 4.2.

RSIC's collection of digital computer codes has increased to include a total of 60 complete code packages, and a set of detailed abstracts describing 39 of the packages has been published.[4] The Center has become a clearing house for these code packages, and a procedure for disseminating them rapidly has been established.[5] Cooperation with the European Nuclear Energy Agency Computer Programme Library has continued, and a basis for computer code standardization and exchange was discussed at a shielding computer codes seminar-workshop held at Ispra, Italy, on April 26–29, 1966.

Considerable interest has been demonstrated in the monthly RSIC newsletter, especially in the accession list of newly received literature. RSIC has made this list more useful by providing microfiche copies of the literature whenever possible. Efforts have begun to include in the newsletter announcements of current shielding efforts by encouraging various installations to submit brief accounts of their shielding activities.

Work has begun on a review of the available data needed to calculate the attenuation of neutrons and gamma rays through concrete. A study of the empirical forms available for albedos and an examination of the state-of-the-art for fallout shielding calculations (see Sect. 4.4) are also under way.

A working group or workshop program has been initiated in which a small group of experts are invited by RSIC to discuss some pressing need of the shielding community. Recommendations by the group will be published. The first such working group met on April 14–15, 1966, to discuss radiological units and other related quantities.

Efforts are being made to incorporate the RSIC computer-based information retrieval system into the more general scheme of information retrieval at ORNL. Many of the locally unique features of the present RSIC system will be used in the larger system. A part of this effort will involve a telecommunication system which should not only accelerate literature searches but reduce by a factor of at least 3 the multiple transcriptions of information that are now necessary.

References

[1]S. K. Penny, D. K. Trubey, and B. A. Maskewitz, *Neutron Phys. Div. Ann. Progr. Rept. Aug. 1, 1965*, ORNL-3858, vol. I, p. 42.

[2]The weapons radiation work is funded by the Defense Atomic Support Agency under DASA order EO-804-66.

[3]The space radiation work is supported by the National Aeronautics and Space Administration under NASA order R-104(10).

[4]Betty F. Maskewitz, *Abstracts of Digital Computer Code Packages Assembled by the Radiation*

Shielding Information Center, ORNL-RSIC-13 (1966).

[5]Hemma Francis, Henrietta Hendrickson, and Juanita Brown, members of the staff of the Central Data Processing Facility at the Oak Ridge Gaseous Diffusion Plant, assist in all phases of RSIC computer code operations, as well as handle production codes for the Neutron Physics Division research staff.

4.2 LITERATURE EXAMINED BY THE RADIATION SHIELDING INFORMATION CENTER

The literature examined by RSIC falls into three broad categories. The literature in these categories is handled separately for reasons of expediency, and the efforts in each case are described separately.

Reactor and Weapons[1]

S. K. Penny D. K. Trubey J. Gurney[2]

The literature collected in the area of shielding against radiations near reactors, from radioisotopes, and in the environment of weapons was increased considerably. A revision of the previously published bibliography (ORNL-RSIC-5) was issued,[3] and abstracts corresponding to the additions in the bibliography were sent to the recipients of ORNL-RSIC-6,[4] a previously issued loose-leaf binder for the collection of abstracts. The volume of literature has become sufficiently large that it was deemed necessary that this bibliography should list documents only under the subject categories which are of major importance. It is expected that the shielding community will begin to depend upon the Center to perform more exhaustive literature searches upon request.

Space and Accelerator[5]

R. G. Alsmiller, Jr. F. S. Alsmiller
J. Gurney[2]

The collection of literature on shielding from radiation occurring in space and near accelerators was continued, and a bibliography was issued (ORNL-RSIC-11).[6] A collection of the abstracts of the literature covered in the bibliography was published as ORNL-RSIC-12.[7] A new service consisting of the automatic and selective dissemination of the literature was initiated, so that persons who provided RSIC with their field-of-interest profiles were alerted as relevant literature of space and accelerator shielding was placed in the system.

Computer Codes

B. F. Maskewitz B. L. McGill
J. Gurney[2]

The literature describing computer codes for shielding calculations is collected along with other literature describing codes to perform calculations in fringe areas of shielding and to perform auxiliary data handling. A bibliography of such literature was published as ORNL-RSIC-15.[8]

References

[1]Work partially funded by the Defense Atomic Support Agency under DASA order EO-804-66.

[2]Jane Gurney, a member of the Central Data Processing Facility staff, is responsible for the data-handling and computer-code operations involved in the RSIC information retrieval system.

[3]S. K. Penny, D. K. Trubey, and J. Gurney, *Bibliography, Subject Index, and Author Index of the Literature Examined by the Radiation Shielding Information Center (Reactor, Radioisotopes and Weapons),* ORNL-RSIC-5 (Revision 1) (1966).

[4]*Abstracts of the Literature Examined by the Radiation Shielding Information Center,* ORNL-RSIC-6 (vol. I).

[5]Work partially funded by the National Aeronautics and Space Administration under NASA order R-104(10).

[6]R. G. Alsmiller, Jr., F. S. Alsmiller, and J. Gurney, *Bibliography, Subject Index, and Author Index of the Literature Examined by the Radiation Shielding Information Center (Space and Accelerator Shielding),* ORNL-RSIC-11 (November 1965).

[7]Abstracts *of the Literature Examined by the Radiation Shielding Information Center (Space and Accelerator Shielding),* ORNL-RSIC-12.

[8]B. F. Maskewitz, B. L. McGill, and J. Gurney, *Bibliography of the Computer Codes Literature*

Examined by the Radiation Shielding Information Center, ORNL-RSIC-15.

4.3 RADIATION SHIELDING INFORMATION CENTER COMPUTER CODE COLLECTION[1]

D. K. Trubey B. F. Maskewitz
S. K. Penny

A large part of the effort of the Radiation Shielding Information Center is the collection and dissemination of computer code packages useful to those engaged in shield research or design. The concept of a computer code "package" as used by RSIC is the inclusion of all the items necessary to make a code operable. These include not only computer material such as card decks (or tapes) and machine listings but also documentation describing the theory and program, auxiliary routines, and data libraries. A sample problem is also included in a package so that each user can verify that the code is operable at his installation.

The collection is described in tabular form on the basis of computer features and theoretical methods. To date, 60 packages have been accepted and assembled.

References

[1]Abstract of paper to be published in *Nucleonics,* August 1966.

4.4 A MONTE CARLO CALCULATION OF FALLOUT GAMMA-RAY DOSE RATES

D. K. Trubey

Several calculations of gamma-ray dose rates due to fallout have been carried out in an effort to determine the difficulty in applying existing Monte Carlo codes to the problem of determining dose rates in shelters both above and below ground.

The first step was the development and use of OGRE-P4 (see Sect. 5.3) to determine the free-field dose in an air-over-ground geometry, since the one-dimensional problem can be solved with comparatively little difficulty. Besides establishing a solution by which to compare a three-dimensional calculation, it was found that (for ^{60}Co contamination) the dose rate 3 ft above the ground was unaffected when the ground was assumed to be air.

The next step was the development of a three-dimensional code based on OGRE-G.[1] The main change required was in the source routine. It was found that the uncollided flux could be computed within 0.1% by picking source positions from a $1/R$ distribution, where R is the distance from the detector. Schemes have also been incorporated to pick the direction and path length from the source site so that the first collision will be likely to occur in air near the detector (or shelter). Russian roulette generally terminates histories unlikely to make further significant contributions.

It has been possible to duplicate the results given by OGRE-P4 (but with a larger variance) for the free-field dose rate. Further development and comparisons will be made for other configurations.

References

[1]D. K. Trubey and M. B. Emmett, *OGRE-G, An OGRE System Monte Carlo Code for the Calculation of Gamma-Ray Dose Rate at Arbitrary Points in an Arbitrary Geometry,* ORNL-TM-1212 (January 1966).

4.5 A MONTE CARLO CALCULATION OF GAMMA-RAY REFLECTION FROM A CONCRETE SLAB

D. K. Trubey B. W. Wieland[1]

A study of the reflected dose rate at point detectors from a ^{60}Co source has been undertaken in an effort to resolve the anomalies apparent in a comparison of an albedo integration[2] and experimental results and to accumulate experience with Monte Carlo reflection calculations using OGRE-P3.[3] It was found that the Monte Carlo results are in good agreement with measured values and that disagreement with the albedo integration will increase with a wider range of source-detector separation distances.

References

[1] General Engineering and Construction Division.

[2] A. B. Chilton, *Backscattering for Gamma Rays from a Point Source near a Concrete Plane Surface*, University of Illinois Engineering Experiment Station Bulletin 471 (1964).

[3] D. K. Trubey and M. B. Emmett, *Neutron Phys. Div. Ann. Progr. Rept. Aug. 1, 1965*, ORNL-3858, vol. 1, p. 47.

5. Mathematics and Computer Programs

5.1 SDC, A SHIELDING-DESIGN CALCULATION CODE FOR FUEL-HANDLING FACILITIES[1]

E. D. Arnold[2] B. F. Maskewitz

A simplified computer code, SDC, is presented for calculating the gamma-shielding requirements for chemical processing, fabrication, or fuel-handling facilities. It is an IBM 7090 FORTRAN code designed to handle 13 source geometries (point, line, disk, plane, slab, cylinder with shield at side, cylinder with shield at end, sphere, ring, rod cluster, skew line, annular cylinder with shield at side, and annular cylinder with shield at end) either unshielded or shielded by slab shields. Materials of construction for shield, cladding, or source volume may be selected from a list of 17. As many as 12 gamma-ray energy groups, covering an energy range 0.10 to 10 MeV, with corresponding source strengths, may be used to describe the gamma spectrum.

Integration of the basic exponential attenuation-point kernel over the various geometries was the method chosen for calculating the uncollided gamma flux. Biological dose rate was obtained by multiplying this uncollided flux by the product of a flux-weighted buildup factor and a dose-conversion factor.

SDC has been used successfully to evaluate shield thickness and/or dose rates for several design jobs, with an average machine time of less than 0.01 h per case. Dose-rate determinations, where compared with experiment or other calculations, have been conservative (+0–50%).

Complete documentation and a code package are available from the Radiation Shielding Information Center.

References

[1]Abstract of ORNL-3041 (March 1966).
[2]Chemical Technology Division.

5.2 DESCRIPTION OF OGRE, A MONTE CARLO SYSTEM FOR GAMMA-RAY TRANSPORT STUDIES, INCLUDING AN EXAMPLE (OGRE-P1) FOR TRANSMISSION THROUGH LAMINATED SLABS[1]

S. K. Penny D. K. Trubey
M. B. Emmett[2]

A system of computer subroutines (called OGRE) has been designed for the study of gamma-ray transport by the Monte Carlo method. The various steps of the procedure have been isolated so that a complete code to solve a specific problem may be easily synthesized. A cross-section system which is easy to use is included. A specific example of the system's use (OGRE-P1) which computes the dose rates from gamma rays penetrating a slab is included.

References

[1]Abstract of ORNL-3805 (April 1966).
[2]Mathematics Division.

5.3 OGRE-P4, AN OGRE SYSTEM MONTE CARLO CODE FOR THE CALCULATION OF GAMMA-RAY DOSE RATE AT ARBITRARY DISTANCES FROM A PLANE SOURCE IN LAMINATED SLAB GEOMETRY

D. K. Trubey

OGRE-P4, an OGRE system Monte Carlo code, has been written for the calculation of dose rate by statistical estimation at arbitrary distances from a plane source in a laminated slab. This code

is similar to OGRE-P1,[1] except that the dose rate is calculated at each region boundary and the source may be placed at any specified boundary. The scattering may be biased toward a specified detector boundary by picking the scattered photon direction from an isotropic plus $\cos^N(\theta)$ distribution (θ = angle measured from slab perpendicular). The probability of picking from the isotropic distribution is controlled by input. The value N increased with the distance from the specified detector.

References

[1]S. K. Penny, D. K. Trubey, and M. B. Emmett, *OGRE, A Monte Carlo System for Gamma-Ray Transport Studies, Including an Example (OGRE-P1) for Transmission Through Laminated Slabs,* ORNL-3805 (April 1966).

5.4 COMPUTER CODES FOR THE CALCULATION OF NEUTRON AND GAMMA-RAY TRANSPORT UTILIZING THE METHOD OF MOMENTS

S. K. Penny

Although there are existing computer codes for the calculation of neutron[1] and gamma-ray[2] transport in an infinite homogeneous medium for simple sources, it has been deemed necessary to write similar codes for important reasons. The most important reason, of course, is that the data produced are badly needed. A second reason is that the codes should be coupled with modern cross-section libraries[3] so that multielement attenuating media can be easily incorporated. Another reason is that the existing codes either are becoming extinct (because of advancing computer technology) or are unavailable from the originators.

Two moments method codes are being written which calculate gamma-ray and neutron transport in any homogeneous media that can be simulated by the cross sections included in the OGRE and O5R cross-section systems. The gamma-ray code is essentially complete for the cases of point isotropic and plane isotropic sources. Development work on the neutron code is about one-third complete.

References

[1]J. Certaine, E. deDufour, and G. Rabinowitz, *Nucl. Sci. Eng.* **12**, 446 (1962).

[2]National Bureau of Standards (unpublished).

[3]D. C. Irving *et al.*, *O5R, A General-Purpose Monte Carlo Neutron Transport Code,* ORNL-3622 (February 1965); S. K. Penny, D. K. Trubey, and M. B. Emmett, *Description of OGRE, A Monte Carlo System for Gamma-Ray Transport Studies, Including an Example (OGRE-P1) for Transmission Through Laminated Slabs,* ORNL-3805 (1966).

5.5 VARIANCE OF THE SURFACE-CROSSING FLUX ESTIMATOR USED IN MONTE CARLO CALCULATIONS[1]

F. H. Clark

An analog calculation was set up to determine the effect of the grazing flux on the surface-crossing flux estimator used in Monte Carlo calculations. It was found that grazing particles make only higher order contributions to current or flux but significantly increase the variance. These effects are more pronounced at internal surfaces than at external boundaries. The use of nonstochastic methods to estimate contributions of grazing particles is justified.

References

[1]Abstract of ORNL-TM-1548 (1966); submitted to *Nuclear Science and Engineering.*

5.6 IMPORTANCE FUNCTIONS FOR MONTE CARLO BIASING IN A SIMPLE ONE-DIMENSIONAL PROBLEM

K. J. Yost R. R. Coveyou

A study is in progress with the primary aim of developing a systematic technique for the determination and subsequent utilization of biasing functions for Monte Carlo transport calculations which yield minimal variance per history. An optimization process in the Monte Carlo context

Table 5.6.1. Comparison of Analytical and Numerical Results for the Various Scoring Techniques

Sampling Technique	Fractional Standard Deviation (%)		Escape Probability		Execution Time per History (sec)
	Analytical	Computed	Analytical	Computed	
Direct Analogue	6.54	7.61	0.01832	0.0203	0.0033
Analogue, Absorption Weight	2.84	2.63	0.01832	0.0199	0.0124
Next Flight Estimator	2.95	3.70	0.01832	0.0172	0.0057
Next Flight Estimator, Absorption Weight	0.69	1.55	0.01832	0.01815	0.0188
Last Event Estimator	2.24	1.85	0.01832	0.0190	0.0051

would in general be directed toward the reduction of the pertinent variance(s) and computer running time per particle history. In practice, both these objectives are seldom if ever simultaneously achieved. The introduction of biasing factors into the random walk formulation usually results in a longer history execution time. One is then forced to think in terms of the most favorable compromise between a reduction of the number of histories required for a certain accuracy through minimizing the variance with a weight function, and the corresponding increase in per-history execution time associated with the greater complexity of the sampling scheme.

The subject investigation is structured to treat problems of progressively increasing complexity both analytically and numerically, the latter by means of Monte Carlo transport codes written specifically for each of the biasing/scoring techniques considered. To this date, work has been completed on a simple problem involving neutron slowing down in a hydrogen-pure absorber medium with constant cross sections. Estimates, variances, and execution times were generated as indicated in Table 5.6.1. The sampling techniques cited in the table have the following definitions:

1. Direct Analogue: score 1 for particle transmission through boundary; score 0 upon absorption before particle reaches boundary.
2. Analogue, Absorption Weight: particle weight factored by survival probability for each collision prior to reaching boundary; upon transmission, score particle weight.
3. Next Flight Estimator: score product of survival probability and probability for transmission to boundary without further interaction at each collision.
4. Next Flight Estimator, Absorption Weight: particle weight factored by survival probability at each collision; score product of particle weight and probability of transmission on succeeding flight at each collision.
5. Last Event Estimator: upon particle absorption, score the quotient of the probability for survival and transmission on the next flight by the probability of absorption.

5.7 ADJOINT AND IMPORTANCE FUNCTIONS IN MONTE CARLO APPLICATION

R. R. Coveyou

In support of current work on the utilization and evaluation of various biasing methods in Monte Carlo calculations, an expository report has been prepared and is in internal circulation with the primary purposes of explaining, clarifying, and making precise the role of adjoint operators and adjoint equations in the selection of feasible and useful weighting and biasing schemes. Some objective criteria of efficiency are discussed, and methods for evaluating biasing schemes in accordance with these criteria are set down.

5.8 IMPORTANCE SAMPLING DEVICES FOR SELECTING TRACK LENGTHS AND DIRECTIONS AFTER SCATTER IN O5R[1]

F. H. Clark N. A. Betz[2]

Several importance sampling schemes are discussed in some detail. A path-length stretching scheme and an exponential transform scheme, both available in O5R, are described analytically and by means of listings and flow charts. A scheme to adapt these two schemes to "never escape selection," not available in O5R, is described analytically only. A scheme for biased selection of laboratory direction after scatter, available in O5R, is described analytically. This last scheme, unlike the others, has not led to good results in any test.

References

[1]Abstract of ORNL-TM-1484 (in publication).
[2]Mathematics Division.

5.9 AUXILIARY ROUTINES FOR O5R: O5RREAD, PICTURE, AND PUNCHSIG

D. C. Irving D. K. Trubey
G. W. Morrison[1]

Several routines, to be used as part of the operations involving the O5R program, have been developed for the CDC 1604 and the IBM 7090 computers. This program, which is available as part of the O5R package through the Radiation Shielding Information Center, includes the subroutines O5RREAD, PICTURE, and PUNCHSIG.

O5RREAD is a machine language subroutine used in analysis routines to read the O5R history tapes. The history tape read operations are buffered to allow simultaneous computation and tape read with a consequent saving in computer time. In addition, O5RREAD handles all the details concerning the actual format of the history tape and the error procedures necessary for the tape operations and thus simplifies the writing of the analysis program.

PICTURE, a diagnostic aid in checking input prepared for the general geometry routine GEOM, produces as printed output a graphical display of arbitrary sections through the three-dimensional geometry specified by the GEOM input. Discrepancies between the intended geometry and that actually resulting from the input may then be easily spotted and corrected.

PUNCHSIG provides a tape-to-card capability for O5R master cross-section tapes. It allows cross-section data contained on any O5R master cross-section tape, such as the cross-section library tapes, to be punched on cards in the O5R format. A special feature in PUNCHSIG facilitates the exchange of cross-section data between the computer installations at ORNL and ORGDP.

References

[1]Central Data Processing Facility, Oak Ridge Gaseous Diffusion Plant.

5.10 A GENERAL MULTIGROUP CROSS-SECTION PACKAGE USING THE O5R CROSS-SECTION LIBRARY

K. J. Yost

A code package designed to generate group average cross sections from the O5R data tape is being developed for use both as a production and a research tool. The number and placement of group boundaries are completely arbitrary. Provision has been made for the averaging of cross sections over arbitrary input flux spectra. The code is programmed to allow for maximum flexibility in such specifics as numerical integration techniques and in the models used to represent various particle interactions and their consequences. This flexibility should be useful in a systematic investigation of the effect upon group cross-section magnitudes of variations in particle interaction models and code execution techniques.

5.11 EVALUATED CROSS-SECTION LIBRARY

D. C. Irving J. Gillen[1]

The compilation of a library of evaluated neutron cross sections containing data on 28 nuclides has been completed. The library is in the format used

by the O5R computer program, and information concerning its contents and use has been distributed to O5R users in the Neutron Physics Division and other divisions. The library is being revised to contain additional nuclides and to incorporate more recent data on the presently available nuclides.

Acquisition of reports and other information concerning cross-section evaluations being performed at other installations is continuing. A sizable library of such documents is maintained as part of the Radiation Shielding Information Center. Programs have been written to convert data from the Aldermaston and United Nuclear Corporation formats into the O5R format, and cross-section libraries obtained from these installations are now available to O5R users at Oak Ridge.

In cooperation with the Reactor Division and other divisions, cross-section evaluations are being coordinated and will be compiled into a Laboratory-wide library. The exchange of cross-section data with other installations will be facilitated through the use of the evaluated nuclear data file format designed by H. Honeck (presently with the AEC). Programs are being developed to utilize this format in preparing data for the Monte Carlo and multigroup codes used at the Laboratory.

References

[1]Central Data Processing Facility, Oak Ridge Gaseous Diffusion Plant.

5.12 FORTRAN-IV VERSIONS OF THE O5R NEUTRON TRANSPORT CODE

E. C. Long[1]

O5R, the highly versatile Monte Carlo neutron transport code invented by Coveyou,[2] was perfected for use on the CDC 1604 and IBM 7090 computers. With the planned replacement of these machines by the IBM 360-series computers at both ORNL and the Central Data Processing Facility, it has become necessary to modify O5R accordingly.

Versions of O5R and its companion cross-section handling program XSECT have therefore been prepared in the FORTRAN-IV language for both the IBM 7090- and 360-series machines. Within the minor limitations imposed by differing machine capabilities, the new versions of the codes are merely direct transliterations of the existing FORTRAN-II and -63 programs. (The FORTRAN-IV 7090 code was used as an intermediate step between the existing versions and the FORTRAN-IV 360 code.) The new versions of O5R and XSECT will serve to keep these codes operable until the completion of O6R (O5R Revised), which is being written directly in FORTRAN-IV (see Sect. 5.13).

References

[1]Central Data Processing Facility, Oak Ridge Gaseous Diffusion Plant.

[2]D. C. Irving *et al.*, *O5R, A General-Purpose Monte Carlo Neutron Transport Code*, ORNL-3622 (1965).

5.13 O6R (O5R REVISED): A GENERAL-PURPOSE MONTE CARLO PARTICLE TRANSPORT SYSTEM FOR IBM 360

R. R. Coveyou

The acquisition of an IBM 360/75 by ORNL and of an IBM 360/50 by Central Data Processing Facility has made necessary the provision of Monte Carlo particle transport programs (O5R or equivalent) for these machines. At the same time the greatly increased capabilities of these machines in speed and memory have made it both desirable and feasible to extend and improve the present O5R system for full utilization of these capabilities. It has hence been decided to undertake a thorough revision and extension of the O5R system. The system as thus revised and extended will be designated O6R (O5R Revised).

The first step will be a transliteration of the present O5R system into a language (FORTRAN-IV) compatible with the IBM 360 system. This project is discussed in Sect. 5.12, this report.

The basic design of the O6R system is essentially complete, and the programming is well begun. Some of the features of O6R which are new or greatly extended over those of O5R are listed and discussed below.

1. Certain problem parameters used in O5R, notably, number of scatterers in a medium, number

of media in the problem, number of anisotropic scatterers in the problem, number of quadric surfaces in a block, number of blocks and zones in the system, and number of energy values at which microscopic cross sections may be specified, are limited to arbitrary maximum values. Every effort will be made to remove such restrictions and to substitute for all of them the single restriction that the resulting code plus data necessary to solving the problem shall fit into the available storage space: fast storage, bulk storage, disks, and tapes.

2. The present supergroup and subgroup energy structure for cross-section handling, with subgroup limits equally spaced in energies, will be preserved. However, the allowed specifications for supergroups will include equal spacing in lethargy (the present method requires supergroups to cover a factor of 2 in energy), equal spacing in energies, or arbitrarily specified supergroup energy limits. In addition, some or all of the cross sections may be tabulated as above, or they may be calculated at the time of use by subroutines supplied by the system or by the user.

3. O5R allows the specification of scattering angular distributions as isotropic, f_1 (or cosine), and in a form which approximates an angular distribution specified by a finite number of Legendre coefficients, all as seen in the center-of-mass coordinate system. O6R will, in addition to these, allow further options in the specification of scattering angular distributions, including specifications by histogram or continuous, piecewise linear distributions, and, with the introduction of special subroutines, anything else within reasonable ingenuity.

The treatment of inelastic scattering will be simplified and, as far as is possible, brought within the general logical framework of the system. Specification of angular distributions in laboratory coordinates will be allowed; center-of-mass specification is required in O5R. Codes to convert center-of-mass scattering data to laboratory scattering data, for use in analysis, will be provided.

4. The general-geometry routine GEOM is being redesigned, both to provide wider options in the types of geometries which can be used and to make simpler the task of input specifications. A more flexible input language is to be used, allowing, for example, quadric surfaces to be specified in simpler and more usual forms than the completely expanded form now required. Further provision will be made for the succinct specification of systems composed of or containing arrays of similar geometric objects. Curved surfaces more complex than quadric surfaces may be introduced by subroutine.

5. Extensive efforts are being made to provide fast, reliable, random variable generators for use in O6R; these efforts are described in Sect. 5.14.

6. The use of adjoint problem specifications is being investigated. There are two plausible ways in which the adjoint specifications may be used in Monte Carlo calculations. First, the adjoint specification may itself be solved by Monte Carlo (means for effecting this and the conditions under which this may be useful are being studied). Second, conventional methods may be used for calculating rough adjoint solutions and solutions used as importance functions.

7. Perhaps the primary purpose of the O6R project is to make feasible the investigation and use of advanced biasing techniques; the bewildering variety of possibilities makes a detailed discussion here impossible. The provision of these extended biasing capabilities will dictate both major and minor changes in the system.

8. Much more sophisticated methods of handling the transport of thermal neutrons are needed. A treatment of thermal scatterers as Maxwell-Boltzmann gases has been developed and will be provided. There are many other models which can be fitted into the O6R framework. Some of these will be investigated, and the requirements of such models will be considered in the overall design.

5.14 RANDOM NUMBER GENERATORS FOR IBM 360

R. R. Coveyou

A random number generator is a procedure for the recursive generation of a sequence of numbers which strongly resembles a sample sequence drawn by repeated independent choices from a probability distribution uniform on the unit interval.

The most important generators are those called linear congruential. The method is as follows: Let P be the number of different nonnegative integers representable as a single machine word. ($P = 2^{35}$, IBM 7090; $P = 2^{47}$, CDC 1604; $P = 2^{31}$, IBM 360; $P = 2^{63}$ is also possible on the IBM 360 at some cost in machine time.)

Let c_0, λ, μ be positive integers less than P,

except that *one* of c_0 and μ may be zero. Define, recursively,

$$c_{n+1} \equiv \lambda c_n + \mu \pmod{P} ,$$

all the c_n being in the range $0 \leq c_n < P$. Finally, let

$$X_n = c_n/P ;$$

the X_n form the sequence which is the output of the random number generator. The choice $\lambda \equiv 5 \pmod 8$ and $\mu = 0$ ensures that $P/4$ different values of X_n occur before repetition; the choice $\lambda \equiv 1 \pmod 4$ and μ odd produces P such different values.

These facts leave nothing to be desired concerning our knowledge of the distribution of the terms of the output sequence when averaged over a full period of the generator; the distribution is essentially perfectly uniform.

Until recently, little has been known of the independence properties of such sequences. The single significant fact known and proved was that, if λ is too small, successive terms in the output sequence would be very seriously correlated. Recent work[1] has provided a method for an essentially complete analysis of the statistical performance of such generators.

Imagine the joint distribution of n successive terms of the sequence as a probability distribution spread over an n-dimensional unit cube. If the method were perfect, this distribution would be uniform and smooth. The work cited shows that departures from uniformity may be visualized as "waves" in this distribution, and, for specific choices of λ and μ, the amplitude and wavelength of these waves may be calculated. Though it is not immediately obvious, reflection will make it clear that such waves are harmful if both amplitude and wavelengths are large.

An important conclusion of this study was that there was a natural limit to the statistical performance of the method, depending only upon P (therefore the machine) and not upon the choice of λ and μ. Further, although it seems that thoroughly reliable generator performance is possible on the CDC 1604 computer, this is not completely clear for the IBM 7090 and is a little more dubious for the IBM 360. The trouble comes mainly in the distribution of quadruplets and longer strings.

Our present concern is with random number generators for the IBM 360/75, since they are necessary in the preparation of Monte Carlo programs for this machine. Several courses are open to us:

1. We can go ahead with presently known methods and hope for the best.
2. Since the actual effect of these correlations on practical calculations is unknown and, realistically, incalculable, we can examine the effect of using such presumably faulty generators in pilot calculations.
3. We can, at a sacrifice of machine time, artificially increase the effective word length to a "safe" value.
4. We can investigate methods other than linear congruential for generators of random numbers. Several such methods, having various degrees of promise, have been devised, and attempts at mathematical analysis have been started.

Course 1, though not hopeless (one might be lucky), is probably unacceptable. We have, temporarily, adopted course 3 in order to have a reliable method for instant use. Course 2 and course 4 will be investigated further.

References

[1]R. R. Coveyou and R. D. MacPherson, *Fourier Analysis of Uniform Random Number Generators*, ORNL-3866 (1965).

5.15 CDC 160-A PROGRAMS FOR PROCESSING DATA FROM NEUTRON TIME-OF-FLIGHT CROSS-SECTION MEASUREMENTS[1]

W. E. Kinney J. A. Biggerstaff[2]

Codes have been written for processing the data from experiments which measure neutron elastic- and inelastic-scattering cross sections by the time-of-flight technique. The data are accumulated in an ND-160 4096-channel pulse-height analyzer and are extracted from it by means of punched paper tape or sent directly to a CDC 160-A computer over a data-link cable. The codes enable the data to be printed, the background to be normalized and

subtracted, the walk in the circuitry to be corrected, and the corrected results to be printed.

References

[1]Abstract of ORNL-TM-1208 (1966).
[2]Physics Division.

5.16 LEGENDRE, A PROGRAM TO CALCULATE LEGENDRE COEFFICIENTS FROM ANGULAR DISTRIBUTIONS[1]

D. C. Irving W. E. Kinney
Pat Rea[2]

LEGENDRE is a FORTRAN program, written for either the CDC 1604 or IBM 7090, to calculate the coefficients of the Legendre expansion of an angular distribution. The angular distribution, represented by either the differential cross section or a probability distribution, may be specified at arbitrary values of the cosine with linear interpolation between given values. The Legendre coefficients are punched on cards in the format used by the O5R cross-section handling package. Comparisons are made between the initial distribution and the calculated Legendre expansion.

References

[1]Abstract of ORNL-TM-1241 (November 1965).
[2]Formerly with Central Data Processing Facility, Oak Ridge Gaseous Diffusion Plant.

5.17 IMPOSSIBLE LEGENDRE COEFFICIENTS[1]

D. C. Irving R. R. Coveyou
R. D. MacPherson

It has long been realized that Legendre polynomial expansions of differential cross sections can result in negative cross-section values due to the truncation of the infinite series. It is also possible that a given set of Legendre coefficients may result in negative cross sections because they do not represent any physically possible, everywhere positive angular distribution. The mathematical criteria that must be satisfied in order that there exist an everywhere positive distribution having a given set of Legendre coefficients are discussed. A check of the Legendre coefficients from several published sources has revealed a surprisingly large number of instances where the coefficients are impossible. A computer program is offered which will examine a set of Legendre coefficients to determine if they can be derived from a possible distribution.

References

[1]Abstract of paper published in *Proceedings of the Conference on Neutron Cross Section Technology, March 22–24, 1966, Washington, D.C.*, sponsored by American Physical Society.

5.18 WATETIME – AN O5R MONTE CARLO ANALYSIS ROUTINE FOR THE TIME BEHAVIOR OF NEUTRON POPULATION

J. T. Mihalczo G. W. Morrison[1]
D. C. Irving

WATETIME is a FORTRAN program for analyzing the neutron history tapes produced by the O5R Monte Carlo neutron transport code[2] and for calculating the neutron population as a function of time. The program was developed for the interpretation of prompt-neutron decay experiments. Source neutrons are injected into the system at time zero. Although the time distribution of source neutrons is a delta function at present, it can be extended to other distributions.

References

[1]Central Data Processing Facility, Oak Ridge Gaseous Diffusion Plant.
[2]D. C. Irving *et al.*, *O5R, a General-Purpose Monte Carlo Neutron Transport Code*, ORNL-3622 (February 1965).

6. Radiation Detector Studies (I)

6.1 DEVELOPMENT OF AN EPITHERMAL NEUTRON SPECTROMETER[1]

T. V. Blosser

The design of a neutron spectrometer for use in the neutron energy range from thermal to approximately 10 keV which has been under development for some time[2] has been completed. The spectrometer is basically a spherical BF_3 counter enclosed in a thick ^{10}B shell, which is penetrated by a 1-in.-diam collimator. Twenty-three ^{10}B filter disks, each of a different thickness, can be successively positioned at the mouth of the collimator to, in effect, peel off greater and greater fractions of the incident neutron spectrum.

The spectrometer has been used in three field tests: a measurement of a portion of a neutron spectrum of the Bulk Shielding Reactor (see Sect. 1.10); measurements of epithermal spectra of the Tower Shielding Reactor (see Sects. 3.3 and 3.5); and measurements of the spectra from beam holes HB2 and HB3 of the High Flux Isotope Reactor. The field tests indicated that the number of filters should be increased by approximately five: three for filling in somewhat large gaps between some filters in the existing sequence and two very thin filters for improving the resolution of the instrument at near-thermal energies.

Analysis of the data obtained with the epithermal neutron spectrometer has turned out to be difficult, and various methods are still being studied. Initially, a strong effort was made to use the quite accurate methods of Burrus *et al.* as embodied in the FERD series of codes.[3] This effort failed, largely because of the intractable shape of the spectrometer response functions. Typically, the response curve for any single filter of the set rises steeply to a rather broad peak, then slowly and monotonically decreases in a $1/v$ fashion. The full width at half maximum of the peak is roughly two energy decades. For the successful application of the FERD codes much sharper cutoffs are needed.

The analysis method which proved successful for the first and second field tests mentioned above consisted fundamentally of making a first guess as to the shape of the measured spectrum and using the measured transmissions of the ^{10}B filters to calculate the number of counts which would have been obtained from such a spectrum. Comparison of the calculated count spectrum with the experimentally obtained counts enabled a second and better guess to be made. This iteration process was carried out until at least ±5% agreement between calculation and experiment was obtained.

Further study of analysis methods is being carried out concurrently with the preparation of the final report and the manual covering the spectrometer, for which outlines are presently being discussed.

References

[1]Work funded by Defense Atomic Support Agency under DASA order EO-851-64.

[2]T. V. Blosser and R. M. Freestone, Jr., *Neutron Phys. Div. Ann. Progr. Rept. Aug. 1, 1965*, ORNL-3858, vol. 1, p. 59; T. V. Blosser, *Neutron Phys. Div. Ann. Progr. Rept. Aug. 1, 1964*, ORNL-3714, vol. 1, p. 84.

[3]W. R. Burrus, *Neutron Phys. Div. Ann. Progr. Rept. Aug. 1, 1964*, ORNL-3714, vol. 1, p. 77.

6.2 ISOTROPICALLY RESPONDING FAST-NEUTRON DOSIMETER[1]

T. V. Blosser

Previous annual progress reports have discussed the design of a highly sensitive, isotropically

responding fast-neutron dosimeter and outlined the goals of its development.[2] The work has been carried on concurrently with the design of the epithermal neutron spectrometer described in Sect. 6.1. Although most of the effort has been on spectrometer design during the past year, a considerable body of calibration data has been accumulated on a dosimeter configuration consisting of a 10-in.-OD polyethylene sphere enclosing a 2-in.-diam spherical, isotropically responding BF_3 proportional counter. Most of the data, unfortunately, are in somewhat disconnected bits and pieces. This is due to the fact that the heavy workload on the facilities required for these calibrations (the 5-MeV Van de Graaff, for instance) has forced our work to fit a "time available" pattern.

At present we have obtained accurate calibrations with 3- and 14-MeV monoenergetic neutrons, with neutrons from Po-Be and Po-B sources, and in a $1/E$ flux behind the 23 ^{10}B filters belonging to the epithermal neutron spectrometer. A long counter, to serve as an accurate flux monitor during calibration runs, was also carefully calibrated.

Since the data are not in order, no attempt has yet been made to perform a careful analysis. However, evidence to date indicates that the combination of the 10-in.-OD sphere with the 2-in.-diam proportional counter (having a double-loop collector and filled to a pressure of $\frac{1}{2}$ atm with enriched BF_3 gas) will have a sensitivity and response similar to, but possibly better than, the end response of the modified long counter used in the survey of the shield of the NS "Savannah."[3] When used in the mode for which it was designed, the latter instrument produced excellent measurements of the multicollision tissue dose.

References

[1]Work funded by Defense Atomic Support Agency under DASA order EO-850-65.

[2]T. V. Blosser, *Neutron Phys. Div. Ann. Progr. Rept. Aug. 1, 1965*, ORNL-3858, vol. 1, p. 61.

[3]E. P. Blizard, T. V. Blosser, and R. M. Freestone, Jr., *The Radiation Leakage Survey of the Shield of the Nuclear Ship "Savannah,"* ORNL-3336 (Aug. 15, 1962).

6.3 PROGRESS IN THE DEVELOPMENT OF INSTRUMENT-RESPONSE UNFOLDING METHODS[1]

W. R. Burrus
B. D. Holcomb[2]
B. Rust[2]
C. Schneeberger
M. Young

For several years we have been concerned with the problem of operating upon experimental pulse-height distributions from scintillation counters in order to obtain the desired neutron or gamma-ray spectrum. At present, the FERDO[3] code is the most advanced general code that we have made generally available. It has a number of restrictive approximations but operates quite fast and gives good results for scintillation counter pulse-height distributions with many channels. A number of small improvements have been made and some errors corrected, and a revised version, FERDOR, will soon be issued as an ORNL report. A complete revision which is not so restrictive, known as FERD, has been completed, checked on several problems, and documented. It is planned to distribute FERD through the Radiation Shielding Information Center. There is a good chance that FERD will prove useful on treating data from threshold activation foils and other few-channel spectrometers, such as the Bonner-sphere spectrometer.[4]

We are still trying to eliminate all ad hoc assumptions or restrictions from the method. Previous attempts at running a complete code using quadratic programming demonstrated the validity of the method, but were plagued by long running times and difficulties with the floating-point tolerance problem. We are trying to adapt the symmetric linear programming method of Talacko[5] for very fast quadratic programming, and hope that judicious use of interval arithmetic or significance arithmetic[6] will eliminate the necessity for prescaling input or worrying with floating-point tolerances. Effort continues on a superspeed approach[7] which requires on the order of 10^3 arithmetic operations for operating on a 100-channel spectrum, as opposed to 10^7 for present methods. It is planned to refine the code in order to deal with NaI(Tl) scintillation gamma spectrometers, and then to attempt to program the method for our PDP-8 computer. We are also trying to get some results outside the narrow context of unfolding pulse-height distributions. We

have just published an algorithm for the generalized inverse[8] which we think is among the most elegant and efficient known. The generalized inverse code was a slight variant of an algorithm used by FERDO (and its predecessor, SLOP). A numerical experiment is now under way on solving systems of equations using programmed arithmetic and input/output routines which have a random rather than a deterministic error. This makes it possible to bring powerful statistical techniques to bear on questions of accumulation of error. We expect to obtain some sharp results which will then have application to actual computers with deterministic finite precision arithmetic and input/output truncation.

References

[1]Work partially funded by the National Aeronautics and Space Administration under NASA order R-104.

[2]Central Data Processing Facility, Oak Ridge Gaseous Diffusion Plant.

[3]W. R. Burrus and V. V. Verbinski, "Recent Developments in Neutron Spectroscopy," *American Nuclear Society Shielding Division Report*, ANS-SD-2 (1965).

[4]S. K. Mehta, *A New Method for the Evaluation of Neutron Emission, Kerma, Kerma Equivalent, Dose Equivalent and the Spectrum Below 1 Mev for (α,n) Sources, Using Bonner Spheres*, ORNL-TM-1171 (Thesis) (1965).

[5]C. Schneeberger and W. R. Burrus, *A Fortran Subroutine Package for Linear Programming*, ORNL-TM-1250 (in press).

[6]W. R. Burrus and B. W. Rust, *Significance Arithmetic for Fortran*, ORNL-TM-1249 (in press).

[7]H. Young and W. R. Burrus, *Neutron Phys. Div. Ann. Progr. Rept. Aug. 1, 1965*, ORNL-3858, vol. I, p. 62.

[8]B. Rust, W. R. Burrus, and C. Schneeberger, *Comm. ACM* 9(5) (1966).

6.4 NEUTRON SPECTROMETRY WITH BULK LIQUID ORGANIC SCINTILLATORS[1]

V. V. Verbinski
R. M. Freestone, Jr.
R. Textor[2]
W. R. Burrus

The development of a fast-neutron spectrometer of high efficiency and relatively large size has been pursued by the Neutron Physics Division because of its importance to a number of past, present, and proposed programs of interest to the Division. These include applications in reactor shielding, fast-neutron albedo and reactor source spectrum determinations, scattering cross-section measurements, determinations of (α,n) and (p,n) yields and cross sections for 0.5- to 50-MeV neutrons, and measurements of cosmic-ray neutrons in and above the earth's atmosphere. The capability of good gamma-ray discrimination with the NE-213 scintillator is of utmost importance in most of these measurements, even where time-of-flight techniques are used.

Both 5- by 5-in. and 2- by 2-in. scintillators have been calibrated and used for a number of measurements where time-of-flight techniques were possible. These calibrations have been carefully made and are quite reliable, as evidenced by the good results obtained and by the use of the published calibrations at several other laboratories. These calibrated detectors are useful in cross calibrating very large scintillator tanks often used with linacs, and this proves to be a very convenient procedure in time-of-flight arrangements.

For time-of-flight applications, only the integral bias efficiency is needed. These are obtained from response functions calculated with a Monte Carlo code.

For measurements where time-of-flight techniques are not feasible, the complete pulse-height distribution for incident monoenergetic neutrons must be known so that unfolding techniques can be applied. These have been obtained with reasonable accuracy from 0.1 to 20 MeV with the O5S Monte Carlo code of Textor. They have been checked for proper shape at a large number of neutron energies, and for absolute differential efficiency at 2.66 and 14.43 MeV.

To obtain reliable spectra with reasonably good energy resolution and a reliable estimation of the statistical uncertainty of the results, it is necessary to have good pulse-shape discrimination capabilities; the electronics must be stable, linear, and yield very reproducible results; the Monte Carlo calculations of the response must be accurate and based on experimental inputs and checks; and a reasonably sophisticated unfolding-type code must be available.

A Forté-type gamma-ray discriminator has been developed to the point where it is stable and can

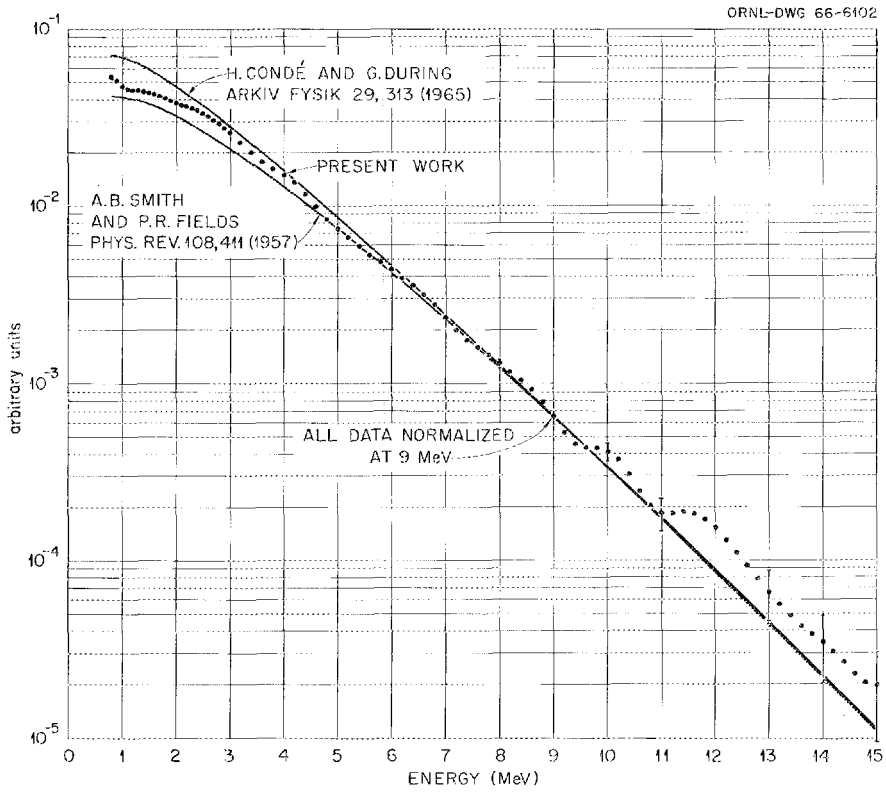

Fig. 6.4.1. ^{252}Cf Spectrum Showing Organic Scintillator Results Compared with Boiloff Spectra Fitted to Published Results.

accept neutron-induced pulses at near 100% efficiency over a pulse-height range that corresponds to recoil protons of about 0.4 MeV (corresponding to a pulse height produced by a 0.050-MeV electron) to 20 MeV. It has been used with conventional amplifiers and an analyzer in gamma-ray environments producing count rates up to 10,000/sec (about 10% of these events were due to neutrons). Proper adjustment of the circuit for this range is not possible without experimental checks. These have recently been improved to the point where good performance and reliability are achieved.

The reliability, linearity, and reproducibility of the electronics have been advanced significantly by proper matching of amplifier and analyzer and by improving the tube-base design. The requirement of obtaining a linear output from the 10th or 11th dynode of a 14-stage photomultiplier operated in a high-current mode leads to severe interelectrode coupling problems. These have been overcome to an extent where two different tube-base designs appear to be reasonably reliable. It is hoped that the problem can be pursued further so that an operable base can be obtained that has nanosecond time slewing, in addition to the above-mentioned requirements of linearity, reproducibility, and good gamma-discrimination capability.

The Monte Carlo calculations have recently shown significant improvement in matching the responses that could be measured at a few points, both as a result of more precise measuring techniques and improved inputs to the calculation. Previously, the mismatch was such that the Gaussian "window widths" generated by the FERDO unfolding code had to be widened additionally by a factor of 1.4 to avoid local aberrations in the neutron spectra. It is expected that this factor can now be reduced, so that the energy resolution of the system should approach that limited by the scintillator itself and not by the heretofore-required additional smearing.

The FERDO code has been carefully checked, including a test case where a published ^{252}Cf spectrum was converted to a pulse-height distribution, using the 2-in. scintillator response matrix.

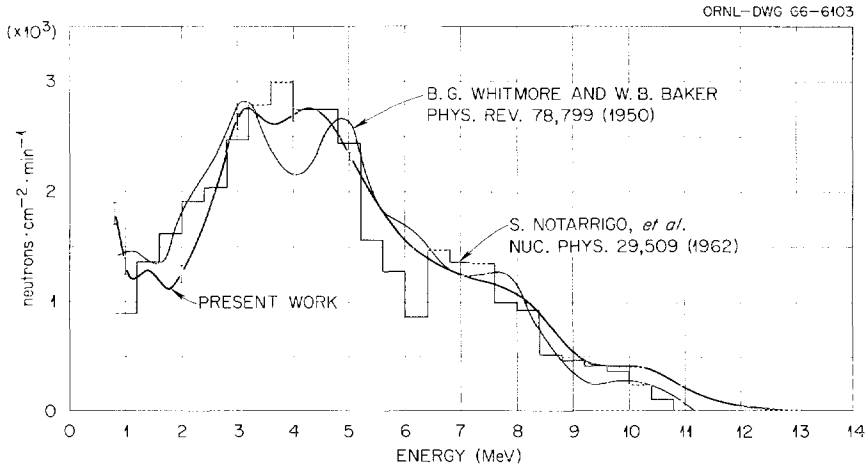

Fig. 6.4.2. Po-Be Spectrum with Organic Scintillator Results Compared with Published Results.

This pulse-height distribution was operated on by the FERDO code, which very satisfactorily reproduced the original spectrum, both in shape and magnitude.

Very recent results of measurements at ORNL, as processed by FERDO, are shown in Figs. 6.4.1 and 6.4.2, where the measured ^{252}Cf and Po-Be source spectra are compared with measurements obtained by nuclear-emulsion and time-of-flight techniques performed at other laboratories.

References

[1]Abstract of paper to be presented at a Conference on Radiation Measurements in Nuclear Power at Berkeley Castle, Berkeley, England, Sept. 12–16, 1966.

[2]Central Data Processing Facility, Oak Ridge Gaseous Diffusion Plant.

Publications

ALSMILLER, F. S.

"A General Category of Soluble Nucleon-Meson Cascade Equations," ORNL-3746 (1965).

ALSMILLER, R. G., Jr.

"Shielding Calculations for High-Energy Accelerators," *Proceedings of the USAEC First Symposium on Accelerator Radiation Dosimetry and Experience, Brookhaven National Laboratory, Upton, New York, Nov. 3–5, 1965,* CONF-651109; also ORNL-TM-1298 (Oct. 14, 1965).

ALSMILLER, R. G., Jr., AND F. S. ALSMILLER

"Bibliography, Subject Index, and Author Index of the Literature Examined by the Radiation Shielding Information Center (Space and Accelerator Shielding)," ORNL-RSIC-11 (November 1965).

ALSMILLER, R. G., Jr., AND J. BARISH*

"Nucleon-Nucleus and Pion-Nucleus Collisions in the Energy Range 2 to 10 GeV," ORNL-3855 (December 1965).

"Calculation of the Nucleon-Meson Cascade in Iron Initiated by 1- and 3-GeV Protons and Comparison with Experiment," *Trans. Am. Nucl. Soc.* **8**, 632 (1965); also ORNL-3852 (December 1965).

"Calculation of the Nuclear Cascade in Steel Initiated by 10- and 19.2-GeV/c Protons and Comparison with Experiment," *Nucl. Instr. Methods* **36**, 309–313 (1965).

ALSMILLER, R. G., Jr., AND H. S. MORAN

"Electron-Photon Cascade Calculations and Neutron Yields from Electrons in Thick Targets," *Trans. Am. Nucl. Soc.* **8**, 634–35 (1965).

ARNOLD, E. D.,* AND B. F. MASKEWITZ

"SCD, A Shielding Design Calculation Code for Fuel-Handling Facilities," ORNL-3041 (March 1966).

BERTINI, H. W.

"Results from Low-Energy Intranuclear Cascade Calculations," ORNL-TM-1225 (Sept. 10, 1965).

"Energy Spectra from Inelastic Nuclear Reactions at Energies Below 450 MeV," *Trans. Am. Nucl. Soc.* **8**, 634 (1965).

"Erratum to 'Low-Energy Intranuclear Cascade Calculations'," *Phys. Rev.* **138**, AB2 (1965).

BERTINI, H. W., H. E. FRANCIS,* AND M. P. GUTHRIE

"Instructions for the Operation of Codes Associated with the Low-Energy Intranuclear Cascade Calculation," ORNL-3844 (March 1966).

BERTRAND, F. E., R. W. PEELLE, T. A. LOVE, R. J. FOX,* N. W. HILL,* AND H. A. TODD*

"A Total-Absorption Detector for 60-MeV Protons Using Lithium-Drifted Germanium," p. 279 in *The IEEE Transactions on Nuclear Science, 10th Scintillation and Semiconductor Counter Symposium, Washington, D.C., Mar. 2–4, 1966,* Vol. NS-13, No. 3.

*Non-Division personnel.

BLONS, J.,* H. DERRIEN,* A. MICHAUDON,* P. RIBON,* AND G. de SAUSSURE
"Study of Resonance Parameters of Pu-239," *International Conference on Study of Nuclear Structure with Neutrons, Antwerp, July 1965,* North Holland Publ. Co., 1966.

"Distributions des parametres des resonances neutroniques du plutonium 239 de 0 a 200 eV," *Compt. Rend.* **262**, 79–82 (Jan. 3, 1966).

BOKHARI, M. S., AND V. V. VERBINSKI
"Measurement of the Neutron Source Distribution in a Pool-Type Reactor," ORNL-TM-1539 (May 27, 1966).

CHAPMAN, G. T.
"Gamma-Ray Attenuation Coefficient for Germanium," ORNL-TM-1237 (Mar. 2, 1966).

CLARK, F. H. S.
"The Eponential Transform as an Importance Sampling Device — A Review," ORNL-RSIC-14 (January 1966).

CLIFFORD, C. E., AND J. LEWIN
"ORNL SNAP Shielding Program," *AIAA Specialists Conference on Rankine Space Power Systems, NASA Lewis Research Center, Cleveland, Ohio, Oct. 26–28, 1965,* CONF-651026.

COURTNEY, J. C., V. V. VERBINSKI, AND N. A. BETZ*
"Fast-Neutron Scattering from Small Cylinders of Steel, Aluminum, Graphite, Concrete, and Lithium Hydride," *Trans. Am. Nucl. Soc.* **8**, 647 (1965).

COVEYOU, R. R., AND R. D. MacPHERSON
"Fourier Analysis of Uniform Random Number Generators," ORNL-3866 (October 1965).

de SAUSSURE, G., J. BLONS,* C. JOUSSEAUME,* A. MICHAUDON,* AND Y. PRANAL*
"Mesure de la Section Efficace de Fission du Plutonium 239 de 0 a 5 kev," *Symposium on the Physics and Chemistry of Fission, Salsburg, Austria, Mar. 22–26, 1965,* paper SM 60/13, IAEA, Vienna, 1966.

DICKENS, J. K.
"Dependence of Proton Optical-Model Parameters upon Experimental Uncertainties," *Phys. Rev.* **143**, 758 (1966); also ORNL-TM-1267 (Sept. 4, 1965).

DICKENS, J. K., F. G. PEREY, AND G. R. SATCHLER*
"Inelastic Scattering of Deuterons from ^{60}Ni and ^{114}Cd," *Nucl. Phys.* **73**, 529 (1965).

GIBSON, W. A.
"Design of Photomultiplier Tube Base with High Gain and Clean Output Signals for Tubes Viewing Organic Scintillator Light Pulses," ORNL-TM-1324 (Jan. 6, 1966).

GWIN, R., L. W. WESTON, AND R. INGLE*
"The Use of a Digital Computer in Time-of-Flight Experiments," *IEEE Trans. Nucl. Sci.*, NS-13, No. 1 (1966).

HARLOW, M. V., Jr., R. L. ROBINSON,* AND B. B. KINSEY*
"Elastic Scattering of 17 to 21 MeV Neutrons from ^{12}C," *Nucl. Phys.* **67**, 249–256 (1965).

IRVING, D. C., R. G. ALSMILLER, Jr., F. S. ALSMILLER, H. W. MORAN, AND J. BARISH*
"The Secondary-Particle Contribution to the Dose from Solar-Flare Protons Incident Isotropically on Slab Shields," ORNL-TM-1210 (October 1965).

IRVING, D. C., W. E. KINNEY, AND P. REA*
"LEGENDRE, A Program to Calculate Legendre Coefficients from Angular Distribution," ORNL-TM-1241 (November 1965).

*Non-Division personnel.

IRVING, D. C., G. W. MORRISON,* AND J. T. MIHALCZO
"O5R Monte Carlo Analysis Routines for Calculating Various Mean Times in Reactor Problems," ORNL-TM-1246 (Feb. 15, 1966).

JOHNSON, E. B., AND R. K. REEDY, Jr.
"Critical Experiments with SPERT-D Fuel Elements," ORNL-TM-1207 (July 1965).

KAM, F. B. K., AND F. H. CLARK
"Numerical Solution of the Lagrange Multiplier Problem with Several Constraints," ORNL-3846 (December 1965).

KINNEY, W. E.
"Calculated Fluxes of Less than 50-MeV Neutrons Diffusing Beneath the Shield of a Meson Production Facility," *Trans. Am. Nucl. Soc.* **8**, 635–36 (1965); also ORNL-TM-1423 (Feb. 23, 1966).

KINNEY, W. E., AND J. A. BIGGERSTAFF*
"Data Reduction Programs for the CDC-160A Computer," ORNL-TM-1208 (April 1966).

LEIMDORFER, M., AND R. T. BOUGHNER*
"Monte Carlo Study of Method for Lunar (Surface) Analysis Based on Spectroscopy of Gamma Rays Following 14-MeV Pulsed-Neutron Bombardment," ORNL-TM-1446 (March 1966).

MAERKER, R. E., AND F. J. MUCKENTHALER
"Measurements and Single-Velocity Calculations of Differential Angular Thermal-Neutron Albedos for Concrete," ORNL-TM-1421 (Apr. 5, 1966).

"Single-Velocity Calculation and Measurement of Differential Angular Thermal-Neutron Albedos for Concrete," *Trans. Am. Nucl. Soc.* **8**, 647–48 (1965).

"Calculation and Measurement of the Fast-Neutron Differential Dose Albedo for Concrete," *Nucl. Sci. Eng.* **22**, 455–462 (1965).

MAGNUSON, D. W.
"Static and Dynamic Transport Calculations for Pulsed-Neutron Experiments with Spheres of Uranyl Nitrate Solutions," ORNL-TM-1213 (Apr. 26, 1966).

MASKEWITZ, B. F.
"Activities of the ANL-ENEA Computer Program Libraries and the ORNL Radiation Shielding Information Center. III. Radiation Shielding Information Center," in *Proceedings of the Conference on the Application of Computing Methods to Reactor Problems, May 17–19, 1965,* ANL-7050.

MIHALCZO, J. T.
"Multiplication Factor of Uranium Metal by One-Velocity Monte Carlo Calculations," ORNL-TM-1220 (Aug. 19, 1965).

"Critical Uranium Metal Annuli Reflected with Polyethylene and Graphite," *Trans. Am. Nucl. Soc.* **8**, 442–43 (1965).

PENNY, S. K.
"Inelastic Effects on Stripping and Other Direct Reactions," ORNL-TM-1414 (March 1966).

PENNY, S. K., D. K. TRUBEY, AND M. B. EMMETT*
"OGRE, A Monte Carlo System for the Study of Gamma-Ray Transport; with an Example OGRE-P1, A Program for Computing Transmission Through Laminated Slabs," ORNL-3805 (April 1966).

SANTORO, R. T., F. E. BERTRAND, T. A. LOVE, AND R. W. PEELLE
"Beam Energy Measurements at the Oak Ridge Isochronous Cyclotron," ORNL-TM-1382 (Jan. 13, 1966).

---

*Non-Division personnel.

SILVER, E. G.
"Status Report on SPERT Programme Including Power Burst Facility," *Nucl. Safety* **6**, 255–59 (1965).

SMITH, W. R.
"The Hauser-Feshbach Nuclear Scattering Computer Code LIANA," ORNL-TM-1234 (Sept. 20, 1965).

"Analysis of Elastic and Inelastic Scattering of Neutrons from ^{206}Pb, ^{208}Pb, and ^{209}Bi Below 4.5 MeV," ORNL-TM-1238 (Sept. 27, 1965).

"DWBA Analysis of the ^{90}Zr(d,p)^{91}Zr Reaction at Energies Between 3.5 and 5.5 Mev," ORNL-TM-1235 (Nov. 22, 1965).

THOMAS, J. T.
"Experimental and Calculated System Criticality," in *Criticality Control of Fissile Materials, Proceedings of a Symposium, Stockholm, Sweden, Nov. 1–5, 1965,* IAEA, Vienna, 1966.

TRUBEY, D. K.
"A Survey of Empirical Functions Used to Fit Gamma-Ray Buildup Factors," ORNL-RSIC-10 (February 1966).

TRUBEY, D. K., AND M. B. EMMETT*
"OGRE-G, An OGRE System Monte Carlo Code for the Calculation of Gamma-Ray Dose Rate at Arbitrary Points in an Arbitrary Geometry," ORNL-TM-1212 (Jan. 17, 1966).

TRUBEY, D. K., S. K. PENNY, AND K. D. LATHROP*
"A Comparison of Three Methods Used to Calculate Gamma-Ray Transport in Iron," ORNL-RSIC-9 (October 1965).

VERBINSKI, V. V.
"Angular Distributions of Low-Energy Neutrons Leaking from Various Scattering Materials," ORNL-TM-1078 (Rev.) (May 20, 1966).

"Slowing-Down Spectra of Neutrons in Lithium Hydride," ORNL-TM-1077 (Rev.) (May 20, 1966).

VERBINSKI, V. V., AND M. S. BOKHARI
"Deuteron Polarization from the ^{9}Be(d,p)^{8}Be Reaction at 3–5 MeV," ORNL-TM-1233 (September 1965).

"Deuteron Polarization from the ^{9}Be(p,d)^{8}Be Reaction at 3–5 MeV," *Phys. Rev.* **143**, 688–691 (1966).

VERBINSKI, V. V., M. S. BOKHARI, J. C. COURTNEY, AND G. E. WHITESIDES*
"Measurements and Calculations of Spectral and Spatial Details of Fast-Neutron Flux in Water Shields," ORNL-TM-1541 (May 26, 1966).

VERBINSKI, V. V., AND J. C. COURTNEY
"Spectra of Bremsstrahlung-Produced Neutrons Emitted from ^{27}Al (at 55 and 93°), ^{206}Pb, ^{208}Pb, and ^{209}Bi (at 90 and 141°)," *Bull. Am. Phys. Soc.* **10**, 541 (1965).

WEBSTER, J. R.
"Some Conclusions Regarding the Use of the S_n Method in Shielding Calculations," ORNL-TM-1196 (Sept. 15, 1965).

---

*Non-Division personnel.

INTERNAL DISTRIBUTION

1. L. S. Abbott
2. F. S. Alsmiller
3. R. G. Alsmiller, Jr.
4. E. D. Arnold
5. H. W. Bertini
6. N. A. Betz
7. J. A. Biggerstaff
8. T. V. Blosser
9. J. Brown
10. W. R. Burrus
11. V. R. Cain
12. A. D. Callihan
13. Y. Cassagsnou
14. G. T. Chapman
15. G. Chilosi
16. H. C. Claiborne
17. F. H. S. Clark
18. C. E. Clifford
19. W. Coleman
20. R. R. Coveyou
21. S. N. Cramer
22. G. de Saussure
23. J. K. Dickens
24. L. Dresner
25. E. Eichler
26. J. F. Ellis
27. M. B. Emmett
28. W. W. Engle, Jr. (K-25)
29. Hemma Francis (K-25)
30. R. M. Freestone, Jr.
31. W. A. Gibson
32. J. Gillen (K-25)
33. L. W. Gilley
34. J. H. Gillette
35. N. M. Greene (K-25)
36. J. Gurney (K-25)
37. M. Guthrie
38. R. Gwin
39. V. M. Hamrick
40. M. V. Harlow
41. M. P. Haydon
42. Henrietta Hendrickson (K-25)
43. K. M. Henry, Jr.
44. B. D. Holcomb (K-25)
45. L. B. Holland
46. J. L. Hull
47. R. Ingle
48. D. Irving
49. E. B. Johnson
50. W. H. Jordan
51. W. E. Kinney
52. G. A. Kistner
53. C. E. Larson
54. J. Lewin
55. E. C. Long (K-25)
56. A. Lottin
57. T. A. Love
58. J. J. Lynn
59. H. G. MacPherson
60. R. E. Maerker
61. D. W. Magnuson

62–86. F. C. Maienschein

87. J. J. Manning
88. B. F. Maskewitz
89. J. T. Mihalczo
90. H. S. Moran
91. G. W. Morrison (K-25)
92. F. J. Muckenthaler
93. F. R. Mynatt (K-25)

94–95. R. B. Parker

96. R. W. Peelle
97. S. K. Penny
98. C. M. Perey
99. F. G. Perey
100. J. W. Poston
101. S. J. Raffety
102. R. K. Reedy
103. E. R. Rohrer
104. B. Rust (K-25)
105. R. T. Santoro
106. C. Schneeberger
107. R. J. Silva
108. E. G. Silver
109. M. J. Skinner
110. E. Solomito
111. E. A. Straker
112. R. Textor (K-25)
113. J. T. Thomas

114. J. H. Todd
115. D. K. Trubey
116. W. C. Tunnell
117. V. V. Verbinski
118. J. Wachter
119. D. R. Ward
120. J. W. Webster
121. A. M. Weinberg
122. L. W. Weston
123. B. W. Wieland
124. G. C. Williams
125. I. R. Williams
126. G. Young
127. M. Young
128. K. J. Yost
129. W. Zobel
130. G. Dessauer (consultant)
131. B. C. Diven (consultant)
132. M. L. Goldberger (consultant)
133. M. H. Kalos (consultant)
134. L. V. Spencer (consultant)
135. Radiation Shielding Information Center
136. Biology Library
137–139. Central Research Library
140. Reactor Division Library
141–142. ORNL – Y-12 Technical Library, Document Reference Section
143–407. Laboratory Records Department
408. Laboratory Records, ORNL R.C.

EXTERNAL DISTRIBUTION

409. Research and Development Division, AEC, ORO
410. J. A. Swartout, 270 Park Avenue, New York, New York
411. W. W. Grigorieff, Assistant to the Executive Director, Oak Ridge Associated Universities
412–783. Given distribution as shown in TID-4500 under Physics category (75 copies – CFSTI)